

WALSH SPECTRAL ANALYSIS

WALSH SPECTRAL ANALYSIS

by

KARL-HANS SIEMENS, B.E.E. (General Motors Institute)

M.Eng. (McMaster)

A Thesis

Submitted to the Faculty of Graduate Studies

in Partial Fulfilment of the Requirements

for the Degree

Doctor of Philosophy

McMaster University

June 1972

DOCTOR OF PHILOSOPHY
(Electrical Engineering)

McMaster University
Hamilton, Ontario, Canada

TITLE: Walsh Spectral Analysis

AUTHOR: Karl-Hans Siemens, B.E.E. (General Motors Institute, 1969)
M.Eng. (McMaster, 1969)

SUPERVISOR: Professor R. Kitai, D.Sc.

NUMBER OF PAGES: (xiv), 151

SCOPE AND CONTENTS:

A study of various definitions of Walsh functions is presented. Hardware implementation of Walsh function generators is based on evaluation algorithms which result from non-recursive forms of Walsh function definitions. A special-purpose instrument, which yields the first 64 Walsh series coefficients of an input signal, is described. Analysis of periodic signals requires two complete cycles of the input. For non-periodic signals, measurement time or sample size may be preset arbitrarily. Decimal readouts of the coefficients are available at the end of the measurement time so that the instrument can be used for real-time applications. Walsh series to Fourier series conversion is discussed. A non-recursive equation for the Fourier transforms of Walsh functions is obtained.

ABSTRACT

Walsh functions are defined both by recursive and non-recursive equations. A synopsis is given of the properties of Walsh functions relevant to this thesis. Two algorithms for simple evaluation of an arbitrary point on a Walsh function that use only the binary codes for the parameters of the Walsh function result from the non-recursive definitions. Direct hardware implementation of the evaluation algorithms yields programmable digital Walsh function generators. One of the generators, which produces functions that are free of hazards or ambiguous states, is modified to produce a parallel array of Walsh functions. This generator is used in a Walsh Spectral Analyzer that evaluates simultaneously several Walsh series coefficients of an input signal.

Walsh series analysis and the concepts of the design of a digital Walsh Spectral Analyzer* are discussed. The equation that is used to determine a Walsh series coefficient is modified so that each portion of the equation can be manipulated conveniently by a digital instrument. Although the instrument was designed primarily to analyze periodic waves, extensions to the design can be made to accommodate aperiodic signals. Signals with frequencies from the audio range downwards can be analyzed by the Walsh Spectral Analyzer.

Walsh series to Fourier series conversion is dealt with. It has been found that the Fourier coefficients of signals that are limited

*A photograph of the Walsh Spectral Analyzer is shown in Fig. AB-1.

either in frequency or in sequency can be evaluated precisely using a finite number of Walsh coefficients of the same signal. A dual relationship holds for Fourier to Walsh series conversion. The Fourier series coefficients of Walsh functions comprise part of the conversion relationships. The Fourier transforms of Walsh functions, from which the above coefficients can be obtained, are derived in non-recursive form.

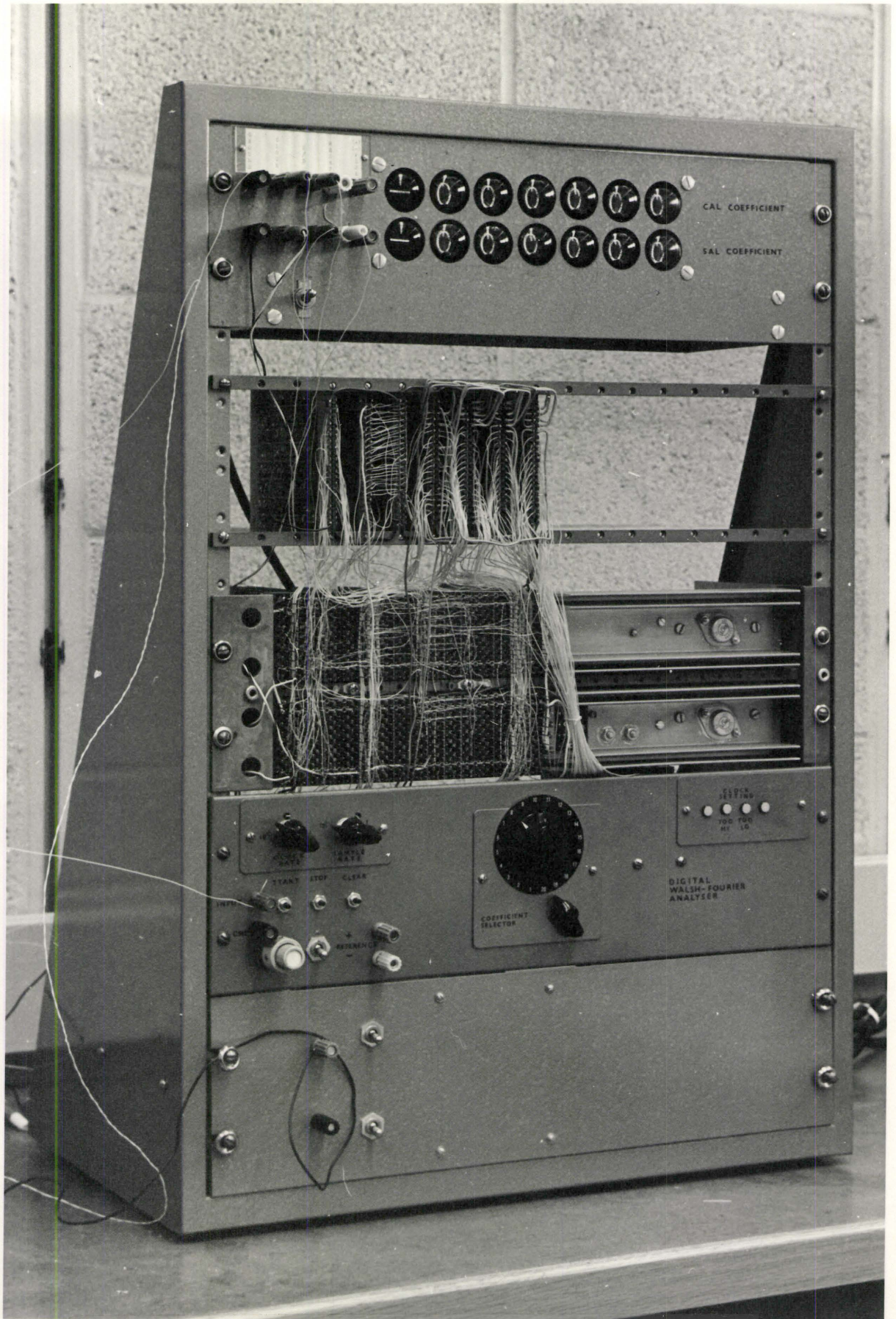


Fig. AB-1 Photograph of Walsh Spectral Analyzer

ACKNOWLEDGEMENTS

The author particularly wishes to thank Dr. R. Kitai for his helpful advice, criticism, and encouragement during the course of this work. The author is also grateful to Mr. K.A. Redish, Dr. R. deBuda and Dr. N.K. Sinha, who, as members of the Supervisory Committee, have aided in stimulating fresh ideas and in assisting with the theoretical aspect of the research. Thanks are due also to Dr. E. Mosca and Milos Novotny who assisted with portions of the mathematical development.

Special thanks are due to Desmond Taylor who first introduced the author to Walsh functions, and to Dr. J. Majithia for his comments and suggestions concerning implementation of the Walsh Spectral Analyzer. Aid by Thomas Pal in preparation of this thesis is gratefully acknowledged. The author wishes to thank Mrs. Kathy Paulin for typing the thesis.

Finally, the author is indebted to the National Research Council of Canada, McMaster University and General Motors of Canada for financial assistance received during the course of this work.

TABLE OF CONTENTS

	<u>Page</u>
CHAPTER 1 - INTRODUCTION	1
CHAPTER 2 - WALSH FUNCTIONS; DEFINITION AND GENERATION	6
2.0 Introduction	6
2.1 Recursive Definitions	6
2.2 Walsh Matrix	10
2.3 Properties of Walsh Functions	12
2.4 Products of Rademacher Functions	14
2.5 A Non-recursive Definition for an Arbitrary Point on a Walsh Function	15
2.6 A Programmable Walsh Function Generator	19
2.7 An Exponential Definition of Walsh Functions	21
2.8 A Hazard-free Walsh Function Generator	25
2.9 An Array Walsh Function Generator	34
2.10 A Hazard-free Gray Code Counter	36
2.11 Conclusion	40
CHAPTER 3 - WALSH SERIES ANALYSIS	42
3.0 Introduction	42
3.1 The Walsh Series	42
3.2 Concepts of a Digital Walsh Spectrum Analyzer Design	45
3.3 Operating Equation for Walsh Spectral Analyzer	48
3.4 Signal Processing in the Walsh Spectral Analyzer	51
CHAPTER 4 - DESIGN OF A DIGITAL WALSH SPECTRAL ANALYZER	55
4.0 Introduction	55
4.1 Complete System	55
4.2 Precision Rectifier	59
4.3 A/D Converter	61
4.4 A/D Converter Controls	63
4.5 Sign Detector	65
4.6 Period Detector	67
4.7 W.F.G. Pulse Generator	73
4.8 Walsh Function Generator	76
4.9 Sample Accumulator Control	77
4.10 Sample Accumulator	78
4.11 Coefficient Readout Counter	81
4.12 System Controls	84
4.13 Conclusions	86

	<u>Page</u>
CHAPTER 5 - WALSH SERIES TO FOURIER SERIES CONVERSION	88
5.0 Introduction	88
5.1 Series Conversion	89
5.2 Sequency-limited Functions	92
5.3 Frequency-limited Functions	92
5.4 Dual Relationship	95
5.5 Instrumentation	96
5.6 Diagonalization of the <u>K</u> Matrix	98
5.7 A Non-recursive Equation for the Fourier Transform of a Walsh Function	115
5.8 Algorithm to Determine Fourier Transform of $Wal(m, \theta)$	122
5.9 Pattern of Non-zero Elements in the <u>F</u> Matrix	123
5.10 Comparison of Walsh and Fourier Series Analysis and Synthesis	125
5.11 Conclusion	138
CHAPTER 6 - CONCLUSIONS	141
APPENDIX	144
APPENDIX A	145

LIST OF ILLUSTRATIONS

<u>Figure</u>		<u>Page</u>
AB-1	Photograph of the Walsh Spectral Analyzer	(v)
2-1	Walsh Functions	11
2-2	Programmable Walsh Function Generator	20
2-3	Sources of Hazards in Exclusive-OR Systems	27
2-4	A Hazard-free Walsh Function Generator	29
2-5	Set of Walsh Functions $\{wal(2^k, \theta)\}$	31
2-6	A Walsh Function Array Generator	35
2-7	Four-bit Gray Code Counter	37
3-1	Quantization	49
3-2	Example of Functions used to Calculate B_3	52
4-1	Walsh Spectral Analyzer	56
4-2	Precision Rectifier	60
4-3	A/D Converter	62
4-4	A/D Converter Controls	64
4-5	Sign Detector System	66
4-6	Period Detector	69
4-7	Waveforms in Period Detector	70
4-8	W.F.G. Pulse Generator	74
4-9	Sample Accumulator Control	77
4-10	Sample Accumulator	79

<u>Figure</u>		<u>Page</u>
4-11	Up/Down Counter with Magnitude and Sign Generation	82
4-12	System Controls	85
5-1	Walsh Spectrum Analysis of a Frequency-limited Function	93
5-2	Convolution Quantities to Form $\text{sal}(3,\theta)$ over the Range $-\frac{1}{2} \leq \theta < \frac{1}{2}$	118
5-3	Spectra of Rectangular Pulse (Duty Cycle = 0.1)	127
5-4	Fourier Series and Walsh Series Synthesis of a Rectangular Pulse (Duty Cycle = 0.1)	128
5-5	Spectra of a Ramp Function	131
5-6	Fourier Series and Walsh Series Synthesis of a Ramp Function	132
5-7	Spectra of a Triangular Wave	134
5-8	Fourier Series and Walsh Series Synthesis of a Triangular Wave	135
5-9	Walsh Series Synthesis of Experimental Waveform	139
5-10	Synthesis of Experimental Waveform using Fourier Series Coefficients Obtained by Conversion Formulae	140

LIST OF TABLES

<u>Table</u>		<u>Page</u>
2-1	The Walsh Matrix	12
2-2	Example of Algorithm for Walsh Function Evaluation	17
2-3	Evaluation of $wal(22, \theta)$ for $\theta = .34429$	30
2-4	Coded Samples of $\{wal(2^k, \theta)\}$ which Form a Gray Code	32
2-5	4-bit Gray Code Count Sequence	38
4-1	Count Sequence Using Magnitude and Sign Detector	83
5-1	Set of 2^M Discrete Walsh Functions	104
5-2	Walsh Series Coefficients of Experimental Waveform and Fourier Series Coefficients Obtained by Walsh to Fourier Series Conversion	137

LIST OF SYMBOLS AND ABBREVIATIONS

T	: period (also used to indicate transpose matrix)
A/D	: analog to digital
D/A	: digital to analog
$\{\phi\}$: original notation for set of Walsh functions
wal(m, θ)	: Walsh function
m	: order of Walsh function
m_k	: bits in binary representation of m
θ	: normalized time
θ_k	: bits in binary representation of θ
cal(s, θ)	: even-ordered Walsh function
sal(s, θ)	: odd-ordered Walsh function
s	: normalized sequency
f	: normalized frequency
y	: Walsh function interval number
M	: number of binary bits in m
[W]	: Walsh matrix
\oplus	: modulo 2 sum or Exclusive-OR
[I]	: identity matrix
$R_k(\theta)$: Rademacher function of order k
G	: Gray code number for m
g_k	: bits in Gray code number G
α	: number of bits equal to ONE in G
γ_k	: bits in Gray code representation of θ

msb : most significant bit
 lsb : least significant bit
 sgn : signum
 IC : integrated circuit
 LSI : large scale integration
 A_s, B_s, W_m : Walsh series coefficients
 $f(\theta)$: time-dependent function
 a_f, b_f, c_f : Fourier series coefficients
 WSA : Walsh Spectral Analyzer
 FFT : Fast Fourier Transform
 FWT : Fast Walsh Transform
 H : sample size
 h : sample number
 p : number of quantization levels
 r : quantization level number
 Q_h : binary-coded sample of $f(\theta)$
 P_h : bits in coded sample
 C.F. : conversion factor
 V : volts
 mv : millivolts
 W.F.G. : Walsh Function Generator
 f_s : sample frequency
 V_R : reference voltage
 e_H : hysteresis voltage
 FF1, FF2 : flip-flops 1 and 2

C_e	: counter enable
C_i	: carry-in
U/\overline{D}	: up/ $\overline{\text{down}}$
BCD	: binary-coded decimal
S	: highest order sequency component
F	: highest order frequency component
$A_{s,f}, B_{s,f}$: Walsh coefficients of sinusoids
$a_{f,s}, b_{f,s}$: Fourier coefficients of Walsh functions
\underline{F}	: matrix containing elements $a_{f,s}$ or $b_{f,s}$
\underline{K}	: matrix $\frac{1}{2} \underline{F} \underline{F}^T$
ROM	: read-only memory
$W_{s,y}$: value of $\text{cal}(s,\theta)$ or $\text{sal}(s,\theta)$ during interval y
$S_{f,y}, C_{f,y}$: integral of sinusoid over interval y
dY	: delay operator
$\delta(\theta)$: unit impulse function
$U(\theta)$: unit step function
$F[f(\theta)]$: Fourier transform of $f(\theta)$

CHAPTER 1

INTRODUCTION

Waves, which are fundamental phenomena in the universe, occur in many forms, such as mechanical vibrations or electromagnetic fluctuations. The concepts of frequency and Fourier spectrum have long provided a basic measure of wave phenomena. Historically, whenever the term frequency is used, reference is generally made to the sine and cosine functions. Since sinusoids occur frequently in nature (e.g., resonance of sound waves in a Kundt's tube) and since time functions used in communications can be represented by Fourier's superposition, sinusoids are used almost instinctively for waveform analysis. Sinusoids also are compatible with linear, time-invariant circuits.

With the advent of pulse and switching technology, wave measurement techniques that were not intuitive by nature before, now become intuitive with respect to the new form of the technology. With the ever-increasing abundance of digital logic hardware, particularly in integrated circuit form, there has been an evolution of thought towards finding a set or sets of functions that are more adaptable to digital hardware than are sinusoidal waves. Ideally, the set of functions should have but two values so that it is compatible with binary logic, and it should be a set of mutually orthogonal functions so all signals can be represented by a superposition of functions in a manner analogous to a Fourier series.

The set of bi-valued mutually orthogonal Walsh functions has been found to be well-suited to signal analysis. Harmuth [1] reports that

probably the oldest use (circa 1900) of Walsh functions in communications was in the area of the transposition of conductors [2]. It was in 1923 that J.L. Walsh [3] introduced the functions into mathematics. Walsh's set was the completion of the orthonormal system presented independently by Rademacher [4] in 1922. Extensive studies of the Walsh system and series expansions in terms of Walsh functions have been conducted since that time, notably by Kaczmarz [5], Paley [6], and Fine [7-9]. In recent years, Harmuth [1, 10-13] has been instrumental in promoting the search for practical applications of Walsh functions. Consequently, research in the area of non-sinusoidal functions in communications has been significantly stimulated [14,15].

This thesis deals principally with a digital instrument that has been designed to perform a Walsh series analysis of a signal in real-time. The salient features of this instrument are as follows:

- 1) A Walsh Spectral Analyzer has been designed specifically for low frequency analysis (audio frequencies and under). There are no low frequency limitations. Since the time-base of measurement for periodic waves can be automatically adjusted to the fundamental period of the input signal, certain error considerations during period determination establish the upper frequency limit.
- 2) For periodic waves with a fundamental period T , the measurement time is $2T$. Since Walsh series coefficient values are then immediately available in sign and magnitude form, the instrument is suitable for real-time applications.

- 3) The instrument design can be extended to analyze aperiodic waveforms. Both measurement time and sample size can be preselected arbitrarily, in which case the measurement time is reduced to T .
- 4) The outputs are in decimal code, but can be displayed in any other code, the only change required being in type of final readout counter. Maximum sample size is restricted only by the size of the output display.
- 5) The instrument can be modified readily to determine the value of any specific component in the Walsh spectrum, or it can yield in parallel as many Walsh series coefficients as are desired.
- 6) The instrument can also be modified to accept either a continuous signal and use its own A/D converter or to use ready-quantized data.
- 7) Since all computations for a sample are complete before the next sample arrives, all programming and unnecessary storage facilities are eliminated.

Walsh functions are defined in a number of ways in Chapter 2.

Both recursive and non-recursive definitions are discussed and a synopsis of the properties of Walsh functions relevant to this thesis is given. Two algorithms for simple evaluation of an arbitrary point on a Walsh function and that use only the binary codes for the parameters of the Walsh function result from the non-recursive definitions. Direct hardware implementation of the evaluation algorithms yields programmable

digital Walsh function generators. One of the generators, which produces functions that are free of hazards or ambiguous states, is modified to produce a parallel array of Walsh functions. This generator is used in a Walsh Spectral Analyzer that evaluates simultaneously several Walsh series coefficients of an input signal.

Chapter 3 deals with Walsh series analysis and the concepts of the design of a digital Walsh Spectral Analyzer. The equation that is used to determine a Walsh series coefficient is modified so that each portion of the equation can be manipulated conveniently by a digital instrument.

An overall view of a digital Walsh Spectral Analyzer is given in the first portion of Chapter 4. Although the instrument was designed primarily to analyze periodic waves, extensions to the design can be made to accommodate aperiodic signals. A detailed description is given of the design of each major section shown in the block diagram of the instrument.

Walsh series to Fourier series conversion for several classifications of waveforms is discussed in Chapter 5. It has been found that the Fourier coefficients of signals that are either frequency-limited or sequency-limited [1] can be determined precisely by using the Walsh coefficients of the same signals. A dual relationship holds for Fourier series to Walsh series conversion. The Fourier series coefficients of Walsh functions comprise part of the conversion relationships. The Fourier transforms of Walsh functions, from which the above coefficients can be obtained, are derived in non-recursive form. A number of graphic

examples of Fourier and Walsh series analysis and synthesis conclude Chapter 5.

In Chapter 6, the significant aspects of the thesis are reviewed briefly. Possible areas for further investigation are suggested. It is felt that Walsh functions and the Walsh spectrum will continue to increase in importance in communications and other areas of information processing, particularly as more hardware systems using Walsh functions become available.

CHAPTER 2

WALSH FUNCTIONS; DEFINITION AND GENERATION

2.0 Introduction

Walsh functions have been paid significant attention in recent years. With the vast amount of research dealing with the properties and applications of these functions, numerous types of definitions and terminology have appeared. It is the intention here to establish the terminology for the Walsh functions that is predominant in this thesis, to derive non-recursive expressions to define the functions,

to develop coding algorithms for evaluation of arbitrary points on a Walsh function, and to develop hardware implementations of the algorithms. Hardware implementations of the algorithms lead to the design of hazard-free binary Walsh function generators, which can be incorporated into a special-purpose computer for Walsh spectral analysis. A synopsis is given of those properties of the Walsh functions that are necessary to define the functions, to develop a Walsh spectral analyzer, and to verify the procedure for Walsh series to Fourier series conversion.

1 Recursive Definitions

In his classic paper, J.L. Walsh introduced [1] a "new closed set of functions $\{\phi\}$ normal and orthogonal on the interval $[0,1]$ ". The Walsh functions, i.e., the set $\{\phi\}$, take only the values +1 and -1, except at a finite number of points of discontinuity, where they assume the value zero. The set $\{\phi\}$, which is ordered according to increasing

number of zero-crossings, has the following recursive definition;

$$\phi_0(\theta) = 1, \quad 0 \leq \theta \leq 1 \quad (2-1)$$

$$\phi_1(\theta) = \begin{cases} 1, & 0 \leq \theta < \frac{1}{2} \\ -1, & \frac{1}{2} < \theta \leq 1 \end{cases}$$

$$\phi_2^{(1)}(\theta) = \begin{cases} 1, & 0 \leq \theta < \frac{1}{4}, \frac{3}{4} < \theta \leq 1 \\ -1, & \frac{1}{4} < \theta < \frac{3}{4} \end{cases}$$

$$\phi_2^{(2)}(\theta) = \begin{cases} 1, & 0 \leq \theta < \frac{1}{4}, \frac{1}{2} < \theta < \frac{3}{4} \\ -1, & \frac{1}{4} < \theta < \frac{1}{2}, \frac{3}{4} < \theta \leq 1 \end{cases}$$

- - - - -

$$\phi_{n+1}^{(2k-1)}(\theta) = \begin{cases} \phi_n^{(k)}(2\theta), & 0 \leq \theta < \frac{1}{2} \\ (-1)^{k+1} \phi_n^{(k)}(2\theta-1), & \frac{1}{2} < \theta \leq 1 \end{cases}$$

$$\phi_{n+1}^{(2k)}(\theta) = \begin{cases} \phi_n^{(k)}(2\theta), & 0 \leq \theta < \frac{1}{2} \\ (-1)^k \phi_n^{(k)}(2\theta-1), & \frac{1}{2} < \theta \leq 1 \end{cases}$$

where $k = 1, 2, 3, \dots, 2^{n-1}$, $n = 1, 2, 3, \dots, \infty$. With respect to $\theta = \frac{1}{2}$, the functions $\phi_{n+1}^{(2k-1)}$ and $\phi_{n+1}^{(2k)}$ are even and odd, respectively. Periodic functions can be developed by means of the set $\{\phi\}$ if the definitions are changed at $\theta = 0$ and $\theta = 1$ so that the value of $\phi_n^{(k)}(\theta)$ is the arithmetic mean of the limits at these points to the right and to the left. Walsh functions may be defined at a point of discontinuity to have the

average of the limits approached on the two sides of the discontinuity.

Walsh used the definition of the functions $\phi_n^{(k)}$ to obtain a formula for $\phi_n^{(k)}(\theta)$. If θ is the set in binary notation,

$$\theta = \frac{y_1}{2^1} + \frac{y_2}{2^2} + \frac{y_3}{2^3} + \dots \quad y_i = 0 \text{ or } 1 \quad (2-2)$$

then if in the binary expansion of θ there exists $y_i \neq 0$ and $i > n$, the following formulas hold for $\phi_n^{(k)}$:

$$\begin{aligned} \phi_0 &= 1 & \phi_1 &= (-1)^{y_1} & (2-3) \\ \phi_2^{(1)} &= (-1)^{y_1+y_2} & \phi_2^{(2)} &= (-1)^{y_2} \\ \phi_3^{(1)} &= (-1)^{y_2+y_3} & \phi_3^{(2)} &= (-1)^{y_1+y_2+y_3} \\ \phi_3^{(3)} &= (-1)^{y_1+y_3} & \phi_3^{(4)} &= (-1)^{y_3} \\ \phi_4^{(1)} &= (-1)^{y_3+y_4} & \phi_4^{(2)} &= (-1)^{y_1+y_3+y_4} \end{aligned}$$

A generalized law that is still in the form of a recursive equation appears from the relations in Eq. (2-3):

$$\begin{aligned} \phi_n^{(1)} &= (-1)^{y_{n-1}+y_n} & (2-4) \\ \phi_n^{(k)} &= \phi_{k-1} \phi_n^{(1)} \end{aligned}$$

where ϕ_{k-1} are members of the set $\{\phi\}$ in order. The definition in the form of Eq. (2-3) can also be developed from a non-recursive equation of a Walsh function, as is described later in this chapter.

A more convenient notation for the set $\{\phi\}$ has evolved. The standard terminology adopted for this thesis uses $wal(m, \theta)$, where m is the order of the Walsh function, and θ is considered to be normalized time. As a comparison of $\phi_n^{(k)}(\theta)$ with $wal(m, \theta)$, $m = n+k$, and n equals the number of bits in the binary expansion of m . Pichler [2] has given distinct notations, $cal(s, \theta)$ and $sal(s, \theta)$, to the even and odd Walsh functions, respectively. They are related to $wal(m, \theta)$ by

$$cal(s, \theta) = wal(m, \theta), \quad m = 2s \quad (2-5)$$

and

$$sal(s, \theta) = wal(m, \theta), \quad m = 2s-1 \quad (2-6)$$

where s is called the sequency [3]; that is, one half the average number of zero-crossings per second. The order m is then related to twice the normalized sequency for a set of sequency-ordered functions.

Using the above terminology, Harmuth [4] has developed a recursive definition of Walsh functions in the form of a difference equation.

$$\begin{aligned} wal(2i+p, \theta) = & (-1)^{[i/2]+p} \{ wal[i, 2(\theta + \frac{1}{4})] \\ & + (-1)^{i+p} wal[i, 2(\theta - \frac{1}{4})] \} \end{aligned} \quad (2-7)$$

where $p = 0$ or 1 ,

$i = 0, 1, 2, \dots$,

$$wal(0, \theta) = \begin{cases} 1 & \text{for } -\frac{1}{2} \leq \theta < \frac{1}{2} \\ 0 & \text{for } \theta < -\frac{1}{2}, \theta > +\frac{1}{2} \end{cases}$$

and $[i/2]$ means the largest integer smaller than or equal to $\frac{1}{2} i$.

Although the definition covers only the interval $-\frac{1}{2} \leq \theta < \frac{1}{2}$, periodic Walsh functions can be formed by duplicating the function over each successive interval. An illustration of the first 16 sequency-ordered, continuous Walsh functions over the interval $0 \leq \theta < 1$ is given in Fig. 2-1.

2.2 The Walsh Matrix

An extremely useful representation of the Walsh functions is in the form of a discrete Walsh matrix. The discrete Walsh functions are sampled versions of the continuous set of $wal(m, \theta)$ in Fig. 2-1; the samples being taken at $\theta_y = y/2^M$ for $y = 0, 1, 2, \dots, 2^M - 1$, and M is the number of binary digits in m . Henderson [5] describes the first 2^M Walsh functions of 2^M arguments as being represented collectively by a square Walsh matrix $[W]$ whose rows are the successive Walsh functions and whose columns correspond to the successive arguments for y over $0 \leq y < 2^M - 1$. The Walsh matrix for $M=3$ is shown in Table 2-1. The value -1 is denoted by $-$. Since the Walsh functions are two-valued, they can easily be coded into binary. A binary Walsh matrix $[W_B]$, each of whose elements is 0 or 1, can be obtained from $[W]$ by the transformation*

$$\begin{Bmatrix} 1 \\ -1 \end{Bmatrix} \text{ in } [W] \leftrightarrow \begin{Bmatrix} 1 \\ 0 \end{Bmatrix} \text{ in } [W_B] \quad (2-8)$$

*This transformation is considered more convenient than that of Henderson [5] in which the 0 and 1 bits are interchanged.

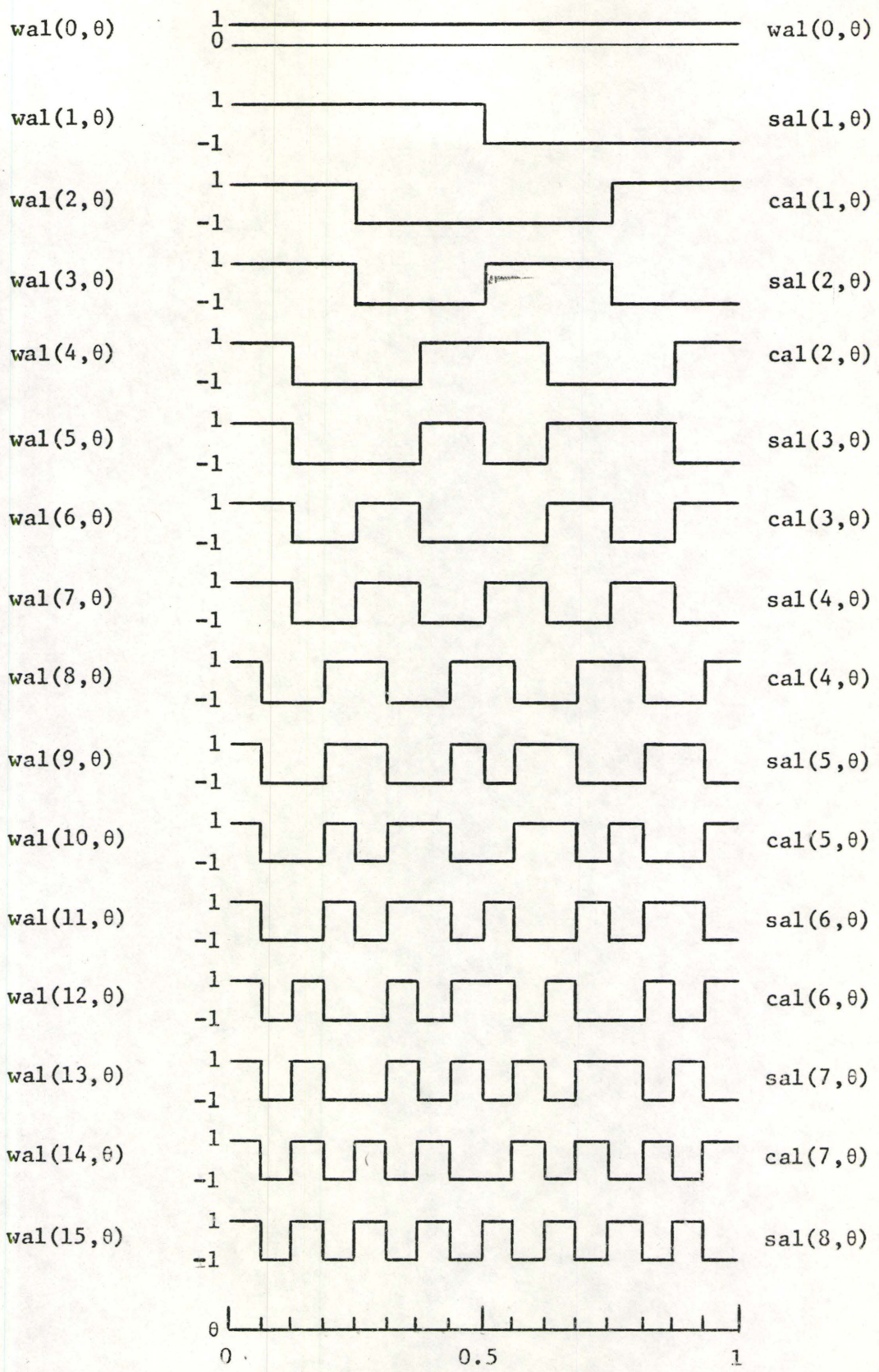


Fig. 2-1 Walsh Functions

$y =$	0	1	2	3	4	5	6	7	
$[W] =$	1	1	1	1	1	1	1	1	wal(0,y)
	1	1	1	1	-	-	-	-	wal(1,y)
	1	1	-	-	-	-	1	1	wal(2,y)
	1	1	-	-	1	1	-	-	wal(3,y)
	1	-	-	1	1	-	-	1	wal(4,y)
	1	-	-	1	-	1	1	-	wal(5,y)
	1	-	1	-	-	1	-	1	wal(6,y)
	1	-	1	-	1	-	1	-	wal(7,y)

Table 2-1 The Walsh Matrix

2.3 Properties of Walsh Functions

Characteristics of the Walsh system are described in detail by Walsh [1], Fine [6], and Harmuth [4]. Presented here is a synopsis only of those properties that are relevant to a basic understanding of Walsh functions, to the development of non-recursive definitions of the functions, and to the design of a digital Walsh spectrum analyzer.

With reference to Fig. 2-1, the Walsh functions $wal(m, \theta)$ are considered periodic over the half-open interval $[0, 1)$. Although the period $[-\frac{1}{2}, \frac{1}{2})$ is used occasionally, we are concerned here with real-time analysis of time functions and will consider the time origin as 0. The arguments m and θ are the order and the normalized time, respectively. Each Walsh function of order m can be divided into 2^M subintervals where M is the number of bits in the binary representation of m . The value of a function is constant at either +1 or -1 over each subinterval. The latter property is useful in digital instrumentation since the Walsh

functions can then be represented as a sequence of ONE and ZERO logic levels.

Several orderings of the Walsh functions are possible [7]. To maintain an analogy with the increasing-harmonic number ordering of Fourier spectrum analysis, the Walsh set used in this thesis is sequency-ordered; that is, ordered according to increasing number of zero-crossings. The number of discontinuities in the range (0,1) is then equivalent to m.

The product of any two Walsh functions yields a single function whose order is determined by the modulo 2 sum of the orders of the multiplied functions [4]; thus

$$\text{wal}(k,\theta)\text{wal}(m,\theta) = \text{wal}(k \oplus m,\theta) \quad (2-9)$$

where \oplus stands for addition modulo 2. If k and m are both binary numbers, \oplus represents add without carry. For example, multiplication of $\text{wal}(6,\theta)$ by $\text{wal}(12,\theta)$ results in $\text{wal}(10,\theta)$, i.e.,

$$\begin{array}{r} \oplus \quad \begin{array}{cccc} 0 & 1 & 1 & 0 \end{array} \quad \begin{array}{c} 6 \\ 12 \\ 10 \end{array} \\ \quad \begin{array}{cccc} 1 & 1 & 0 & 0 \end{array} \\ \hline \quad \begin{array}{cccc} 1 & 0 & 1 & 0 \end{array} \end{array}$$

This multiplicative property of the functions can be used to demonstrate one of the most important properties of the set; Walsh functions form a complete set of mutually orthogonal functions [1] over [0,1). Hence

$$\int_0^1 \text{wal}(k,\theta)\text{wal}(m,\theta)d\theta = \begin{cases} 0, & k \neq m \\ 1, & k = m \end{cases} \quad (2-10)$$

Since the $\text{wal}(m,\theta)$ are mutually orthogonal, the Walsh matrix [W] has some interesting properties. The rows of [W] and the columns of its transpose $[W]^T$ are also mutually orthogonal. The matrix of the

product $[W][W]^T$ will therefore be nonzero only on its main diagonal, and because each element of $[W]$ is either +1 or -1,

$$[W][W]^T = 2^M [I] \quad (2-11)$$

where $[I]$ is the identity matrix. It is evident from Eq. (2-11) that the inverse of $[W]$ is

$$[W]^{-1} = 2^{-M} [W]^T \quad (2-12)$$

The matrix $[W]$ is symmetrical [5] and hence equal to $[W]^T$. From this relationship,

$$\text{wal}(m,y) = \text{wal}(y,m) \quad (2-13)$$

2.4 Products of Rademacher Functions

The complete set of Walsh functions can be obtained as direct products of the subclass of these functions known as Rademacher functions $R_k(\theta)$ [6]. $R_k(\theta)$ can be associated with specific Walsh functions by

$$R_k(\theta) = \text{sal}(2^k, \theta) = \text{wal}(2^{k+1}-1, \theta) \quad (2-14)$$

where $k = 0, 1, 2, 3, \dots$

According to Paley's modification [6] of the Walsh system, if the order m of $\text{wal}(m, \theta)$ is given by the dyadic expansion

$$m = \sum_{k=0}^{M-1} m_k 2^k \quad (2-15)$$

then the Walsh functions are given by

$$\text{wal}(0, \theta) = 1 \quad (2-16)$$

$$\text{wal}(m, \theta) = \prod_{k=0}^{M-1} m_k \{R_k(\theta)\}$$

where m_k is a binary presence operator*. The modified set defined by Eq. (2-16) is not sequency-ordered as in Walsh's original definition. However, it was found by Henderson [5] that the sequency-ordered set could be obtained by selecting products of $R_k(\theta)$ according to bits in the reflected binary code. That is, if the bits g_k in the Gray code for m are found in the usual manner from

$$g_k = m_{k+1} \oplus m_k \quad (2-17)$$

then

$$\text{wal}(m, \theta) = \prod_{k=0}^{M-1} g_k \{R_k(\theta)\} \quad (2-18)$$

where g_k is a presence operator similar to m_k . Non-recursive definitions in terms only of the arguments m and θ are derived from Eq. (2-18) to evaluate any arbitrary point on a Walsh function.

2.5 A Non-recursive Definition for an Arbitrary Point on a Walsh Function

Lackey and Meltzer [8] have presented a technique for solving Eq. (2-18) by listing sample values of those Rademacher functions that correspond to the ONE-bits in the Gray code for the order m . Corresponding samples of the $R_k(\theta)$ are multiplied to synthesize a discrete Walsh function. A simple extension [9] of this method allows evaluation

* m_k is a binary operator such that $m_k\{x\}$ equals the logical operation $\overline{m_k} \cdot \overline{x} = \overline{m_k + x}$. Hence,

$$\text{for } m_k = 0, \quad m_k\{x\} = 1$$

$$\text{and for } m_k = 1, \quad m_k\{x\} = x.$$

of any arbitrary point on the m th Walsh function without listing tables of $R_k(\theta)$ and it yields a concise non-recursive definition for the point.

Let the Rademacher values $+1$ and -1 be given the binary coding ZERO and ONE, respectively. If θ has the limits $0 \leq \theta < 1$, the coding of each of the 2^M intervals in a set of the first M Rademacher functions is equivalent to the first M bits in the binary fraction representation of any point θ within that interval. Lesser significant bits that locate points within an interval can be ignored since the value of a Walsh function is constant over each of its sections. The ONE-bits in a bit-reversed Gray code for the order m enable the corresponding bits in the code for θ to be operated on by a parity check for an even number of ONE's. The parity check serves as a multiplier of the appropriate Rademacher functions. Since ONE's represent Rademacher values of -1 , an even number of ONE's yields a Walsh value of $+1$ from the parity check. An odd number of ONE's yields -1 . The Gray code for m is bit-reversed since the least significant bit (lsb) g_0 controls $R_0(\theta)$, which is represented by the most significant bit (msb) of θ .

An example of a Walsh function evaluation algorithm that is developed from the above form of coding is shown in Table 2-2. In the example, $wal(22, \theta)$ is evaluated at $\theta = .34429$. In binary, $\theta = .010110---$. Thus, the point θ is located in the twelfth of 32 intervals, and it is sufficient to evaluate $wal(22, \theta)$ at the beginning of the interval (i.e., at $\theta = 11/32 = .01011$).

$22_{10} =$	10110_2		Binary notation for $wal(22, \theta)$
	↓		
	11101		Gray code for 22
	↓		
	10111	G	Bit-reversed Gray code
$\theta = .34429_{10} =$	$\frac{0.01011}{00011}$	K	Binary notation for θ
		L	Bits of K enabled by G
	↓		
	1		Parity check for even number of ONE's in L.
	↓		
	+1		Value of $wal(22, .34429)$

Table 2-2 Example of Algorithm for Walsh Function Evaluation

The evaluation algorithm of Table 2-2 lends itself to several forms of non-recursive expressions defining $wal(m, \theta)$. First express the position θ_y as an integer y by

$$y = 2^M \theta_y \quad (2-19)$$

where 2^M is the number of intervals contained in $wal(m, \theta)$. Then if y is expressed in binary as

$$y = \sum_{k=0}^{M-1} y_k 2^k, \quad y_k = 0 \text{ or } 1 \quad (2-20)$$

the parity check on the bits of y enabled by the bits of the Gray code G forms a product realization of the Walsh function as

$$\text{wal}(m, \theta_y) = \prod_{k=0}^{M-1} (-1)^{y_k g_{M-1-k}} \quad (2-21)$$

$$= \prod_{k=0}^{M-1} (-1)^{g_k y_{M-1-k}}$$

Eq. (2-21) can also be written in summation form as

$$\text{wal}(m, \theta_y) = (-1)^{\sum_{k=0}^{M-1} y_k g_{M-1-k}} \quad (2-22)$$

For a specific Walsh function, the Gray code bits in Eq. (2-22) can be omitted by summing only those bits y_k for which $g_{M-1-k} = 1$. In this manner, the same formulas as originally found by Walsh in Eq. (2-3) can be obtained from a non-recursive equation. Eq. (2-22) also turns out to be a simplified form of the Walsh-Kaczmarz equation [10];

$$\text{wal}(m, \theta_y) = \exp j\pi [y_0 m_{M-1} \oplus \sum_{k=1}^{M-1} y_k (m_{M-k} \oplus m_{M-1-k})] \quad (2-23)$$

In some of the literature on Walsh functions, $\text{wal}(m, \theta)$ is considered periodic over the interval $[-\frac{1}{2}, \frac{1}{2})$. To use the definitions of Eqs. (2-21) and (2-22) for negative values of θ_y , one uses the 2's-complement bits of y . This is easily seen by observing that the values of a Walsh function at $-\theta_y$ and at $1-\theta_y$ are equivalent. In binary, the 2's complement of $|\theta_y|$ equals $1-\theta_y$ for $-1 \leq \theta_y < 1$.

The coding algorithm of Table 2-2 has also proved useful in computer evaluation of a Walsh function and in the design of a programmable Walsh function generator. A description of the generator follows.

2.6 A Programmable Walsh Function Generator

The definition of Eq. (2-21) evaluates only one point on a Walsh function. If the binary code is cycled through one period from 0 to 2^M-1 , a complete Walsh function can be obtained. Using the coding ZERO and ONE for Rademacher values 1 and -1, respectively, the outputs of a binary up-counter form the set of Rademacher functions. The msb of the counter represents $R_0(\theta)$. In the Walsh function generator design* shown in Fig. 2-2 the Gray code bits of the order of the desired Walsh function control AND gates that enable the appropriate coded Rademacher functions to pass through to a parity check for an even number of ONE's. The design is thus a direct implementation of the algorithm of Table 2-2.

The circuit in Fig. 2-2 can easily be implemented using IC logic. The latest available packages that can be used in the TTL line are given in the diagram. This generator design has the feature that it can be programmed by changing the input binary code for the order of the desired Walsh function. The code can be changed at any time during the operation. The Walsh functions are always in phase with the synchronous counter, regardless of changes in the input code. $Wal(0,\theta)$, which is not a product of Rademacher functions according to Eq. (2-16), is produced when the input code is set to 0.

The generator does, however, have a characteristic that could prove detrimental in certain applications. Since the binary counter has

*This design was implemented independently several months before identical subsequent designs were published [10,11]. At that time, publication of the design was rejected since only an example of the accompanying algorithm, rather than a proof, was given.

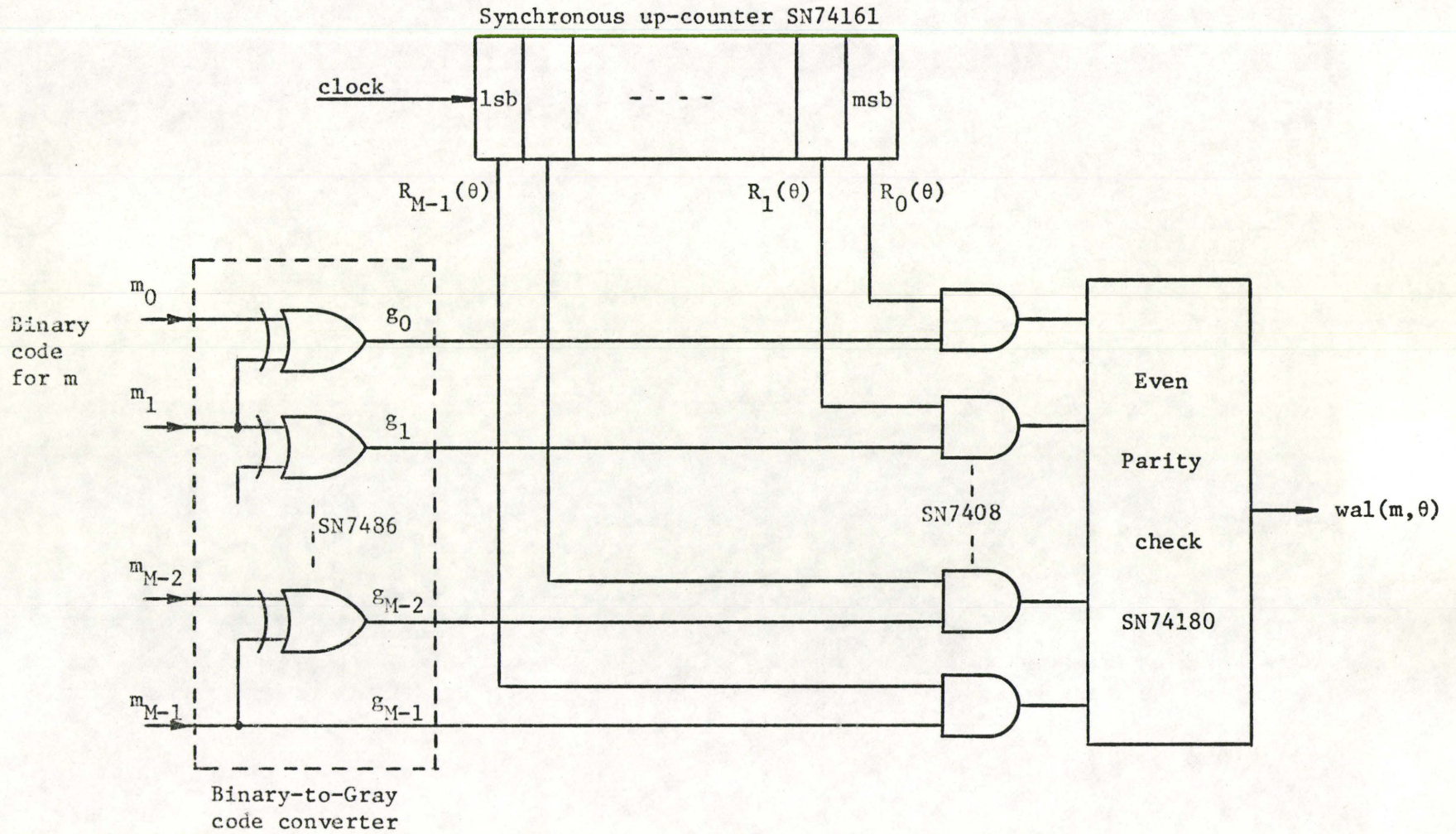


Fig. 2-2 Programmable Walsh Function Generator

outputs that can change simultaneously, there is the possibility that the Walsh functions may contain ambiguous states, i.e., voltage spikes, or hazards [12]. Consequently, in the following section, another definition of Walsh functions is developed and it results in implementation of a hazard-free Walsh function generator [13].

2.7 An Exponential Definition of Walsh Functions

It is well known [4] that any Walsh function can be formed by the product of two or more Walsh functions where the order of the new function is the modulo 2 sum of the orders of the multiplying factors [See Eq. (2-9)]. However, if we consider the new function $wal(m, \theta)$ to consist only of products of those functions in the set $\{wal(2^k, \theta)\}$, it is readily shown that the modulo 2 sum operation can be replaced by arithmetic addition. Since the binary representation of 2^k contains only 1 ONE in the k th position (where $k = 0, 1, 2, 3, \dots$),

$$\begin{aligned} wal(1, \theta)wal(2, \theta)wal(4, \theta) \dots &= wal(1 \oplus 2 \oplus 4 \oplus \dots, \theta) \\ &= wal(1 + 2 + 4 + \dots, \theta) \end{aligned} \quad (2-24)$$

where \oplus denotes addition.

If m_k are bits in the binary representation of m , then it follows that $wal(m, \theta)$ may be formed by products of those members of the set $\{wal(m_k 2^k, \theta)\}$ for which $m_k = 1$. If, for example, $m = 13$,

$$\begin{aligned} wal(13_{10}, \theta) &= wal(1101_2, \theta) && (2-25) \\ &= wal(1000 + 100 + 1, \theta) \\ &= wal(8 + 4 + 1, \theta) \\ &= wal(8, \theta)wal(4, \theta)wal(1, \theta) \end{aligned}$$

Since the order of the result is the arithmetic sum of the order of the components, Walsh functions generated in this manner are sequentially ordered. Then, from the above,

$$\begin{aligned}
 \text{wal}(m, \theta) &= \prod_{k=0}^{M-1} m_k \{\text{wal}(2^k, \theta)\} & (2-26) \\
 &= \prod_{k=0}^{M-1} \text{wal}(m_k 2^k, \theta) \\
 &= \text{wal}\left(\sum_{k=0}^{M-1} m_k 2^k, \theta\right)
 \end{aligned}$$

In the first row of Eq. (2-26), m_k acts as a binary presence operator. Note also that if $m_k = 0$ for all k ,

$$\text{wal}\left(\sum_{k=0}^{M-1} m_k 2^k, \theta\right) = \text{wal}(0, \theta) = 1 \quad (2-27)$$

The definitions of Eq. (2-26) are, however, in recursive form and they give no direct evidence that they can lead to the design of a hazard-free Walsh function generator. First, the equation must be modified by viewing the set $\{\text{wal}(2^k, \theta)\}$ as a set of hard-limited sinusoids; that is,

$$\begin{aligned}
 \text{wal}(1, \theta) &= \text{sgn} \sin 2\pi\theta & (2-28) \\
 \text{wal}(2, \theta) &= \text{sgn} \cos 2\pi\theta \\
 \text{wal}(4, \theta) &= \text{sgn} \cos 4\pi\theta \\
 &\vdots \\
 \text{wal}(2^k, \theta) &= \text{sgn} \cos 2^k \pi\theta
 \end{aligned}$$

The hard-limited sinusoids are related to exponential functions by;

$$\operatorname{sgn} \sin 2\pi\theta = \exp j\pi \langle \theta \rangle \quad (2-29)$$

$$\operatorname{sgn} \cos 2\pi\theta = \exp j\pi \langle 2\theta \rangle$$

$$\operatorname{sgn} \cos 4\pi\theta = \exp j\pi \langle 4\theta \rangle$$

$$\vdots$$

$$\operatorname{sgn} \cos 2^k \pi\theta = \exp j\pi \langle 2^k \theta \rangle$$

where $\langle 2^k \theta \rangle$ denotes the nearest integer to $2^k \theta$ and θ is in the range $[0,1)$. Hence, each member of $\{\operatorname{wal}(2^k, \theta)\}$ can be represented by an exponential expression;

$$\operatorname{wal}(2^k, \theta) = \exp j\pi \langle 2^k \theta \rangle \quad (2-30)$$

where $k = 0, 1, 2, 3, \dots$,

$$0 \leq \theta < 1.$$

Similarly,

$$\begin{aligned} \operatorname{wal}(m, \theta) &= \operatorname{wal}\left(\sum_{k=0}^{M-1} m_k 2^k, \theta\right) \quad (2-31) \\ &= \exp j\pi \left[\sum_{k=0}^{M-1} \langle m_k 2^k \theta \rangle \right] \end{aligned}$$

Evaluation of $\exp j\pi \langle m_k 2^k \theta \rangle$ depends only on whether $\langle m_k 2^k \theta \rangle$, which is an integer, is even or odd. In the binary product of m and θ , only the digits immediately to the left and to the right of the binary point are needed to determine if the product is even or odd; that is, if the product $m_k 2^k \theta$ is of the form ---0.1--- or ---1.0--- then $\langle m_k 2^k \theta \rangle$ is an odd integer and $\exp j\pi \langle m_k 2^k \theta \rangle = -1$. If $m_k 2^k \theta$ is of the form ---0.0--- or ---1.1--- then $\langle m_k 2^k \theta \rangle$ is even and $\exp j\pi \langle m_k 2^k \theta \rangle = +1$. Since $m_k 2^k$ in binary always contains only 1 ONE in the k th position, it simply serves to shift the binary point of θ to the right by k places. Then if $m_k = 1$, the bits around the binary point can be

considered as θ_{k-1} and θ_k . (Since θ is a binary fraction, the bit θ_{-1} for $k=0$ is the integer portion and always $\theta_{-1} = 0$.) Addition of these two bits effectively determines the evenness or oddness of $\langle m_k 2^k \theta \rangle$. Consequently,

$$\exp j\pi \langle m_k 2^k \theta \rangle = \exp j\pi m_k (\theta_{k-1} + \theta_k) \quad (2-32)$$

Then

$$\text{wal}(m, \theta) = \exp j\pi \left[\sum_{k=0}^{M-1} m_k (\theta_{k-1} + \theta_k) \right] \quad (2-33)$$

The value of the expression in Eq. (2-33) does not change if the addition of θ_{k-1} and θ_k is replaced by the modulo-2 sum or exclusive-OR operation. Hence, the following non-recursive definition* of a point on a Walsh function in exponential form is derived as

$$\text{wal}(m, \theta) = \exp j\pi \left[\sum_{k=0}^{M-1} m_k (\theta_{k-1} \oplus \theta_k) \right] \quad (2-34)$$

If the exclusive-OR operation is performed between each pair of adjacent bits in binary θ , that is, each pair $\theta_{k-1} \oplus \theta_k$, the binary representation is changed to a Gray code. Let the Gray code bits be γ_k , where

$$\gamma_k = \theta_{k-1} \oplus \theta_k \quad (2-35)$$

Since the exponential in Eq. (2-35) can take only the values +1 or -1 and since the binary bits can be replaced by a Gray code bit, the previous definition can be modified to

* A summary of Walsh function definitions used in this thesis is given in Appendix A.

$$\text{wal}(m, \theta) = (-1)^{\sum_{k=0}^{M-1} m_k \gamma_k} \quad (2-36)$$

$$= \prod_{k=0}^{M-1} (-1)^{m_k \gamma_k}$$

It can be seen that the above equation is similar in form to Eq. (2-22). However, whereas in Eq. (2-22), the order of the Walsh function was expressed in Gray code bits, the order is now expressed in binary; whereas the position bits were expressed in binary, they are now expressed in Gray code. Consequently, for a $2^M \times 2^M$ Walsh matrix, Eqs. (2-22) and (2-36) may be used to show what was stated but not proved by Henderson [5], that the Walsh matrix is symmetrical.

An equally important development of Eq. (2-36) is that combinations of a Gray code count, which is a unit-distance code, rather than outputs of a binary counter, as in Fig. 2-2, can be used to generate a Walsh function. The functions generated in this manner are free of hazards. This characteristic of the Walsh function definition of Eq. (2-36) will become more apparent in the following description of the design of a hazard-free Walsh function generator [13].

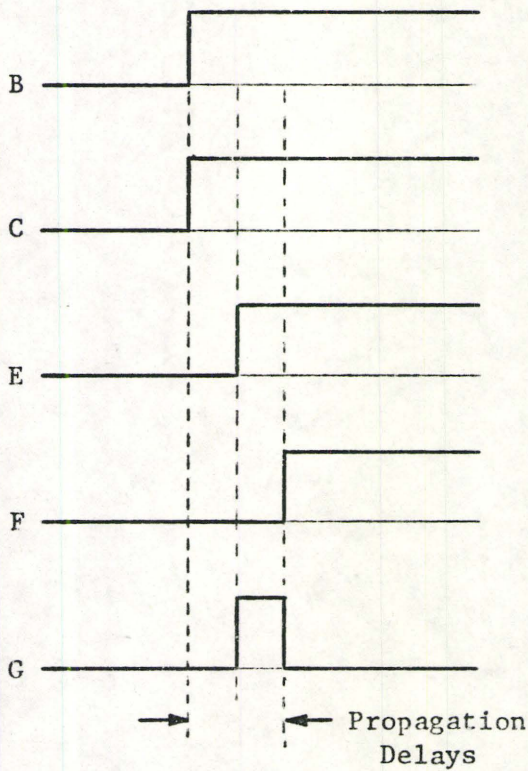
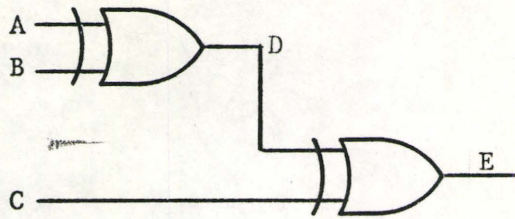
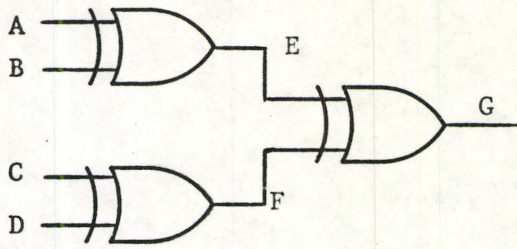
2.8 A Hazard-free Walsh Function Generator

The Walsh function generator of Fig. 2-2 was found to contain undesired spikes due to small differences in propagation times of two or more simultaneous logic transitions through its combinational logic gates. Other Walsh function generators [4,14,15] that were investigated were also found to be susceptible to hazards, while a different design [16], which uses differentiation, was considered to be unsuitable

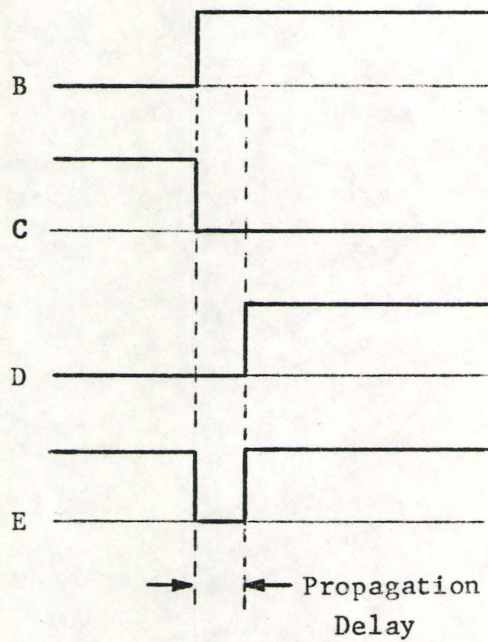
because of its susceptibility to noise.

Hazards in combinational irredundant circuits are particularly significant if memory elements (e.g., flip-flops) are to follow the circuit, so that a hazard could set a flip-flop into an incorrect state. One technique for eliminating hazards is to introduce redundancies into the combinational circuits [12]. Such a technique, however, does not lend itself readily to most Walsh function generator designs in that the complexity of the gating circuit requirements becomes excessive. Alternative techniques are either to strobe the output or to custom-build compensating delay networks, but this again is wasteful. The design presented here uses the unit-distance property of the Gray code to avoid hazards. It is simple to implement, can be programmed, and generates the Walsh functions in order of sequency.

Most Walsh function generators [4,14,15,17 and Fig. 2-2] use the outputs of a binary counter in a form of exclusive-OR combinatorial system to synthesize the required functions. Fig. 2-3 shows two exclusive-OR formations commonly used in these systems that display propensity to hazards. If there are simultaneous changes on the inputs shown in Fig. 2-3(a), and if the input exclusive-OR gates have unequal propagation delays, then the output G has an undesired pulse. (It is assumed that gating of an exclusive-OR module cannot produce a hazard state within itself. A check on a number of IC gates showed this to be a justifiable assumption.) Similarly, Fig. 2-3(b) shows an unwanted ZERO-going pulse due to propagation delay of signal D, whereas there is no delay in input C. If the changes on the input lines were not



(a)



(b)

Fig. 2-3 Sources of Hazards in Exclusive-OR Systems

simultaneous, hazards would be even more likely. In both cases shown in Fig. 2-3, it can be seen that if only one input at a time were allowed to change, only one transition would propagate through the system and no extra pulses could occur.

The Walsh function definition of Eq. (2-36) indicates that any point on $wal(m, \theta)$ may be evaluated using a parity check for an even number of ONE's in the Gray code number for the position θ that have been enabled by the binary bits of m . From this definition, a coding algorithm comparable to Table 2-2 can be devised (see Table 2-3). Direct implementation of the algorithm of Table 2-3 is a Walsh function generator design (shown in Fig. 2-4) in which outputs of a Gray code counter, rather than outputs of a binary counter, are enabled by AND gates that are controlled by bits m_k in the binary code for m to pass to a parity check, which consists of exclusive-OR configurations of the type shown in Fig. 2-3. Due to the unit-distance property of a Gray code, only one bit of the code changes with each count and only one transition at a time can propagate through the parity check system, resulting in hazard-free operation. Note that the most-significant bit (msb) of the Gray code is enabled by the least significant bit (lsb) of the binary code; the lsb of the Gray code is enabled by the msb of the binary code.

A more graphical visualization of the hazard-free characteristic of using a combination of Gray code bits can be made by recalling that Eq. (2-36) was derived from a product of members of the set $\{wal(2^k, \theta)\}$,

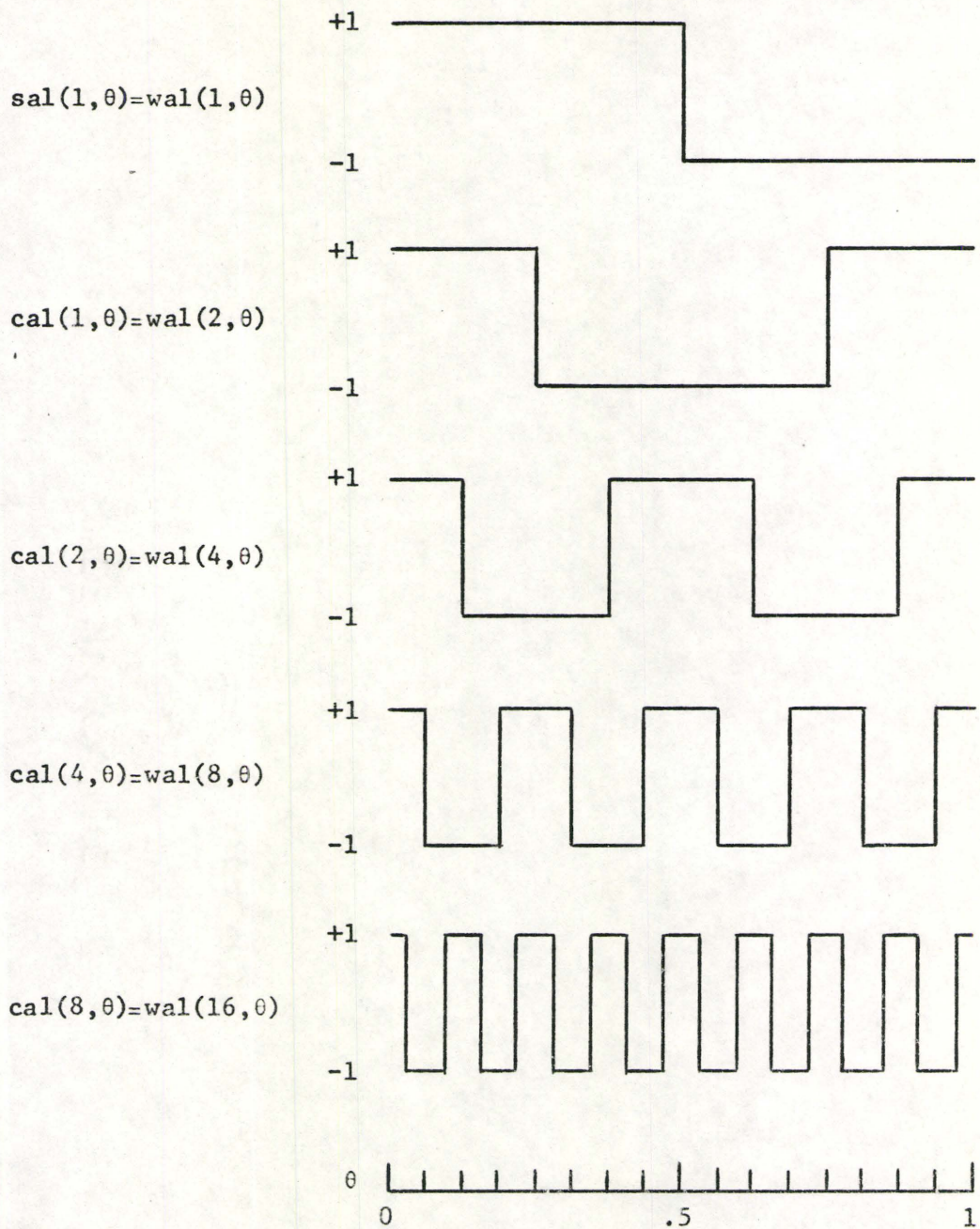


Fig. 2-5 Set of Walsh Functions $\{\text{wal}(2^k, \theta)\}$

$2^M \theta_y$	sampled $g_3 \equiv \text{wal}(1, \theta)$	sampled $g_2 \equiv \text{wal}(2, \theta)$	sampled $g_1 \equiv \text{wal}(4, \theta)$	sampled $g_0 \equiv \text{wal}(8, \theta)$
0	0	0	0	0
1	0	0	0	1
2	0	0	1	1
3	0	0	1	0
4	0	1	1	0
5	0	1	1	1
6	0	1	0	1
7	0	1	0	0
8	1	1	0	0
9	1	1	0	1
10	1	1	1	1
11	1	1	1	0
12	1	0	1	0
13	1	0	1	1
14	1	0	0	1
15	1	0	0	0

Table 2-4 Coded Samples of $\{\text{wal}(2^k, \theta)\}$ which Form a Gray Code.

$\theta=0$ and $\theta=.5$. The remainder of the set comprises the even functions $\text{cal}(2^{k-1}, \theta)$. Since this latter set consists of evenly-symmetric square waves having 2^{k-1} segments within the interval $0 \leq \theta < 1$, $\text{cal}(2^{k-1}, \theta)$ has transitions at $\theta_m = [(1+2m)/2^{k+1}]$. If the transitions for any other cal function within the above set, say $\text{cal}(2^{x-1}, \theta)$, are at $\theta_y = [(1+2y)/2^{x+1}]$, it is shown below that the transitions of the latter do not coincide with those of the former; that is,

$$\frac{1+2m}{2^{k+1}} \neq \frac{1+2y}{2^{x+1}} \quad (2-37)$$

where $k \neq x$ and k, m, x , and y are positive integers. Eq. (2-37) can be rewritten

$$\left(\frac{1+2m}{1+2y} \right) \left(\frac{2^{k+1}}{2^{x+1}} \right) \neq 1 \quad (2-38)$$

Let

$$\frac{2^{k+1}}{2^{x+1}} = 2^z \quad (2-39)$$

where $z = k-x$. Since $k \neq x$, $z \neq 0$. Both $(1+2m)$ and $(1+2y)$ are odd integers, and since 2^z is always an even integer with no odd factors,

$$\frac{1+2m}{1+2y} \neq \frac{1}{2^z} \quad (2-40)$$

Hence each cal function in the set has a unique set of level transition positions. Furthermore, these positions do not match those of $sal(1, \theta)$ since $[(1+2m)/2^{k+1}]$ cannot equal 0 or 0.5. No simultaneous state changes occur among different members of $\{wal(2^k, \theta)\}$. In Fig. 2-4 then, the outputs of the Gray code counter, which constitute the coded set of $\{wal(2^k, \theta)\}$, allow at most one transition at each clock pulse to pass through the AND system and the parity check.

The system of Fig. 2-4 was implemented using TTL integrated circuits. Attention needs to be paid to the Gray code counter since some designs are not hazard-free. For example, a system comprising a binary counter feeding a binary-to-Gray code converter would likely not provide hazard-free operation. A particularly elegant design is of the iterative type [18] in which the clock is gated to only one of the flip-flops at each count. The design from [18] that was modified for use in the Walsh Function generator is discussed in more detail in section 2.10. The AND gates used in the generator are type SN7408 and the parity check is SN74180. At the highest available clock frequency, 10 MHz, the Walsh waves were stable, were free of hazards, and had clean rising and falling edges. The selection of the Walsh

function $wal(m,\theta)$ to be generated is made simply by providing a binary-coded input for m .

2.9 An Array Walsh Function Generator

Each of the Walsh function generators previously described produces a single, programmed function. In some applications, such as spectral analysis or multiplexing, several Walsh functions may be required simultaneously. Previous Walsh function array generators [4,19] display hazards. A simple extension of the design method of Fig. 2-4 yields a parallel array of Walsh functions that are free of hazards (see Fig. 2-6). Each of the Walsh functions is hardware-programmed as a binary combination of outputs of a Gray code counter. For any given function $wal(m,\theta)$, one combines, using exclusive-OR gates, those functions of the set $\{wal(m_k 2^k, \theta)\}$ for which $m_k = 1$. Since the output of an exclusive-OR system is ONE if there are an odd number of ONE's at the input, each output of an exclusive-OR network is complemented by an inverter to produce a binary Walsh function in which +1 is coded as ONE and -1 is coded as ZERO.

Gating for certain Walsh functions may be simplified by using the outputs of exclusive-OR gates that are already engaged in forming other Walsh functions. For example, $wal(7,\theta)$ is the complement of $\overline{wal(1,\theta) \oplus wal(2,\theta) \oplus wal(4,\theta)}$, as shown in Fig. 2-6. However, $\overline{wal(1,\theta) \oplus wal(2,\theta)}$ was used already in forming $wal(3,\theta)$. Thus, one can use $\overline{wal(3,\theta) \oplus wal(4,\theta)}$ to form $wal(7,\theta)$. In this manner, one needs at most, one additional exclusive-OR gate for each new Walsh function. In this simplification procedure, care must be taken that

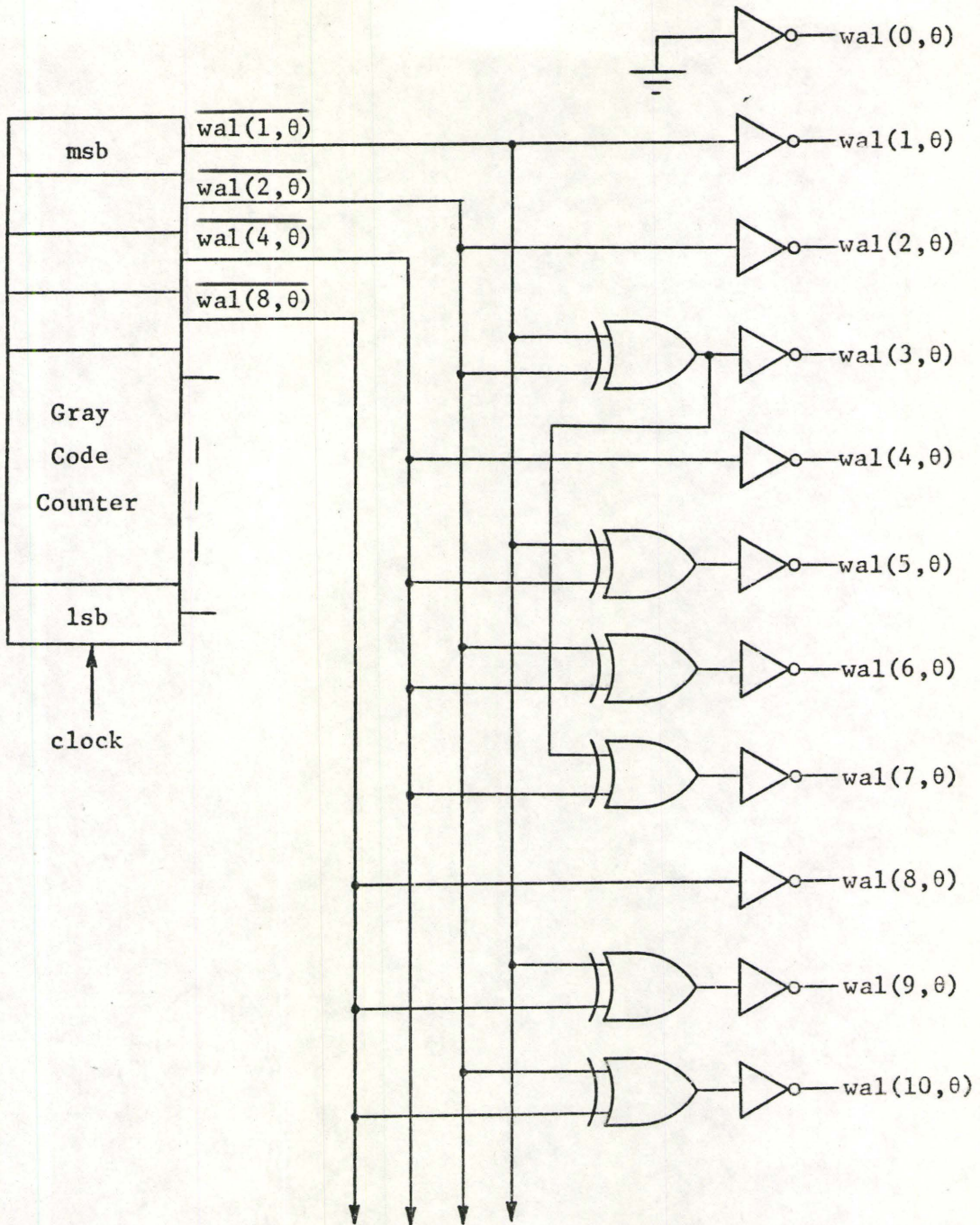


Fig. 2-6 A Walsh Function Array Generator

redundant functions are not used in generating a new function.

According to Eq. (2-26), only a binary combination of $\{\text{wal}(2^k, \theta)\}$ will give hazard-free operation. To illustrate, let us generate $\text{wal}(5, \theta)$. With reference to Fig. 2-6 and Eq. (2-26), $\text{wal}(5, \theta)$ must be formed using $\text{wal}(1, \theta)$ and $\text{wal}(4, \theta)$. $\text{Wal}(3, \theta)$ and $\text{wal}(2, \theta)$ will not produce $\text{wal}(5, \theta)$ since $\text{wal}(3, \theta)$ already contains the elements $\text{wal}(1, \theta)$ and $\text{wal}(2, \theta)$. $\text{Wal}(2, \theta)$ can not be used again with this combination. Not only may hazards occur but according to Eq. (2-9), the wrong Walsh function will result.

2.10 A Hazard-free Gray Code Counter

Both the programmable Walsh function generator of Fig. 2-4 and the array generator of Fig. 2-6 are stipulated to be hazard-free. Although it has been established that a combination of Gray code bits accomplishes the hazard-free requirement of the generators, such discussion is useless unless the outputs of the Gray code counter portion of each generator are themselves free of irregularities.

A Gray code counter that is a modified version of a design by Majithia [18] can have only one of its outputs change with any clock pulse, since the clock input of only one of the J-K flip-flops that yield a Gray code bit is enabled at any step. Hence, this counter, which is of the iterative type shown in Fig. 2-7, cannot be the source of any hazard states.

Majithia's design [18] uses an auxiliary flip-flop A (see Fig. 2-7) to complement the lsb of the Gray code, g_0 , at every alternate

count. The g_0 flip-flop in the counter is to be complemented when A is in state 1 and a count pulse is presented. From the 4-bit Gray code count sequence shown in Table 2-5 it is seen that the A flip-flop must be initially preset to ONE. Hence, A must be a presettable flip-flop. Simple T-type or J-K flip-flops suffice to generate the Gray code bits.

Decimal Count	Gray Code				A
	g_3	g_2	g_1	g_0	
0	0	0	0	0	1
1	0	0	0	1	0
2	0	0	1	1	1
3	0	0	1	0	0
4	0	1	1	0	1
5	0	1	1	1	0
6	0	1	0	1	1
7	0	1	0	0	0
8	1	1	0	0	1
9	1	1	0	1	0
10	1	1	1	1	1
11	1	1	1	0	0
12	1	0	1	0	1
13	1	0	1	1	0
14	1	0	0	1	1
15	1	0	0	0	0

0	0	0	0	0	1

Table 2-5 4-bit Gray Code Count Sequence

The flip-flop g_1 is to be complemented when g_0 is at 1, A at zero, and a clock pulse (c.p.) arrives. Similarly, g_2 is to be complemented when g_1 is at 1, all lesser significant stages are at 0, and a c.p. is present. If this argument is extended to the k th flip-flop, one obtains the following conditions:

Use a c.p. to complement g_k if

$$g_{k-1} \bar{g}_{k-2} \dots \bar{g}_0 \bar{A} = 1 \quad (2-40)$$

for $k \neq 0$. If $k = 0$, complement for $A = 1$.

Examination of the above conditions for complementing the k th flip-flop and of Table 2-6 indicates that at the end of one Gray code count cycle, the msb of the Gray code is ONE and all other flip-flops are in state 0. The next count pulse would leave the msb of the Gray code as a ONE and merely complement flip-flop A. This, in effect, initiates a reverse Gray code count. Consequently, Majithia's design has been slightly modified in Fig. 2-7 to use the count pulse that would normally complement the $(k+1)$ flip-flop to reset the k th flip-flop. Fig. 2-7 shows the entire counter being reset by this condition, but this is done to simplify the incorporation of an external reset. One necessary condition for the count pulse arises due to the modification. Since changes in the g outputs may occur at rising or falling edges of the count pulse, this pulse must be kept as short as possible.

It can be seen that the design of the counter prevents hazard states in the g outputs. From the complement conditions of Eq. (2-40), only one g flip-flop may be complemented at any count. The final count in a cycle resets only the msb of the Gray code. Consequently, this design of a Gray code counter in conjunction with the combinational logic of Fig. 2-4 or Fig. 2-6 is used for generation of hazard-free binary Walsh functions.

2.11 Conclusion

The definitions of the Walsh functions have been developed from Walsh's original recursive equations to several forms of non-recursive expressions. With the variety of relationships available, one must take care before selecting which to use in specifying the ordering of the Walsh functions [7], in defining the period ($[-\frac{1}{2}, \frac{1}{2})$, $[0,1)$, etc.), or in defining the position (binary fraction over $0 \leq \theta < 1$, or integral interval number $y = \theta 2^M$). Properties of the various definitions should be considered before use. For instance, the definition [Eq. (2-36)] in which the Gray code bits for the position and the binary bits for the order are used has been utilized to design a Walsh function generator that is free of hazards. On the other hand, a definition that is similar [Eq. (2-21)] but uses binary bits for the position and a Gray code for the order does not lead to hazard-free operation. For convenience, all the equations that are mentioned in this chapter with regard to sequency-ordered Walsh functions are summarized in Appendix B.

Software programming for evaluating Walsh functions is simplified using the coding algorithms described in this chapter.

The orthogonal property of the Walsh functions, which are also conveniently two-valued, makes this set of functions particularly attractive in the design of a digital instrument for spectral analysis of signals. The functions can be used to represent a waveform in a Walsh series in much the same way as sinusoidal waves are used to form a Fourier series. Walsh series analysis is discussed in greater detail

in the following chapter. Based on this analysis, a digital instrument that determines the coefficients of the Walsh series of a waveform in real-time has been designed. The hazard-free Walsh function generators of Fig. 2-4 and Fig. 2-6 play an integral role in the development of such an instrument.

CHAPTER 3

WALSH SERIES ANALYSIS

3.0 Introduction

Characterization of signals and systems by the frequency domain has been well established. The concepts of frequency analysis and spectrum can be more generally perceived by observing other complete orthogonal sets. One set of functions that is well-suited for this purpose is the set of Walsh functions. Using this set of functions for the description of time-dependent functions in the frequency domain is as meaningful as the description of the same signal in the frequency domain since both series expansions converge to the signal in the least mean squares fit [1]. This chapter concerns itself initially with signal analysis by means of expansion into a Walsh series. Emphasis is then placed on specifications for a digital special-purpose instrument that will determine the Walsh series coefficients of a function in real-time using samples of the input waveform. The basic equations of the Walsh series coefficients are modified into operating equations that can be handled by the digital instrument. Instrumentation requirements to process each portion of the operating equation are then discussed.

3.1 The Walsh Series

A function $f(\theta)$ which is of period 1 and Lebesgue integrable on $(0,1)$ may be expanded into a Walsh series [2], viz.

$$f(\theta) = \sum_{m=0}^{\infty} W_m \text{wal}(m, \theta) \quad (3-1)$$

$$= A_0 + \sum_{s=1}^{\infty} A_s \text{cal}(s, \theta) + \sum_{s=1}^{\infty} B_s \text{sals}(s, \theta)$$

where θ is the normalized time and where A_0 , A_s , B_s and W_s are the coefficients of the terms of the series. The set of Walsh series coefficients forms the Walsh spectrum [1-13]. According to Theorem II of Walsh [1], if $f(\theta)$ is continuous in the interval $(0,1)$, the series expressed in Eq. (3-1) converges uniformly to the value $f(\theta)$ if the terms are grouped so that each group contains all the 2^{M-1} terms of a set $\{\text{wal}(m, \theta)\}$, where M is the number of binary bits in m . Walsh's Theorem II can be extended to include discontinuous functions $f(\theta)$ if $f(\theta)$ is integrable in the sense of Lebesgue.

The objective now is to derive relations which will yield the Walsh series coefficients of an unknown signal. According to the standard procedure for determining the equation for the coefficients of an orthogonal series [14], both sides of the series expansion of Eq. (3-1) are multiplied by $\text{wal}(k, \theta)$ and then integrated over one period T . Thus,

$$\int_0^T f(\theta) \text{wal}(k, \theta) d\theta = \int_0^T \sum_{m=0}^{\infty} W_m \text{wal}(m, \theta) \text{wal}(k, \theta) d\theta \quad (3-2)$$

Since Walsh functions form a mutually orthogonal set [see Eq. (2-10)], all terms on the right side of Eq. (3-2) will integrate to zero except for the product of the Walsh functions for which $k = m$. Then

$$\int_0^T \sum_{m=0}^{\infty} W_m \text{wal}(m, \theta) \text{wal}(k, \theta) d\theta = \int_0^T W_k \text{wal}^2(k, \theta) d\theta = W_k T \quad (3-3)$$

therefore

$$W_k = \frac{1}{T} \int_0^T f(\theta) \text{wal}(k, \theta) d\theta \quad (3-4)$$

Similarly, for the average value A_0 and for the coefficients of the even and odd components, A_s and B_s , respectively,

$$A_0 = \frac{1}{T} \int_0^T f(\theta) d\theta \quad (3-5)$$

$$A_s = \frac{1}{T} \int_0^T f(\theta) \text{cal}(s, \theta) d\theta$$

$$B_s = \frac{1}{T} \int_0^T f(\theta) \text{sal}(s, \theta) d\theta$$

The amplitude spectrum of the ordinary Fourier transform is defined as the square root of the power spectrum. This definition is based on the relation

$$\begin{aligned} a_f \cos 2\pi f\theta + b_f \sin 2\pi f\theta &= (a_f^2 + b_f^2)^{\frac{1}{2}} \cos[2\pi f\theta - \arctan(b_f/a_f)] \\ &= c_f \cos[2\pi f\theta - \arctan(b_f/a_f)] \quad (3-6) \end{aligned}$$

Such a relationship does not hold for the Walsh spectrum [15].

Consequently, there is no simple relationship between W_m , A_s and B_s .

A_s and B_s are commonly interpreted individually as Walsh amplitude spectra of the symmetric and the skew symmetric parts of $f(\theta)$.

3.2 Concepts of a Digital Walsh Spectrum Analyzer Design

A special-purpose instrument is to be designed that meets the following general specifications:

- a) the instrument should yield the Walsh spectral coefficients of a waveform at audio frequencies and lower,
- b) the process should be carried out in real-time,
- c) the instrument should use as few cycles of the input (if it is periodic) as possible to complete the measurement, and
- d) the system should have as little memory as possible.

Primarily, there is a choice between designing a digital or an analog instrument. A digital design was selected since digital logic is obviously compatible with Walsh functions, which have only two states, and can be coded easily using binary logic. A digital instrument adapts itself more readily to low frequency analysis (say under 1 Hz) than does an analog device. Arithmetic operations, storage, and numerical readouts are facilitated using digital hardware. At this time cost considerations generally give digital components an additional advantage over analog components.

Secondly, the spectral analyzer design can employ the straightforward approach of sampling the input waveform and processing the

samples using the coefficients equation of Eq. (3-5), or one can implement the Fast Walsh Transform (FWT) [16,17] which is comparable to the FFT (Fast Fourier Transform). The direct approach was selected since it is felt to have certain advantages over a Fast Walsh Transformer. A machine that processes each sample of a waveform before the next sample arrives and which calculates in parallel as many Walsh coefficients as desired can be made more versatile and can operate faster than a Fast Walsh Transform device.

The digital Walsh Spectrum Analyzer that is described in detail in Chapter 4 has various modes of operation:

- 1) for periodic waveforms; there is automatic period detection using successive positive-going zero crossings of the input. Calculations are time-locked to the waveform period, and measurement is complete at the end of the second cycle of the input wave.
- 2) for periodic waveforms with more than two zero crossings per cycle; there is automatic period detection using successive positive-going crossings of an arbitrarily set reference voltage. Again the processes are time-locked to the signal and there is two-cycle operation.
- 3) for any waveform; a second input control makes provision for a square wave or a set of marker pulses to be used to start the calculations and to set the period of measurement arbitrarily. This period is automatically measured within the instrument

and calculations are made similar to modes 1 and 2.

Several additional modes of operation could be built into a Walsh spectral analyzer as described in 4) - 6) below. However, the minor changes that would be required in the control system to accommodate them have not been included in the design of Chapter 4:

- 4) the period of measurement could be selected arbitrarily by presetting the period detector. This operation would enable single cycle measurement of the coefficients.
- 5) a pre-selected number of samples (say 2^M) could be used for the measurement. The period of the signal to be analyzed is determined by the sample size and the sampling interval. Again, single cycle operation is enabled.
- 6) a set of digital samples could be analyzed by bypassing the A/D converter that would normally be used to sample the analog input:

A Walsh spectral analyzer that can operate in any of the above modes is a more versatile machine than a Fast Walsh Transformer. Whereas an FWT requires a predetermined number of samples to be stored before any processing is done on the samples, the Walsh Spectral Analyzer (hereafter denoted WSA) can process each of an indeterminate number of samples before the next sample is taken. Thus, the WSA completes processing by the time the FWT begins its sample processing. If desired, the WSA can operate in a similar way to the IWT by preselecting the

number of samples (see mode 5) but again calculations are complete immediately after the arrival of the last sample. Consequently, the WSA is closer to a real-time instrument than the FWT.

It is not generally possible for the FWT to operate in modes 1) to 4). The FWT would be difficult to synchronize with a periodic wave or the time window of an arbitrarily set period. The only storage requirement of the WSA is the final readout storage for each of the Walsh series coefficients, whereas the FWT must provide storage for a complete set of data samples.

3.3 Operating Equation for Walsh Spectral Analyzer

The Walsh Spectral Analyzer that has been implemented is a digital instrument, so that data from a signal is in the form of quantized samples. Since discrete samples are used to describe $f(\theta)$, integration in Eq. (3-5) is replaced by summation. If there are H samples of $f(\theta)$ during the period T , where T is normalized to 1, then

$$d\theta = \frac{1}{H} \quad (3-7)$$

and the equations in Eq. (3-5) can be rewritten as

$$A_0 = \frac{1}{H} \sum_{h=1}^H f(\theta)_h \quad (3-8)$$

$$A_s = \frac{1}{H} \sum_{h=1}^H f(\theta)_h \text{ cal}(s, \theta)_h$$

$$B_s = \frac{1}{H} \sum_{h=1}^H f(\theta)_h \text{ sal}(s, \theta)_h$$

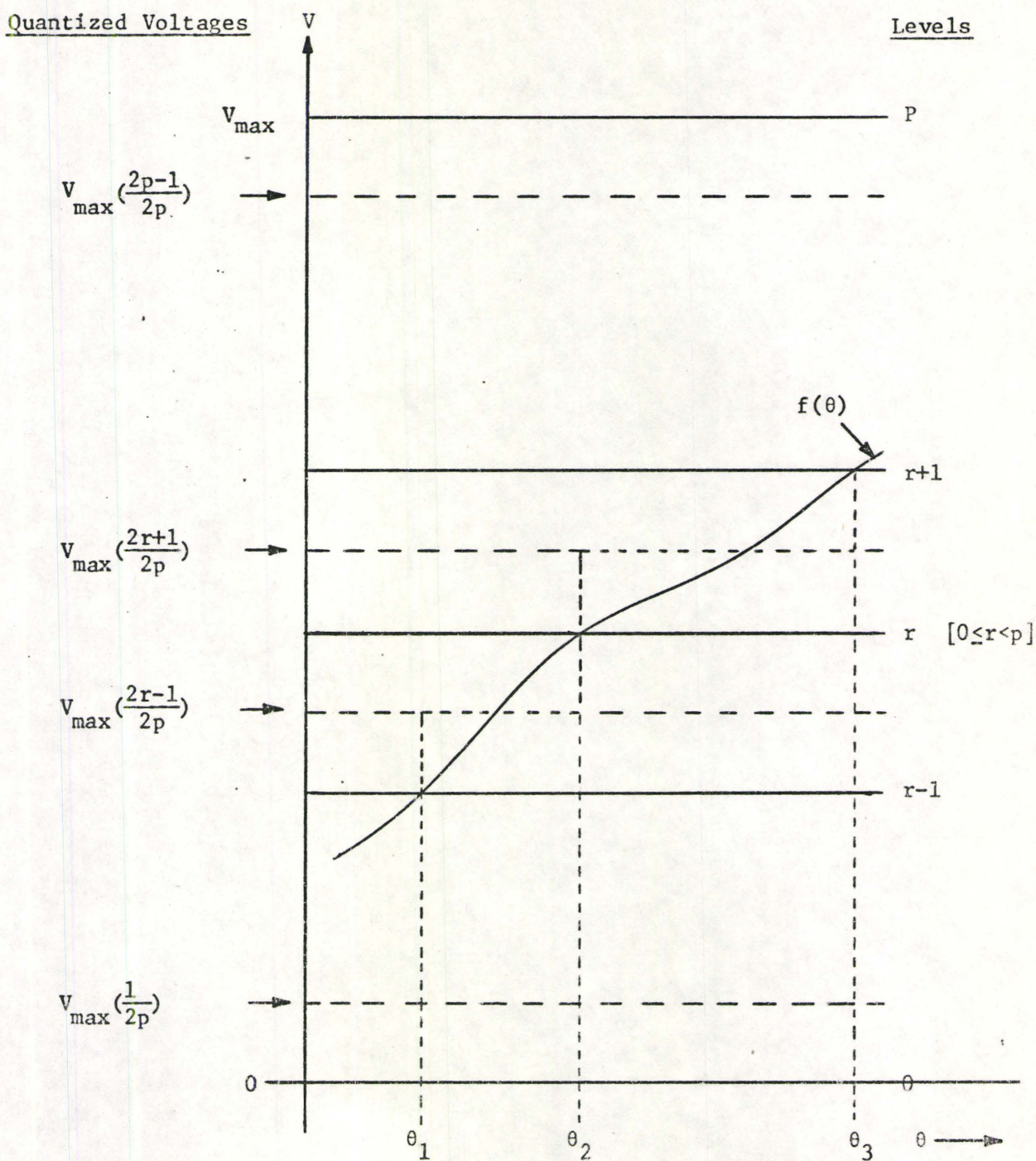


Fig. 3-1 Quantization

where $f(\theta)_h$, $\text{cal}(s,\theta)_h$ and $\text{sal}(s,\theta)_h$ are the values of the respective functions at the time of the h th sample.

The samples of the continuous wave $f(\theta)$ are processed by a binary-coded analog-to-digital (A/D) converter. Quantization of the waveform during the coding process means that all of the samples within the range of voltages specified for any given level are represented by the same value. For example, in Fig. 3-1, if the A/D converter has a range of 0 to V_{\max} volts and has p quantization levels, then the signal $f(\theta)$ is considered to have the quantized value $[V_{\max}(2r+1)/2p]$ volts when $f(\theta)$ lies between the levels r and $r+1$. Fig. 3-1 shows $f(\theta)$ lying in this range between the normalized times θ_2 and θ_3 .

However, since the A/D converter yields only a binary-coded signal, each sample of the wave $f(\theta)_h$, which is taken between times θ_2 and θ_3 is represented by the binary-coded value of $r + \frac{1}{2}$. Let this binary number be designated Q_h . To change the coded value back into a voltage value, a conversion factor (C.F.) is introduced.

$$f(\theta)_h = \frac{V_{\max}(2r+1)}{2p} = (\text{C.F.})Q_h \quad (3-9)$$

where

$$Q_h = r + \frac{1}{2} = \frac{2r+1}{2} \quad (3-10)$$

Hence

$$(\text{C.F.}) = \frac{V_{\max}}{p} \quad (3-11)$$

and

$$f(\theta)_h = \frac{V_{\max}}{p} Q_h \quad (3-12)$$

The A/D converter used can accept waveforms in the range 0 to +10 volts. An AC input signal is rectified before it is sampled by the A/D converter. In this way, samples with the same absolute value are given the same coding, and an additional signal is used to indicate the sign of $f(\theta)$. A logic ONE level is used to represent the positive portion of the signal and a logic ZERO level is used to indicate that $f(\theta)$ is negative. Now $f(\theta)_h$ can be rewritten as

$$f(\theta)_h = \frac{V_{\max}}{p} |Q_h| \text{sgn } f(\theta)_h \quad (3-13)$$

Consequently, the operating equations that can be handled by a digital Walsh Spectral Analyzer to perform Eq. (3-5) have the final form

$$A_0 = \frac{V_{\max}}{pH} \sum_{h=1}^H |Q_h| \text{sgn } f(\theta)_h \quad (3-14)$$

$$A_s = \frac{V_{\max}}{pH} \sum_{h=1}^H |Q_h| \text{sgn } f(\theta)_h \text{ cal}(s, \theta)_h$$

$$B_s = \frac{V_{\max}}{pH} \sum_{h=1}^H |Q_h| \text{sgn } f(\theta)_h \text{ sal}(s, \theta)_h$$

3.4 Signal Processing in the Walsh Spectral Analyzer

The stages of signal processing in the WSA are determined by the operating equations Eq. (3-14). With reference to the example in Fig. 3-2, which shows a signal [Fig. 3-2(a)] that is to be analyzed according to mode 1, the first step is to rectify $f(\theta)$ [Fig. 3-2(b)] and provide

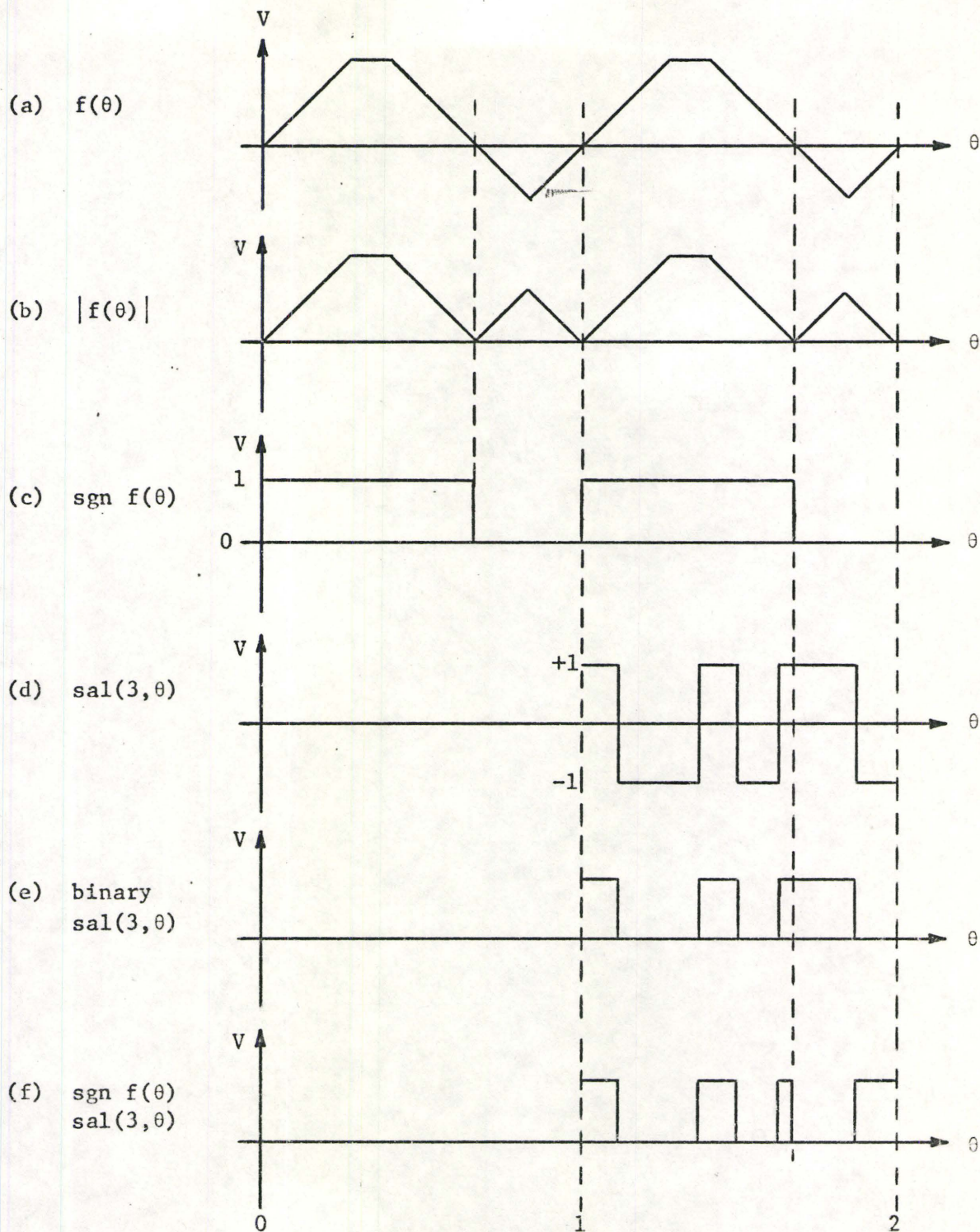


Fig. 3-2 Example of Functions used to Calculate B_3

a logic signal that indicates the sign of the input [Fig. 3-2(c)]. In mode 1), the first cycle of the periodic wave is used to determine a measure of the time of one period. During the second cycle the Walsh coefficients are calculated. Eq. (3-14) requires that the input wave be multiplied by a Walsh function corresponding to the coefficient to be evaluated and the function must be correctly timed and have the same period as the analyzed signal. Consequently, Fig. 3-2(d) shows a Walsh function [in this case, $\text{sal}(3,\theta)$] generated during the second cycle of the input. The binary equivalent of $\text{sal}(3,\theta)$ is shown in Fig. 3-2(e). The summation of samples of $f(\theta)$ according to Eq. (3-14) is best handled by adding or subtracting the binary samples of $|f(\theta)|$, where the addition or subtraction is dependent on the product of the signals $\text{sgn } f(\theta)$ and $\text{sal}(3,\theta)$, as indicated by Fig. 3-2(f). The latter signal enables the Walsh coefficient B_3 to be determined.

The other modes of operation follow the same basic structure of the processes outlined by Fig. 3-2. In mode 2), if the signal has more than two zero-crossings per cycle, a reference level is adjusted positively or negatively to a point where there are only two crossings of the reference level per cycle. The steps of Fig. 3-2 then begin with the first positive-going crossing of the reference level. In mode 3), marker pulses on a control input channel, rather than the analog signal to be processed, initiate the period measurement and analysis.

Preselection of the period of measurement according to modes 4) and 5) enables the operation to begin immediately at a point equivalent

to the beginning of the second cycle shown in Fig. 3-2. Successive time windows of a function could be used to evaluate a time-varying Walsh spectrum by operating in modes 4) and 5). A digital Walsh Spectral Analyzer that is designed to operate in any of the first three modes is discussed in detail in the following chapter.

CHAPTER 4

DESIGN OF A DIGITAL WALSH SPECTRAL ANALYZER

4.0 Introduction

The operating equation (3-14) provides the basis for the design of a digital Walsh Spectral Analyzer. A special-purpose instrument has been designed and constructed to operate in the first three modes of operation as outlined in Chapter 3. A detailed description of each section of this analyzer follows an overall view of the system.

4.1 Complete System

The block diagram corresponding to the complete Walsh Spectral Analyzer is shown in Fig. 4-1. Portions of the operating equation of Eq. (3-14) which relate to the various blocks are indicated on the diagram.

After being interfaced by a high input impedance voltage follower, the analog input is directed along three paths: the first leads to the conversion of the input $f(\theta)$ into a series of quantized, binary-coded samples. The second path is used simply to determine the sign of the input signal. The third path leads to controls which use information concerning the period of the input in order to process the binary-coded samples from the first path. When the switch SW1 of Fig. 4-1 is connected to the mode (3) control, the analog input is led only to the first two paths so that external information must be provided to determine the period of measurement. The input to the mode (3) control

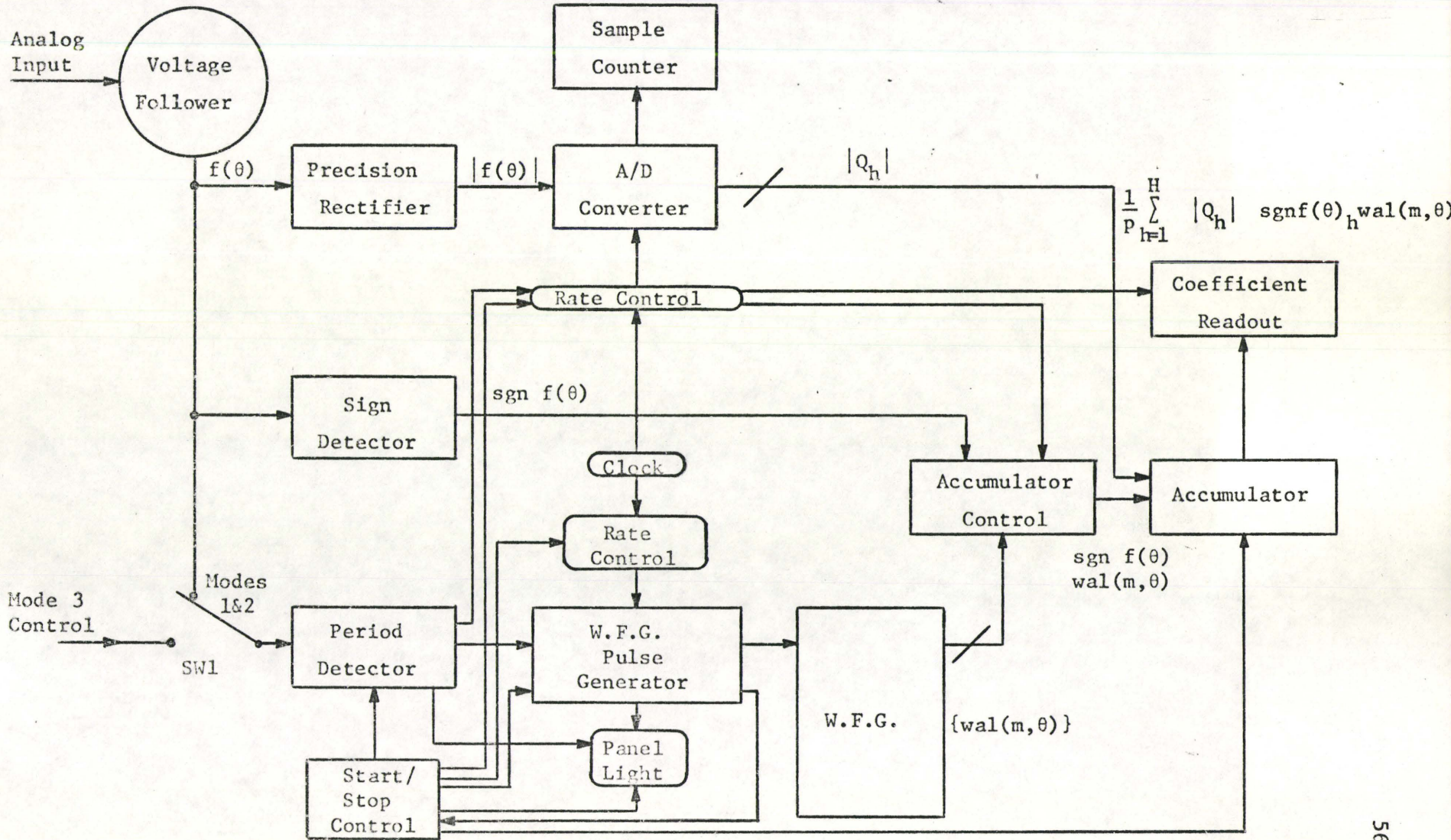


Fig. 4-1 Walsh Spectral Analyzer

should be a sequence of pulses or a rectangular wave with a period equivalent to the desired period of measurement.

The first path contains two major components, a rectifier and an A/D converter. Rectification is positive so that the input to the A/D converter is restricted to the range 0 to +10 volts. The output of the rectifier $|f(\theta)|$ is sampled by the converter. The samples $|Q_n|$ are quantized and given a binary coding. The digits of the coding appear on parallel output leads. Since the first cycle of the input signal or the mode (3) control signal is used only to determine the period of measurement, controls permit the A/D converter to operate only during the second cycle. A counter is used to total the number of samples. Since the input has been rectified, the second path contains a sign detector which provides a binary signal $\text{sgnf}(\theta)$.

Concurrently, in the third path, $f(\theta)$ passes to a period detector, which detects crossings of a reference level either by the analog input or by the mode (3) control input signal. This information is necessary since all system operations are to begin with the first positive-going voltage reference level crossing and Walsh functions are to be generated with a time-base equal to the measurement period. The period detector provides signals that indicate whether the system is in the first or second cycle of operation and whether all calculations are complete. These signals are sent to panel light indicators and to a pulse generator that produces correctly-timed pulses for the Walsh function generator (W.F.G.). The W.F.G. pulse generator transmits pulses that enable the Walsh function generator to produce a parallel array of

functions with the correct time-base during the second cycle of operation, as shown in the example in Fig. 3-2. If the clock system controlling the generator is not operating at a rate sufficient to calculate the measuring period within certain error limits, the system stops and panel lights indicate whether the clock rate should be increased or decreased.

Each Walsh function generator output ties into the following blocks; an accumulator control, an accumulator, and a coefficient readout. Since the analyzer that was constructed was a prototype, facilities were provided to calculate only two Walsh series coefficients at a time out of a possible 64. The two coefficients to be measured are selected before operation by rotary switches. The accumulator control has an output signal $\text{sgnf}(\theta) \text{ wal}(m, \theta)$. This signal determines whether the samples of $|f(\theta)|$ from the A/D converter should be added to or subtracted from the previous total in the accumulator. Each of the accumulators is designed to divide the accumulation of sample values by the number of quantization levels p as required by Eq. (3-14). Thus, the final stage is a bank of counters that count the overflow from each accumulator. Each of these last stages hold a count equivalent to

$$\left(\frac{1}{p}\right) \sum_{h=1}^H |Q_h| \text{sgnf}(\theta)_h \text{ wal}(m, \theta).$$

Numerical indicators can be used to display the counter contents. The final count value differs from Eq. (3-14) by the factor V_{\max}/H . $V_{\max} = 10$, and H is supplied by a separate counter. In using the prototype instrument, it is left to the operator to multiply the coefficient readout by $10/H$. However, the Walsh coefficient equation is sometimes derived (i.e., [1]) without the factor $1/H$. In this case, simple

multiplication by 10 suffices.

H is also used to determine the frequency of the fundamental component of the series. If the sample frequency is f_s , then the time between samples is $1/f_s$. The time for H samples is $H/f_s = T$, and the fundamental frequency or sequency is f_s/H .

In addition to the main blocks of the instrument, some peripheral controls are required. There is a master clock whose frequency can be reduced in decade steps to determine the sample rate of the A/D converter and the W.F.G. pulse generator. Start, stop and clear controls, which regulate several portions of the analyzer, complete the design of the digital Walsh Spectral Analyzer. Detailed descriptions of each section of the instrument follow. Due to continually changing availability of components, reference to commercial devices used in the construction of a prototype instrument are limited to a few specific cases.

4.2 Precision Rectifier

A precision rectifier [2] with negligible distortion in the range D.C. to 5 KHz was built using high slew-rate operational amplifiers (250 V/ μ sec) and stable precision resistors. The rectifier circuit is shown in Fig. 4-2.

When the input V_{IN} to the rectifier is negative, the voltage V_{O1} from the first operational amplifier is essentially zero and the second operational amplifier acts as an inverter with unity gain so that the output is given by

$$V_0 = -V_{IN} \quad (4-1)$$

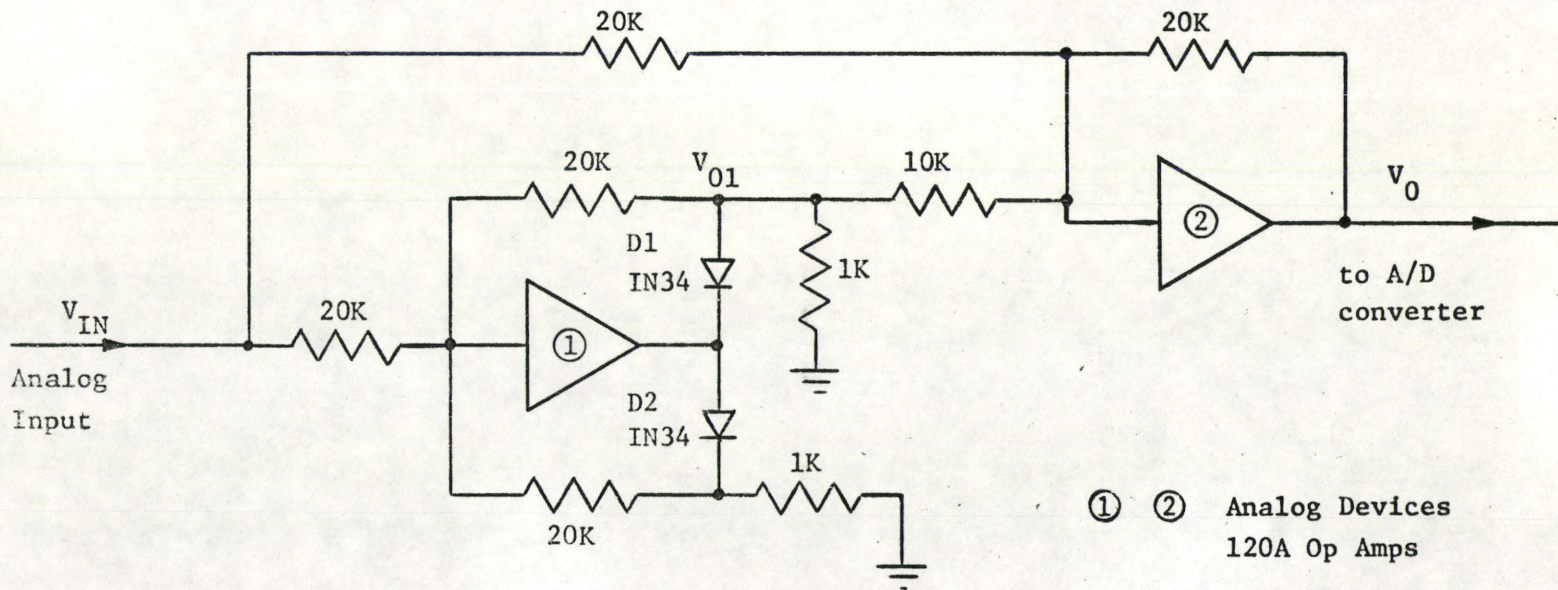


Fig. 4-2 Precision Rectifier

When the input V_{IN} is positive, the diode D1 conducts making $V_{O1} = -V_{IN}$, since the gain of the first inverting amplifier is also unity. The second amplifier now acts as a summing and inverting amplifier with an output given by

$$\begin{aligned} V_0 &= -V_{IN} - 2V_{O1} \\ &= -V_{IN} + 2V_{IN} \end{aligned} \quad (4-2)$$

The precision resistors were matched to maintain accurate ratios on the summing inputs of the amplifiers. Measurements of the rectifier that was constructed indicated that there was a maximum error of 6.8 mv. on the output for an input in the range ± 25 mv. to ± 10 V. Propagation delay through the rectifier is less than 1 μ sec.

4.3 A/D Converter

After rectification, the waveform being analyzed is sampled and quantized. The samples are given a binary coding, with each bit of the code appearing on a separate lead. An 8-bit successive approximation A/D converter with a built-in reference supply is used [3]. A diagram of the A/D converter is shown in Fig. 4-3. 8-bit quantization, in which case the quantization steps are approximately 39 mv. wide, yields an amplitude error which is a tolerable .4%.

The sample accumulation system which is described later requires the bits in the coding from the A/D converter to be processed serially in time. The A/D start pulse ripples through a time delay network, and the delayed pulses can be tapped to enable successively each bit of the coding, beginning with the m.s.b.. The outputs P_n of the enabling network

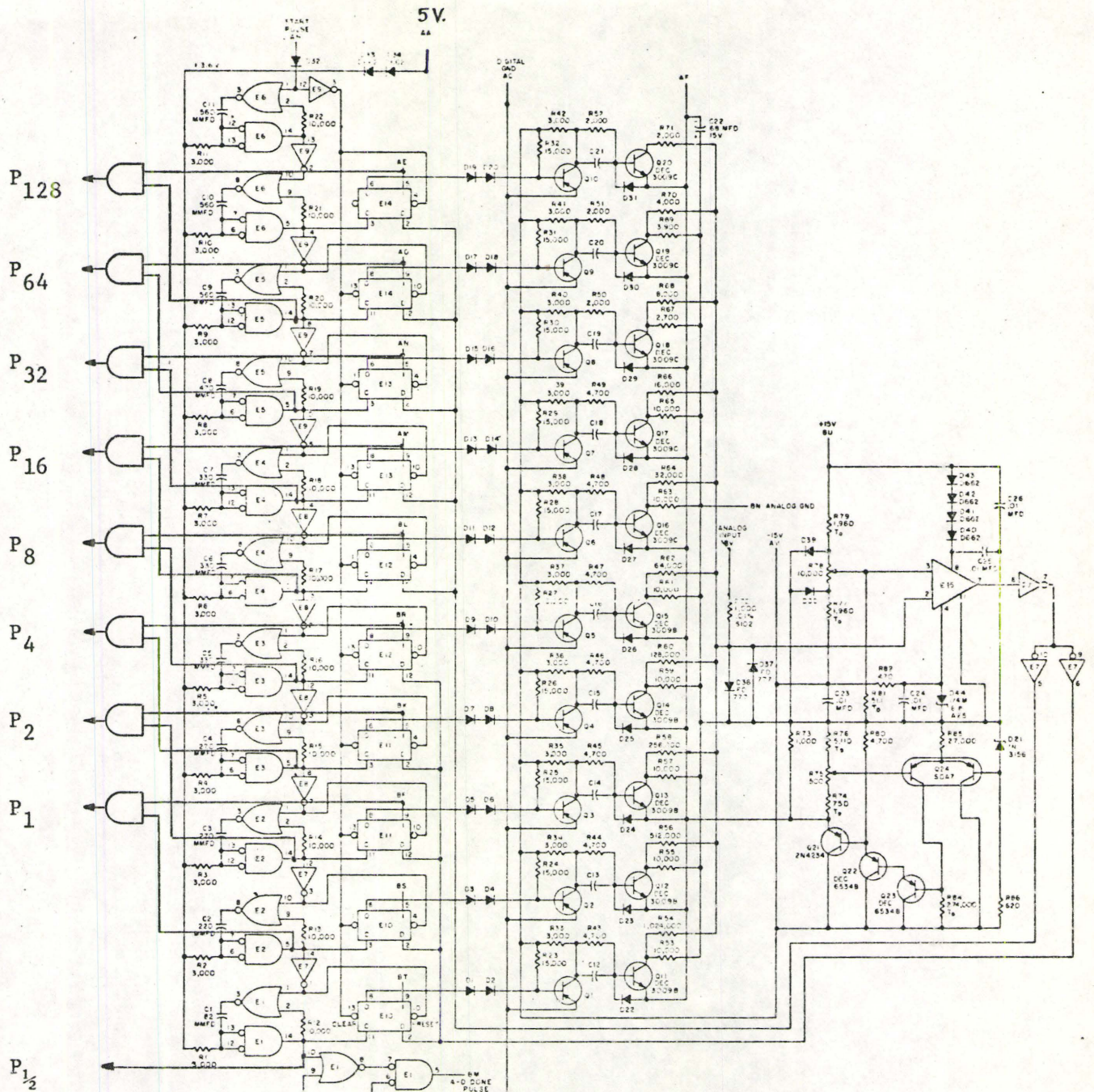


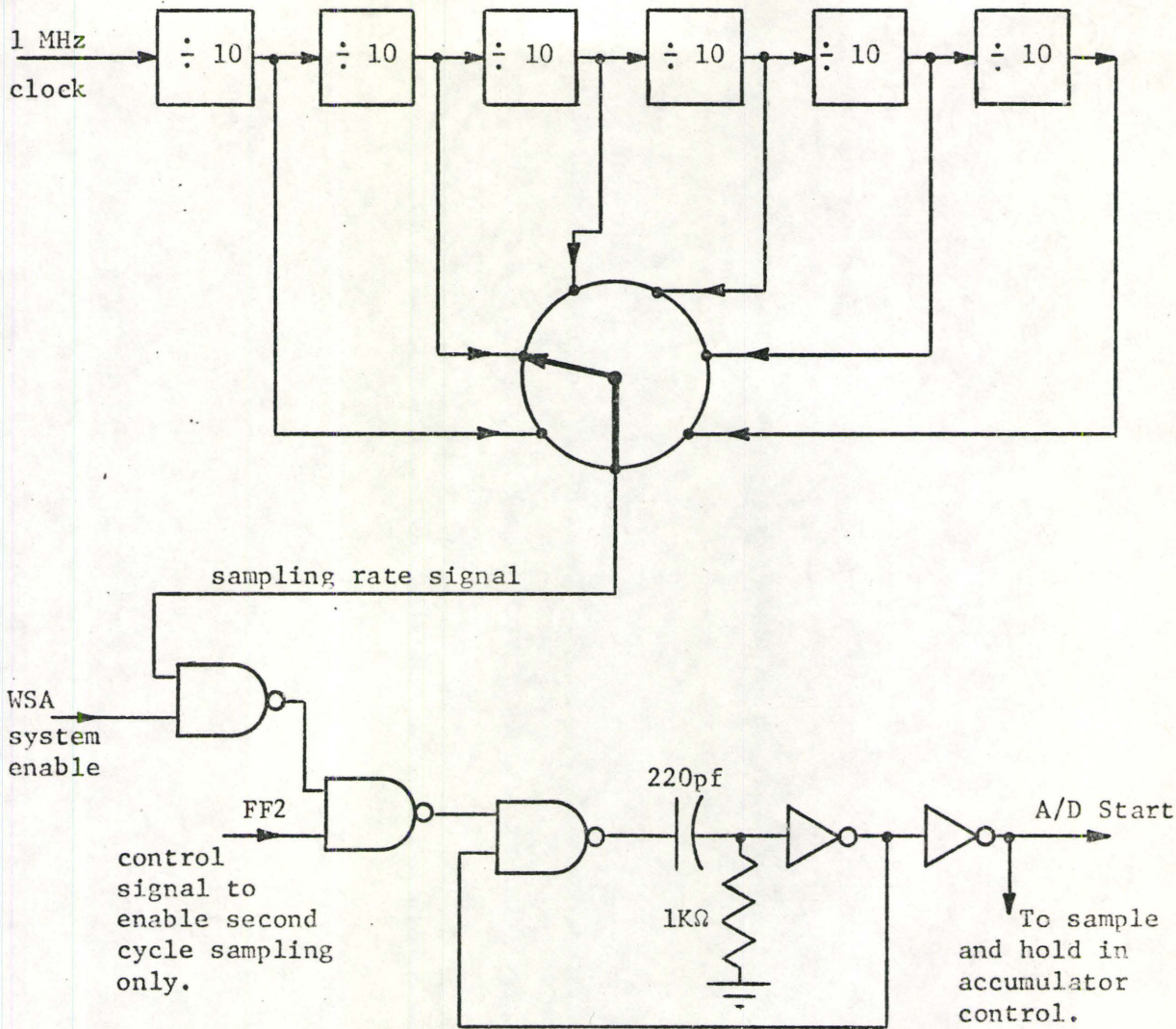
Fig. 4-3 A/D Converter

are indicated in Fig. 4-3. The subscript of the bits P_h gives the binary count value represented by each pulse. There are 9 points in the converter from which the delayed pulses may be tapped. Eight of them are used to produce the coded pulses equivalent to level r . The ninth pulse is used for sample counting and to represent a binary $\frac{1}{2}$ signal which enters into the sample accumulation regardless of the coding. The $\frac{1}{2}$ - bit addition with each sample is a requirement of Eq. (3-10).

Test measurements on the converter showed that the conversion is complete within 9 μ sec. Thus, a maximum sampling rate of 100 KHz. allows 1 μ sec. settling time between the end of conversion and the beginning of the next start pulse. Controls to determine sampling rate and duration of sampling, and to generate the A/D start pulses are described in the following section.

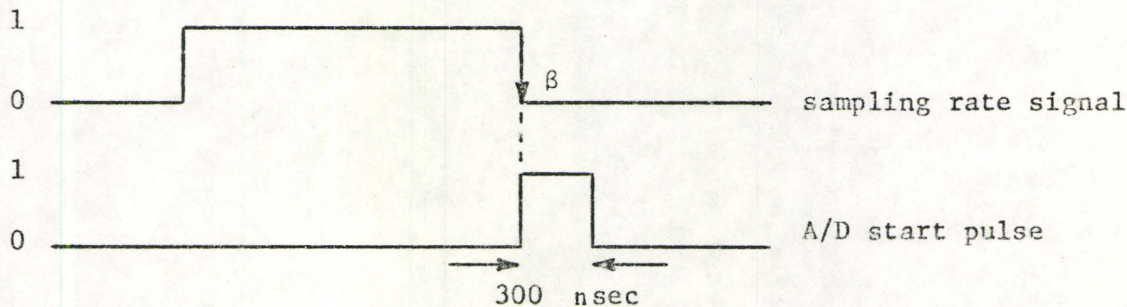
4.4 A/D Converter Controls

The control system of Fig. 4-4(a) sends constant width pulses at a preselected rate to the start pulse input of the A/D converter. The pulse rate from the 1 MHz master clock in the Walsh Spectral Analyzer is reduced through 6 decade counters. A rotary switch is used to select sampling rates from 100 KHz down to 1 Hz. Three control signals enable the timing pulses to pass to the constant width pulse generator. The sampling rate signal is enabled only when the W.S.A. system enable signal and the FF2 signal (a control signal from the period detector that permits sampling to take place only during the second cycle of operation) are at logic ONE levels.



constant pulse generator

(a)



(b)

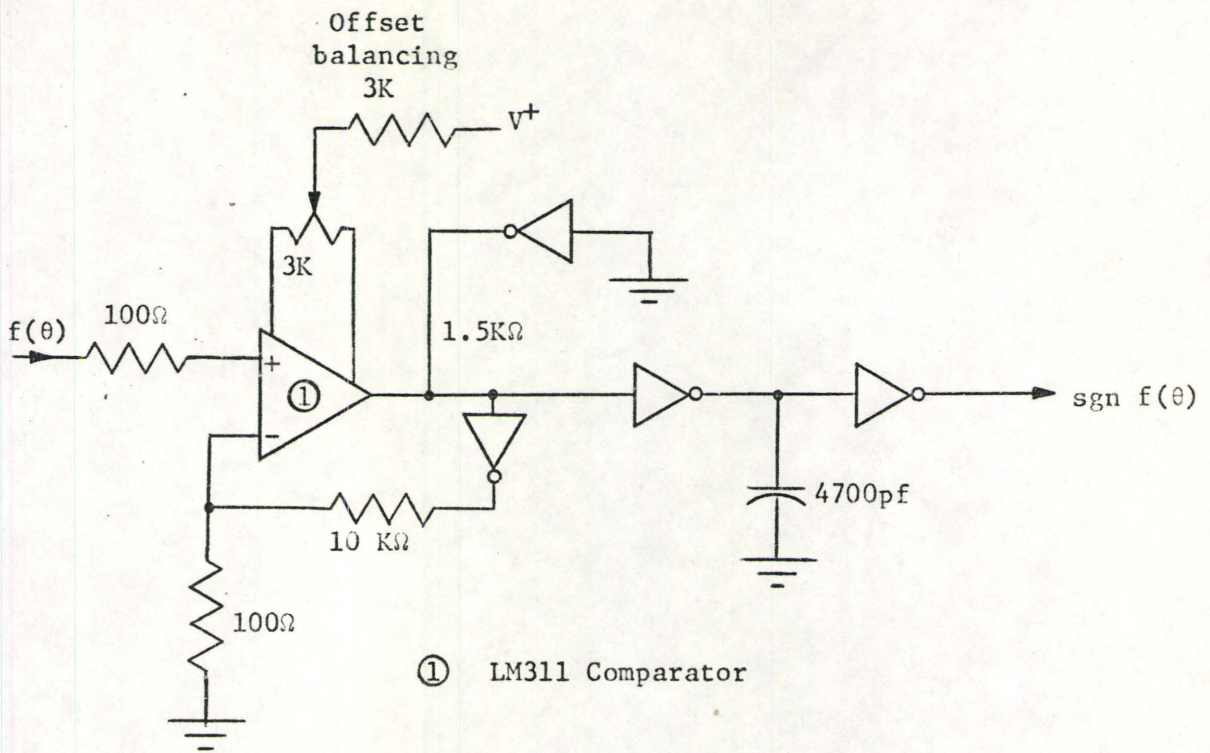
Fig. 4-4 A/D Converter Controls

According to the A/D converter specifications [3], the start pulse must have a width between 100 nsec. and 500 nsec. The constant width pulse generator allows a pulse with a width in the specified range to be produced on a change from logic 1 to 0 of the sampling rate signal, as shown in Fig. 4-4(b). On the constructed system, the pulse was found to maintain a width of approximately 300 nsec. The A/D start pulse serves a dual function; it is also used as the timing control for the digital sample and hold within the accumulator control, which is described in a later section.

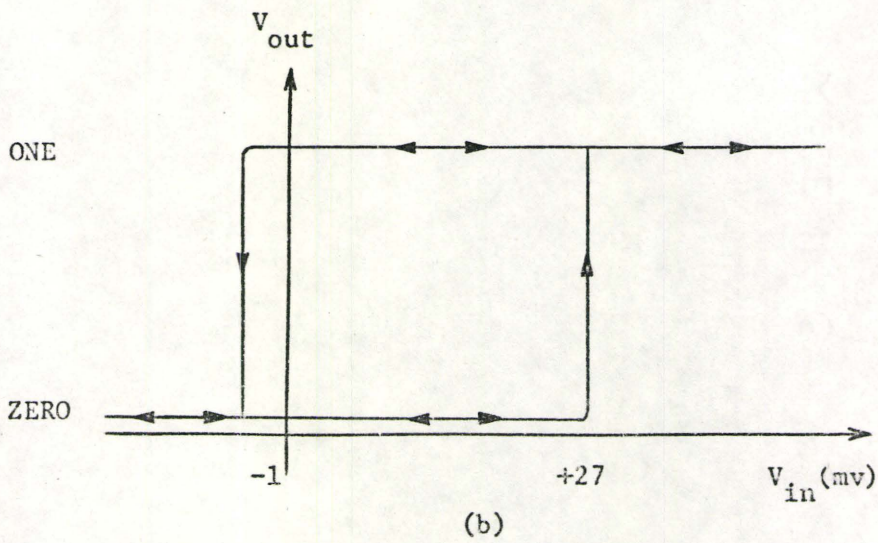
4.5 Sign Detector

Since the input is rectified for use in the A/D converter, a binary signal $\text{sgn } f(\theta)$ representing the sign of the input is needed. The detector, shown in Fig. 4-5(a) uses a National Semiconductor voltage comparator LM311, which has a response time of approximately 200 nsec. Several other voltage comparators were tried, but no other types could provide as noise-free switching on the output signal for input waveforms of very low frequency (i.e., under 0.1 Hz.). One type of comparator could not tolerate use of hysteresis at a zero-reference level. Hysteresis is the difference in the reference level voltage that determines the comparator switching point, where the level depends on the output state of the comparator. It is necessary in order to eliminate erratic switching of the comparator due to additive noise in the signal.

The LM311 has an open-collector output so that its output can be made compatible with the TTL circuits that are used throughout the WSA.



(a)



(b)

Fig. 4-5 Sign Detector System

Fig. 4-5(a) shows the output tied through a resistor to a logic level ONE, so that the high output is also a logic ONE level.

The detector should be adjusted so that sign changes on $f(\theta)$ are detected within one quantization interval either side of 0V. Since the first level ranges from 0 mv. to 39 mv., the hysteresis was adjusted by a voltage divider in the feedback loop tied to the inverting input so that the output switches on a rising signal above 27 mv. and on a decreasing voltage below -1 mv. An inverter in the feedback loop provides a constant reference voltage to determine the amount of hysteresis. The switching characteristic of the sign detector is given in Fig. 4-5(b).

The low-value resistance on the non-inverting input is used to match input resistances on both inputs. The pair of inverters on the output provide better fanout characteristics for the detector and allow a capacitor to filter out possible high-frequency noise on the edges of logic-level transitions without loading the comparator.

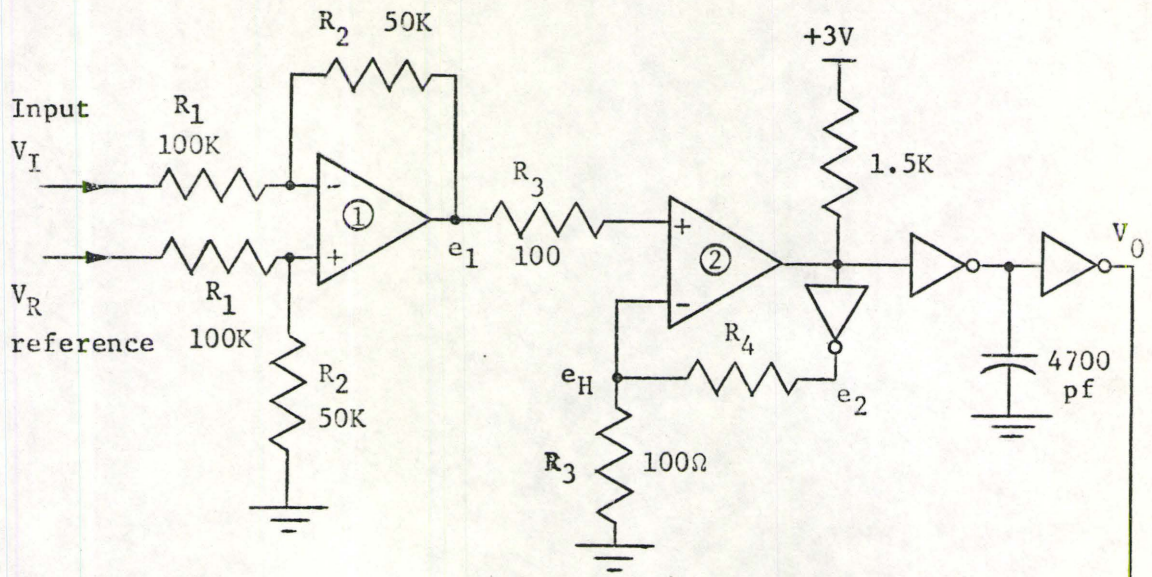
4.6 Period Detector

In each of the modes in which the instrument is to function, all operations are to begin with the first positive-going reference crossing of either $f(\theta)$ or a marker signal. If these inputs were always periodic with only two zero-crossings per cycle (as in mode (1) operation) then the sign detector signal would suffice to determine the measuring periods. However, in modes (2) and (3), the signals used to determine the period may have more than two zero-crossings per cycle or they may not cross zero at all. Hence, a reference level is shifted positively

or negatively over a range -10 V to $+10\text{ V}$ to a point where the signal crosses the reference only twice in each cycle. The period detector must indicate whether the instrument is operating in the first or second cycle of the input, since a measure of the period is taken during the first cycle and coefficients are calculated during the second cycle. Operations cease at the end of the second cycle. The period detector is shown in Fig. 4-6. It consists of two parts; a reference crossing detector, i.e., a Schmitt trigger, and a pair of flip-flops whose output information determines whether the instrument is functioning in the first or second complete cycle of the input.

In conventional Schmitt trigger circuits, the hysteresis may cause switching at a level that is not precisely the programmed reference level, or the hysteresis may vary depending on the output loading. Furthermore, some Schmitt triggers have a very restricted range for reference level inputs. The reference level must often be unipolar. The first part of the period detector in Fig. 4-6 is a Schmitt trigger circuit whose output is compatible with TTL circuits and which has a predetermined, fixed amount of hysteresis. The reference level can be varied from -10V to $+10\text{V}$ and the transition (logic 1 to 0) which triggers the period numbering circuit, occurs very close to the point at which the input has a positive-going crossing of the input reference level.

The operation of the circuit is explained by referring to the waveforms shown in Fig. 4-7. The input waveform is V_I . With the reference level set at V_R , the output switches from high to low at points A and B. The reverse will occur when the input falls to a value below V_R , as determined by the hysteresis. The μA741 operational amplifier



- ① μ A 741 Op Amp
- ② LM311 Comparator

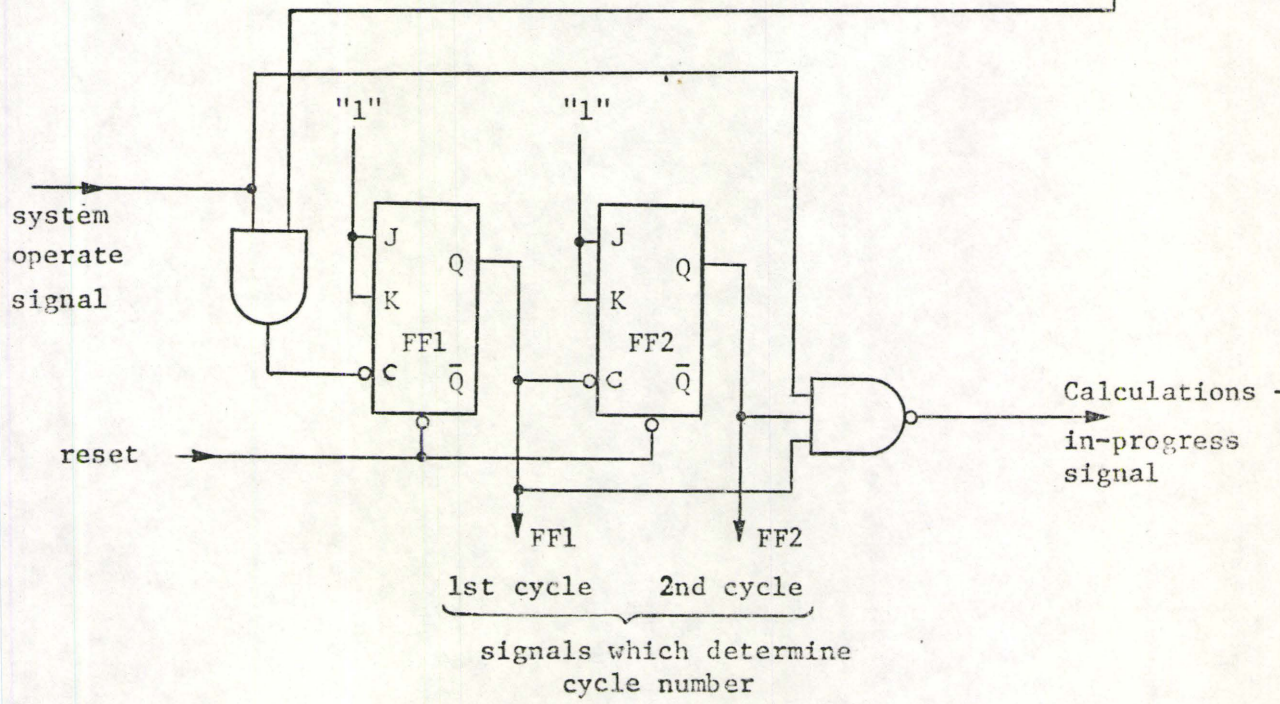


Fig. 4-6 Period Detector

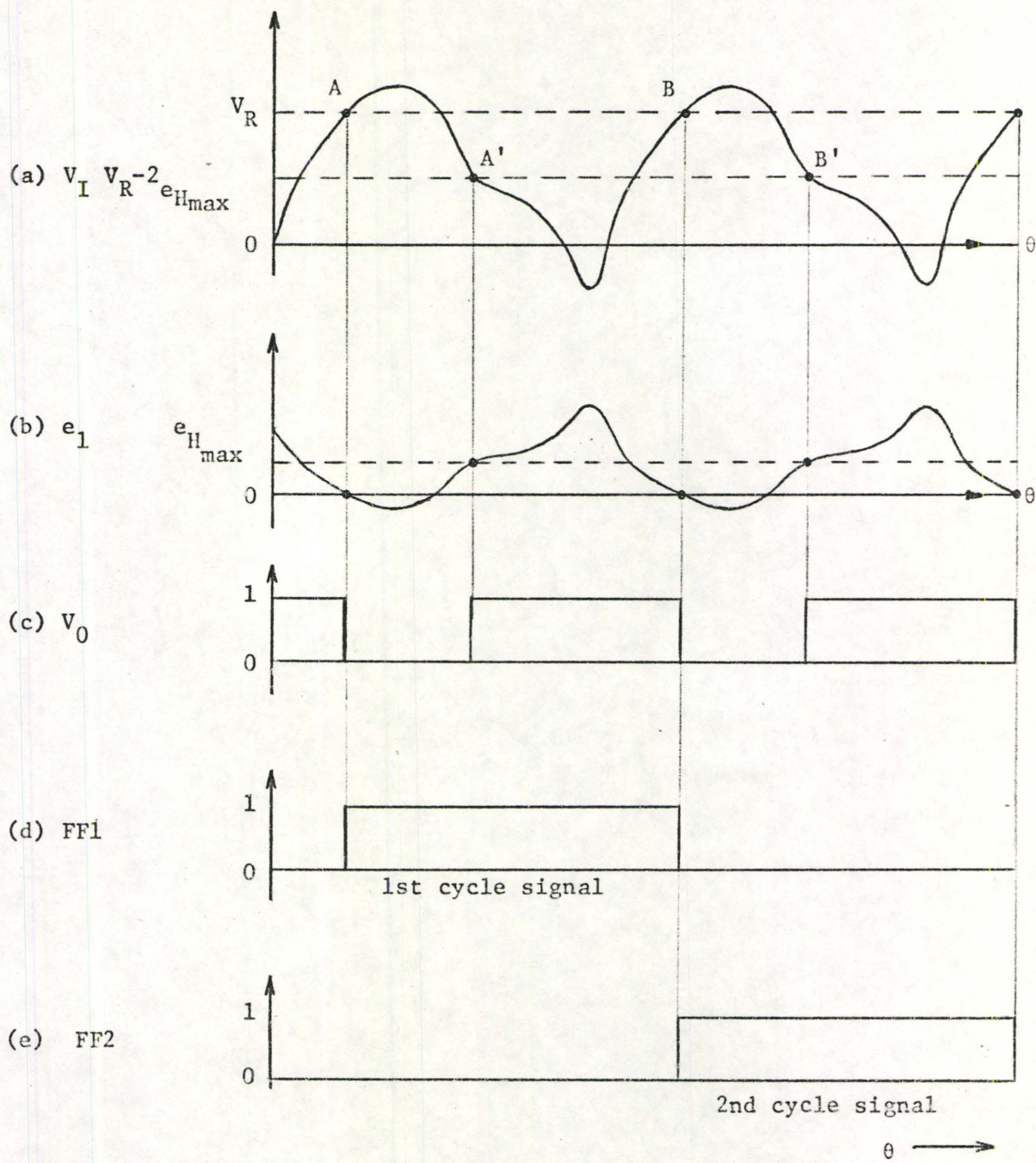


Fig. 4-7 Waveforms in Period Detector

of Fig. 4-6 is used as a subtractor with the output e_1 given by

$$e_1 = \frac{R_2}{R_1} (V_R - V_I) \quad (4-3)$$

as shown in Fig. 4-7(b). If both V_I and V_R have limits of +10V and -10V then $R_2/R_1 = 0.5$ to restrict e_1 to $\pm 10V$. This causes the overall hysteresis to be double that of the comparator circuit alone. The comparator LM311 has one input e_1 and the other determined by the feedback loop. Since the LM311 comparator has two output states, logic ZERO and logic ONE, e_2 in Fig. 4-6 also has two states. The comparator hysteresis is then given by

$$e_H = e_2 \left(\frac{R_3}{R_3 + R_4} \right) \quad (4-4)$$

Thus, if R_3 and R_4 are fixed, the hysteresis of the comparator is fixed by the logic inverter output e_2 . The inverter is included in the feedback loop to make the hysteresis e_H independent of variations in the output voltage due to loading and to ensure the proper direction of switching of the hysteresis voltage e_H for stable operation.

Generally $R_4 \gg R_3$ so that $e_{H_{\min}}$ is effectively zero. As seen in Figs. 4-7(b) and (c), when e_1 is high, then $e_{H_{\min}} \approx 0$ volts and the comparator will switch at points A and B. As soon as the comparator switches to logic ZERO, e_H rises to approximately $\frac{3.5R_3}{R_3+R_4} = e_{H_{\max}}$ volts, since $e_{2_{\max}} = 3.5V$. The input e_1 must rise above this level (at points A' and B') before the comparator switches to its previous state.

Consequently, the hysteresis voltage e_H determines the minimum peak-to-peak amplitude of the input voltage that will cause the Schmitt trigger

to be able to detect a complete cycle. Since the overall hysteresis of the system is $2e_H$, the latter voltage is the required minimum for the input.

Measurement of $e_{H_{\min}}$ for the constructed system was approximately 7.5 mv. Since the switching voltage at points A and B on Fig. 4-7(a) is $V_R - 2e_{H_{\min}}$, the output will first trigger the cycle numbering system when the input rises to within 15 mv. below the reference level. This level is acceptable since it is well within one quantization interval. The total hysteresis measurements show that the minimum peak-to-peak input signal that can be handled by the WSA is approximately 275 mv.

The Schmitt trigger output is enabled by the system operate ("start" signal) to control a pair of flip-flops which are connected as a 2-bit binary counter. Since clean trigger edges are essential to prevent erratic responses by the flip-flops, a decoupling capacitor is placed on the Schmitt trigger output to eliminate noise at the time of switching. The first flip-flop FF1 is in state 1 during the first cycle, while FF2 is in state 1 during the second cycle. These signals control various portions of the instrument that are to operate only during specified cycles of the input.

A panel light is ON when the calculations-in-progress signal is a ONE (See Fig. 4-6). At the beginning of the third cycle of the input, all inputs to the gate which determines the latter signal become logic ONE and the calculations-in-progress signal switches to logic ZERO. Not only does the panel light turn off, but the ZERO signal causes all operations in the Walsh spectrum analyzer to stop.

4.7 W.F.G. Pulse Generator

The Walsh spectrum analyzer has been designed to calculate the first 64 Walsh series coefficients of an input waveform. According to the steps outlined in Chapter 3 the Walsh functions $wal(0,\theta)$ to $wal(63,\theta)$ are generated simultaneously and they have a time-base equivalent to the fundamental period of the input. From the definitions and properties of the Walsh functions, a generator producing 64 functions requires 64 uniformly-spaced clock input pulses during one cycle. The W.F.G. (Walsh function generator) pulse generator here described forms a measure of the duration of the fundamental period and uses that measure to generate the 64 uniformly-spaced pulses during the second cycle of operation. The system diagram of the generator is shown in Fig. 4-8.

Referring to Fig. 4-8, at the start of the first complete measuring cycle, the first binary up-counter in the pulse generator is enabled to count clock pulses. This counter, which contains 20 bits, accumulates the pulses throughout the first cycle of the input. At the end of the cycle the counter stops and it now contains a number, in terms of its binary state, representing the period T of the first cycle. It is required to generate pulses every $1/64$ of that period throughout the second cycle. A number which represents very nearly $1/64$ of the period is simply the number stored in the 14 most significant bits of the 20-bit counter. This is so because binary division by 64, or 1000000 in binary, merely means shifting the binary point 6 places to the left.

Thus, clock pulses to a second counter containing 14 bits are enabled by the period numbering signal FF2 during the second cycle of operation. The bits of this counter are compared continually with the

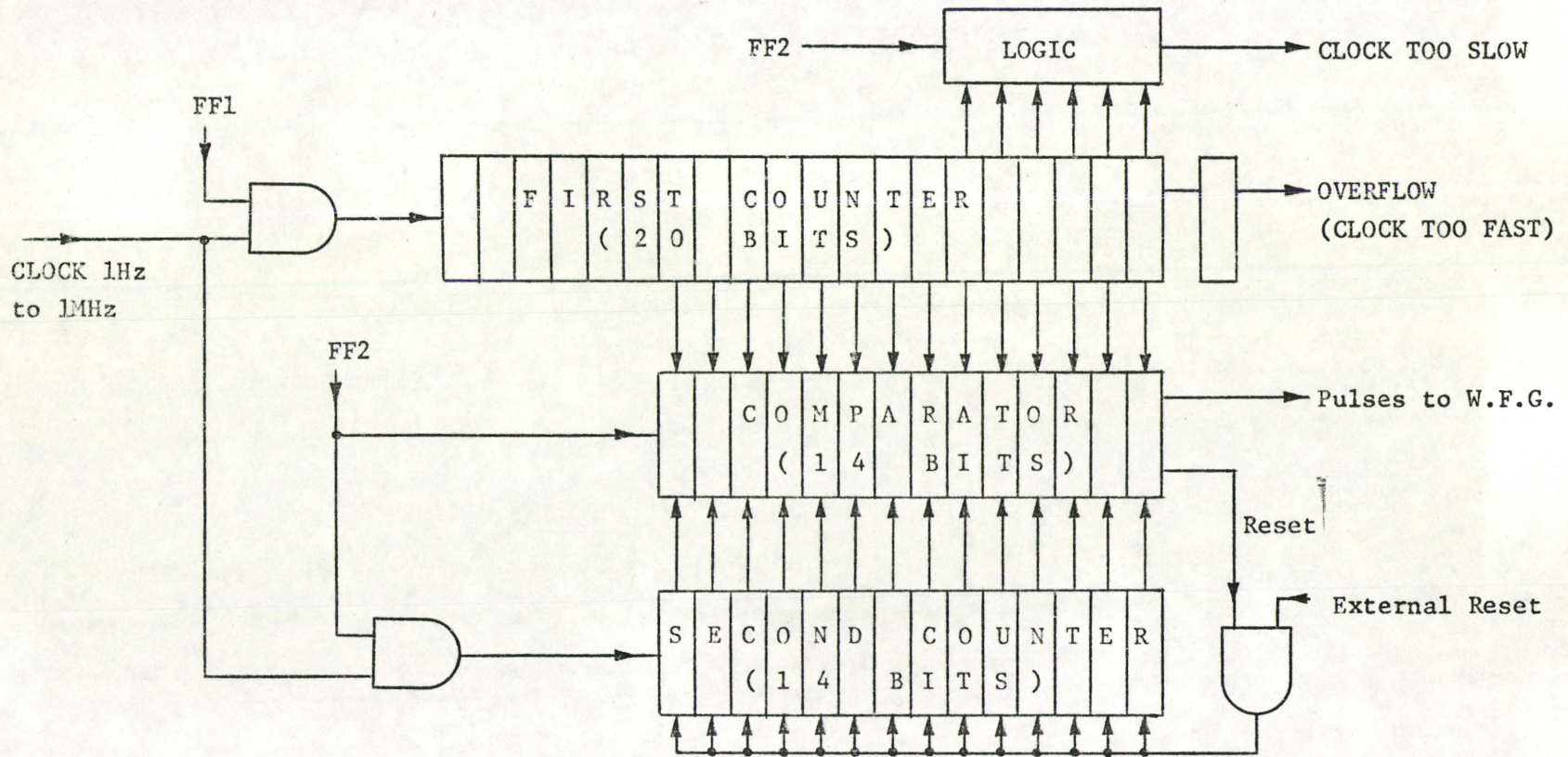


Fig. 4-8 W.F.G. Pulse Generator

corresponding 14 most significant bits of the first counter. When the two numbers under comparison are equal, a pulse appears at the comparator output. The first pulse occurs at $T/64$ seconds after the beginning of the second cycle. This pulse, which is approximately 50 nsec. in duration, feeds back to reset the second counter. The process of counting, comparing, and resetting takes place 64 times. In this way, a pulse at the digital comparator output is generated every $1/64$ of a cycle during the second cycle.

Overflow from the 20th counter binary in the first counter is detected by a 21st flip-flop and is used to indicate too fast a clock rate for the input pulses. The last six stages of this counter are used to indicate too slow a clock rate. An output from either of these indicators is shown on panel light indicators and it also stops the measurement. Observation of the panel light signals allows the operator of the instrument to increase or decrease the input clock rate in decade steps.

In the system described, there will generally be a remainder in the first six binaries of the larger counter, representing a timing error of 63 pulses maximum. This maximum possible error is halved by a small modification in the reset of the counter, prior to measurement. The sixth binary of the first counter is preset to state ONE while the remaining 19 are preset to state ZERO. By adding this count of 32 to the period measurement, the timing error now has a range +32 to -31 clock pulses. In the system shown in Fig. 4-8, the first counter content must reach at least the 15th binary by the time the second cycle begins. Hence, the maximum frequency error in generating the Walsh functions is

$32/2^{14} \approx .2\%$. Also, if the highest clock rate allowable is 1 MHz, then the time for the count to reach the 15th binary is 16,384 μ sec., corresponding to a fundamental frequency of nearly 61 Hz. Clearly, using this process, the maximum possible timing errors may be reduced by extending the number of binaries, but with a given input clock rate, this is done at the expense of the shortest time-base that can be used in the analysis. The inclusion of five additional binary stages allows a range of signal frequencies of 64:1 to be accommodated. The recommended clock rate is 1 MHz. for signals with fundamental frequencies in the range 1 to 60 Hz, and 100 KHz for signals in the range .1 to 6 Hz, etc. With a 1 sec. clock rate, the designed system can analyze waves with a fundamental frequency as low as one cycle in 11.6 days. By decreasing the input clock rate, the lower limit of fundamental frequency of signals that can be analyzed can be extended indefinitely.

4.8 Walsh Function Generator

An array of 64 Walsh functions are generated simultaneously during the second cycle using a hazard-free generator of the type shown in Fig. 2-6. The generator is clocked by the 64 pulses sent from the pulse generator described in the previous section. Each of the Walsh functions feeds a system comprising an accumulator control, a sample accumulator, and a final readout system. The block diagram of Fig. 4-1 shows this system for only one Walsh function output.

4.9 Sample Accumulator Control

The sample accumulator control in Fig. 4-9 generates the signal $\text{sgn } f(\theta) \text{ wal}(m, \theta)$. This signal determines whether the samples $|Q_n|$ from the A/D converter are to be added to or subtracted from the sample accumulation. Since both the $\text{sgn } f(\theta)$ signal and $\text{wal}(m, \theta)$ are coded as logic ONE for +1 and logic ZERO for -1, a comparison gate performs the $\text{sgn } f(\theta) \text{ wal}(m, \theta)$ logic, i.e., $\text{sgn } f(\theta) \oplus \overline{\text{wal}(m, \theta)}$ or $\overline{\text{sgn } f(\theta)} \oplus \text{wal}(m, \theta)$. If the $\text{sgn } f(\theta) \oplus \overline{\text{wal}(m, \theta)}$ form is used, then the bank of inverters in the array Walsh function generator of Fig. 2-6 can be eliminated.

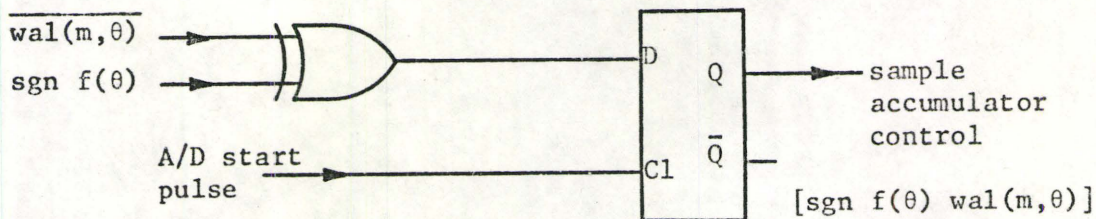


Fig. 4-9 Sample Accumulator Control

There is a possibility that the sign of the input function could change during a sample conversion. The D-type flip-flop in the accumulator control acts as a digital sample and hold. The A/D start pulse is used to

clock the flip-flop to prevent control line switching on the sample accumulator during the sampling interval.

4.10 Sample Accumulator

Several possible systems could be devised to accumulate sample values. The bits comprising the binary coded samples of $f(\theta)$ appear on 9 parallel lines from the A/D converter. Hence, a synchronous parallel adder/subtractor with a buffer register could be used. With such a system, timing pulses and a binary to 2's-complement converter for the subtraction process would be required. Since the accumulation results in long word lengths, the 2's-complement numbers and the adder/subtractor would have to be correspondingly large. If a serial adder/subtractor were employed, both a parallel to serial converter and a binary to 2's-complement converter would be needed. Again, extra timing pulses are required. In each of the above cases, it requires additional hardware to provide for a decimal digit display readout.

The accumulator design shown in Fig. 4-10 is a parallel processor that operates asynchronously and requires no additional timing pulses. The amount of hardware is minimal and decimal digit readout is facilitated. The accumulator consists mainly of two 9-bit binary counters with parallel feeds. The upper counter in Fig. 4-10 processes the samples when it is enabled by a signal which indicates that $\text{sgn } f(\theta) \text{ wal}(m, \theta)$ is positive. Except for the first flip-flop, the clock input of each J-K flip-flop is controlled by an exclusive-OR gate. The exclusive-OR gates are used to permit flip-flop clocking from either the pulse input or a level change from a lesser significant bit. Since the pulse inputs arrive serially

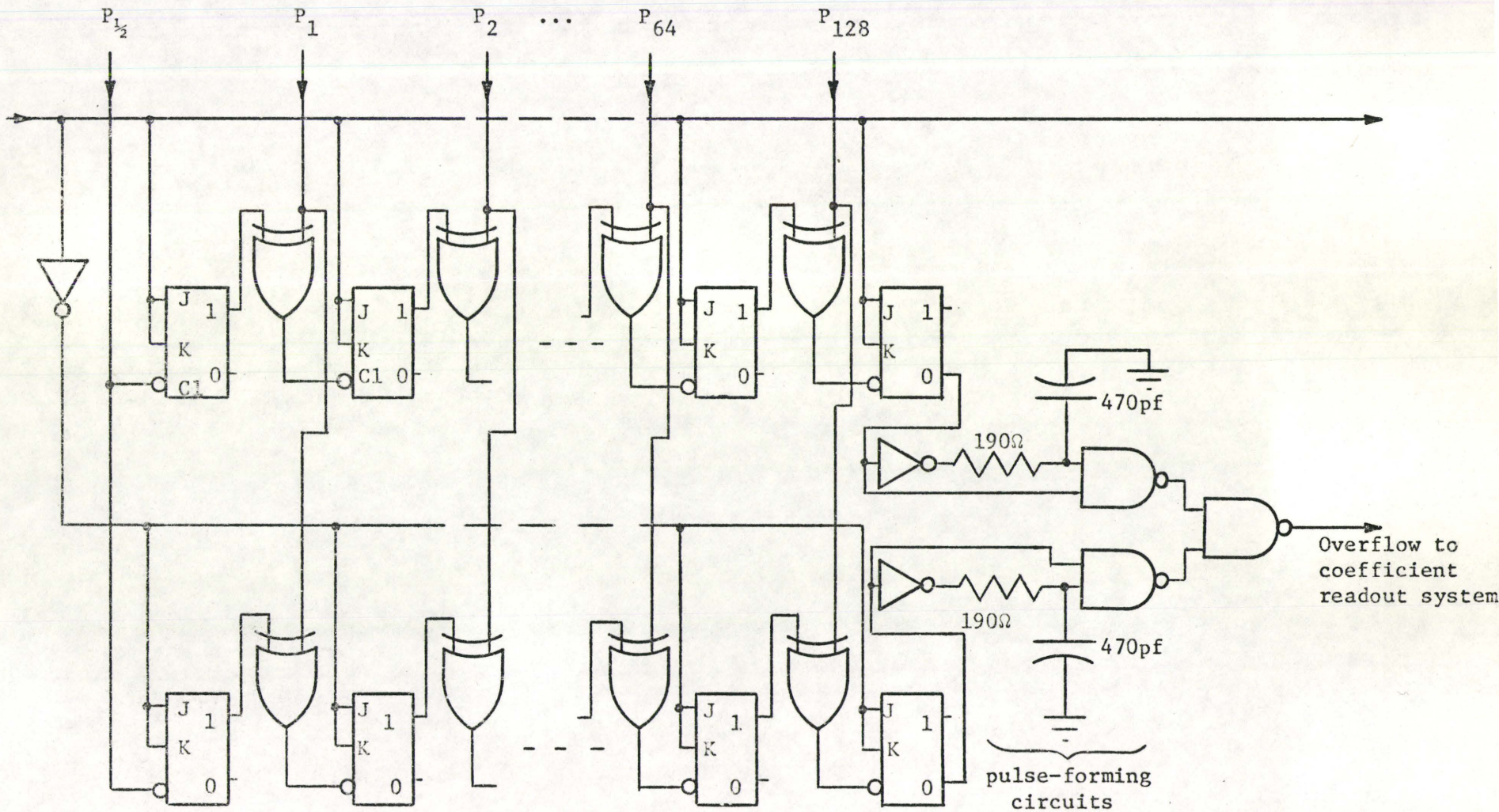


Fig. 4-10 Sample Accumulator

in time from the A/D converter, with the msb arriving first, there is no conflict or race condition between the two triggering sources. The sample and hold unit in the accumulator control of Fig. 4-9 prevents changes on the counter enable control during the time that pulse inputs from the A/D converter are being processed. Thus, erroneous counts are impeded if the J-K inputs (counter enable signal) should switch from ONE to ZERO. A similar procedure is followed by the lower counter, which accumulates samples whenever $\text{sgn } f(\theta) \text{ wal}(m, \theta)$ is negative.

As pulses are accumulated in each of the counters, there will be overflows from the 9th bits. These overflows feed a reversible counter that can operate in any code that is desired. The overflows take place before a sampling interval is complete so that the counter enable control of the accumulator can also control the direction of counting in the output counter, which is used to display final coefficient values. The overflows from each counter generate pulses using the pulse-forming circuits shown in Fig. 4-10. The pulses are gated by OR logic to the clock of the readout counter.

Sample values are accumulated according to the values of the nine input pulses $P_{1/2}$ to P_{128} , where $P_{1/2}$ represents a value $1/2$, P_1 represents a value 1, etc. A full accumulator count represents 255.5. A sample accumulation of 256 causes an overflow, so that the number which appears in the final readout counter is $1/256$ of the total sample value count. However, 256 is the number of quantization levels p that have been used in the A/D converter. Thus the number stored in the output counter corresponds, except for a possible small remainder in the two accumulator counters, to the expression

$$W_m \left(\frac{H}{V_{\max}} \right) = \frac{1}{P} \sum_{h=1}^H |Q_h| \operatorname{sgn} f(\theta)_h \operatorname{wal}(m, \theta)_h \quad (4-5)$$

The Walsh coefficient W_m may then be obtained by multiplying the readout value by V_{\max}/H , where $V_{\max} = 10$.

4.11 Coefficient Readout Counter

The final readout should permit a decimal digit display. To this end, the overflow from the sample accumulator feeds a BCD (binary-coded decimal) synchronous up/down counter consisting of Signetics' 8285 counters [4]. Light emitting diode numerical displays with BCD decoders included are ideal for the readout. Since the coefficient values can be either positive or negative, it is desirable to produce the absolute value of a number and its sign. Without a decoding system to provide these features, an up/down counter would normally yield 1's or 2's-complement representations for negative numbers. The magnitude and sign capability of the configuration shown in Fig. 4-11(b) simplifies the decoding of negative numbers for a counter made with the Signetics 8285 [Fig. 4-11(a)].

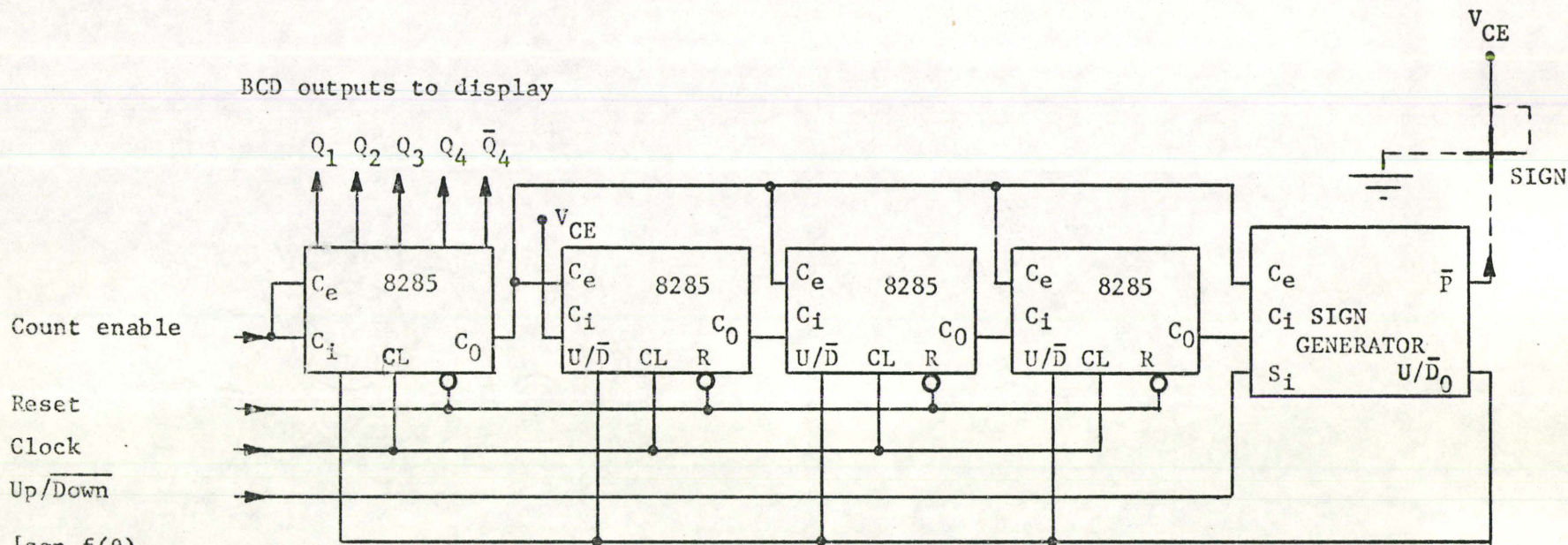
As shown in Fig. 4-11(b), gates 1 to 4 form a D-type latch. The U/\bar{D} input, which is the $\operatorname{sgn} f(\theta) \operatorname{wal}(m, \theta)$ signal, is transferred to the point P (gate 3) when the combined carry-out ($C_e \cdot C_i$) goes to a "1" level. The function generated at the output U/\bar{D}_0 is

$$U/\bar{D}_0 = S_i \cdot P + \bar{S}_i \bar{P} \quad (4-6)$$

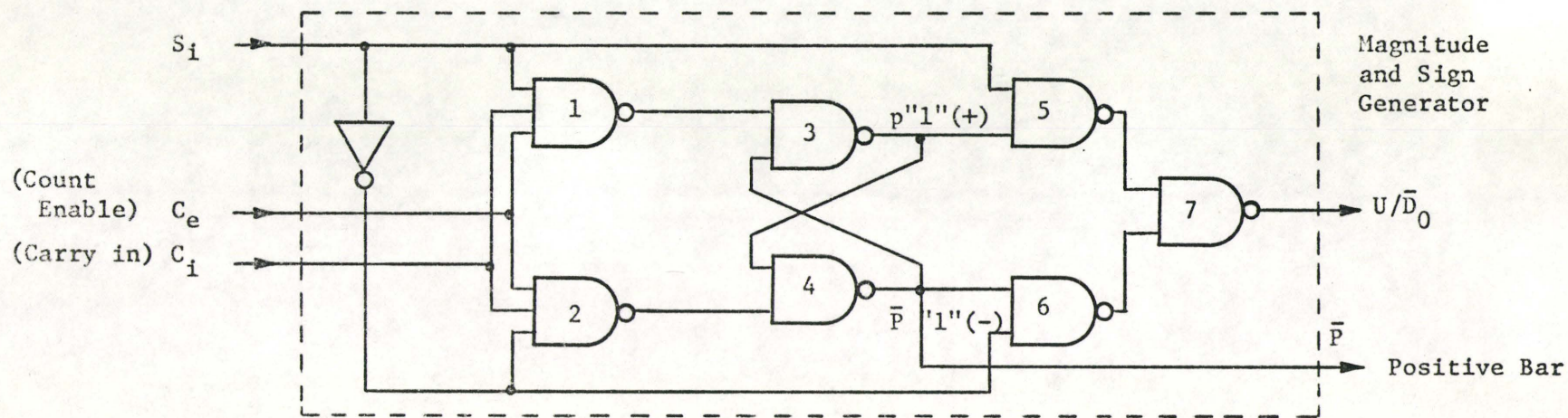
where

$$P = "1" \quad (\bar{P} = "0") \quad \text{then } N \geq 0$$

$$P = "0" \quad (\bar{P} = "1") \quad \text{then } N \leq 0$$



(a)



(b)

Fig. 4-11 Up/Down Counter with Magnitude and Sign Generation

N = number of counts

$S_i = "1"$, count positive

$S_i = "0"$, count negative.

The latch (P) is enabled when carry-in ($C_e \cdot C_i$) goes to "1". This occurs at all zero crossings. Table 4-1 shows the count sequences generated for a single 8285 BCD decade counter with the magnitude and sign generator connected.

S_i^*	Carry-Out $C_e \cdot C_i$	P	U/\bar{D}	N Clock	Binary	Decimal
0	0	1	0	0	0 0 1 1	+3
0	0	1	0	1	0 0 1 0	+2
0	0	1	0	2	0 0 0 1	+1
0	0	1	0	3	0 0 0 0	-0
0	1/0	0	1	4	0 0 0 1	-1
0	0	0	1	5	0 0 1 0	-2
0	0	0	1	6	0 0 1 1	-3
1	0	0	0	7	0 0 1 0	-2
1	0	0	0	8	0 0 0 1	-1
1	0	0	0	9	0 0 0 0	+0
1	1/0	1	1	10	0 0 0 1	+1
1	0	1	1	11	0 0 1 0	+2
0	0	1	0	12	0 0 0 1	+1
0	0	1	0	13	0 0 0 0	-0
0	1/0	0	1	14	0 0 0 1	-1

* $S_i = "1"$ → Count Up $S_i = "0"$ → Count Down

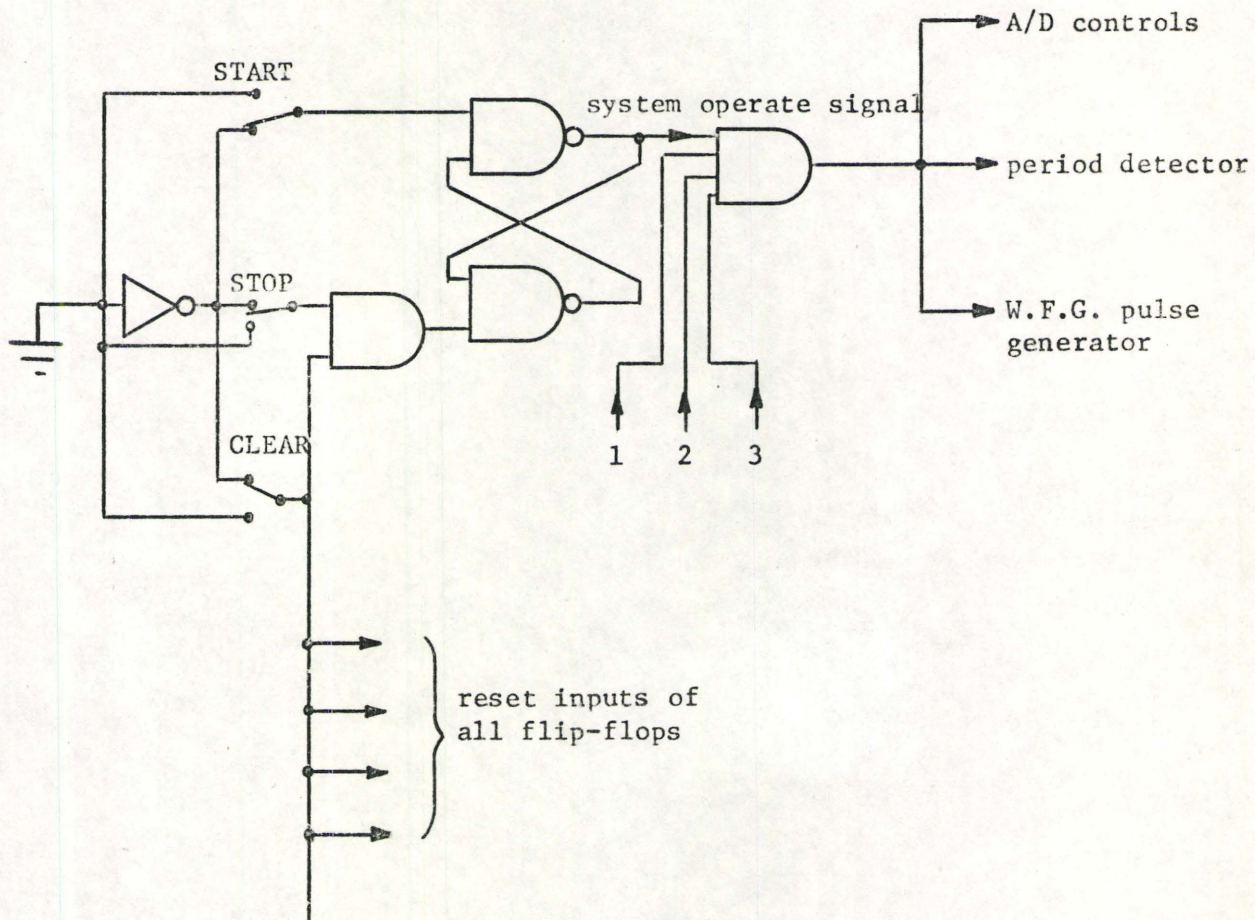
Table 4-1 Count Sequence Using Magnitude and Sign Detector

In a Walsh Spectral Analyzer in which several Walsh series coefficients are calculated in parallel, there is a readout counter of the type in Fig. 4-11 for each coefficient. These counters and the counters in the sample accumulator constitute the only memory in the system. Outputs from the final counter stages would be multiplexed to the numerical displays so that say two coefficient values would be displayed visually at a time. The outputs could also be recorded on a typed printout or, by using D/A (digital to analog) converters, the spectrum could be displayed on an oscilloscope.

4.12 System Controls

Three manually-operated switches control the start, stop, and clear or reset operations in the WSA. A pair of NAND gates, shown in Fig. 4-12, form an R-S flip-flop which prevents contact bounce on the switches from affecting the rest of the instrument. The reset signal not only clears all memory elements (flip-flops) in the system but also stops all further operations. The start signal is further gated by an AND operation with indicators that determine whether the clock rate into the W.F.G. pulse generator has been too fast or too slow or if the calculations are complete, i.e., the input waveform is going into its third cycle.

Two additional controls are available to the operator of the instrument. The switch SW1 in Fig. 4-1 places the WSA in mode (3) operation, in which the period of measurement is set arbitrarily by the function on the control input channel. For mode (2) operation, the reference level input to the period detector can be varied continuously from -10V to +10V.



- 1 P.G. clock rate too high
- 2 P.G. clock rate too low
- 3 Calculations-in-progress

Fig. 4-12 System Controls

4.13 Conclusions

An instrument based on the design described in this chapter was constructed and was found to operate satisfactorily in determining the first 64 coefficients of the Walsh series of a signal. Frequency limitations on a signal that can be analyzed are governed by the maximum sampling rate capability of the A/D converter and by the clock rate feeding the W.F.G. pulse generator. An analog sample and hold in conjunction with a faster A/D converter is recommended to increase the sampling rate. A higher clock rate to the W.F.G. pulse generator would enable the time-base of measurement to be shortened while maintaining the specified accuracy in time-base measure.

An additional feature that could be designed into the machine is preselection of a time-base (mode (4) operation) by presetting the 14 most significant bits in the first counter of the pulse generator in Fig. 4-8. This feature enables the frequency of the fundamental component in an analyzed signal to rise to a maximum of $1/64$ of the clock rate (assuming that 64 Walsh functions are to be generated). There are no error bits to consider in the 6 least significant bits of the counter so that the minimum count beyond these bits is 1. There is no need to fill the counter to the 15th binary to maintain accuracy as outlined in section 4.7. Comparison of this minimum count with the second counter content could cause an output pulse with each clock pulse input, thereby creating a minimum measuring time-base of 64 clock pulses in duration. Foreknowledge of the input clock rate allows precise presetting of the time-base. In this mode of operation, the instrument controls require modification to allow single cycle operation. In accordance with the

sampling theorem, care must be taken to ensure a minimum sampling rate of 64 samples per cycle.

If a preselected number of samples (mode (5) operation) is used for the analysis, the Walsh function time-base is adjusted to the sampling rate. Preferably the number of samples will be an integral power of two, say 2^x . Then, if 64 Walsh coefficients are to be calculated, the first counter in the W.F.G. pulse generator would be preset to 2^x . The clock rate to the pulse generator and the sampling rate would be identical so that a pulse would be sent to the Walsh function generator every $2^x/64 = 2^{x-6}$ samples (where $x \geq 6$). Again single cycle operation is used in this mode.

Mode (6) operation is the analysis of previously digitized samples. In this mode, the A/D converter in the system is bypassed. Depending on the information that is known about the samples (e.g., sample size; are the samples from a periodic signal, etc.) the system could operate in a manner similar to the other modes. However, additional equipment such as a digital period detector may be required.

A system that could perform the Fast Walsh Transform generally requires a fixed number of samples, storage of all the samples before calculation, and is not generally adaptable to an arbitrary time-base of measurement. The digital Walsh Spectral Analyzer described in this chapter can operate in the various modes that have been discussed and all calculations are complete within one clock pulse period after the last sample has been taken. Hence the WSA is considered to be more versatile than an FWT system.

CHAPTER 5

WALSH SERIES TO FOURIER SERIES CONVERSION

5.0 Introduction

Sinusoidal functions have long held a dominant position in communications and other branches of science. This dominance is related to the availability of linear, time invariant circuit components in practical form. The arrival of semiconductor technology has led to more intense investigation of non-sinusoidal functions, primarily Walsh functions. In an effort to make better use of the new technology instruments such as the Walsh Spectral Analyzer of Chapter 4, that are simpler and faster than Fourier analyzers, have been developed to yield a finite number of Walsh series coefficients of a signal [1-3]. In many instances the Walsh spectrum of a signal is as meaningful as the Fourier spectrum, and sometimes it is preferable. Nevertheless, because of bandwidth restrictions of transmission channels, the Fourier spectrum corresponding to a given Walsh spectrum may often be required. A brief comparison of some examples of Walsh and Fourier spectrum analysis and synthesis is given in the latter section of this chapter.

Given the Walsh coefficients of a signal, the corresponding Fourier coefficients may be evaluated by either a general-purpose or a special-purpose computer, using conversion formulae derived here. In practical conversion systems, two forms of truncation error may arise. First, the word lengths in the system hardware may be inadequate: Such roundoff errors are here considered to be negligible. Since, in general, the

conversion equation for each Fourier coefficient is an infinite sum of products of constants and the given Walsh coefficients, a second and more important source of error is truncation of the infinite series because the number of Walsh coefficients will always be finite.

Signals fall into four spectral categories;

1. infinite Walsh series with infinite Fourier series,
2. finite Walsh series with finite Fourier series,
3. finite Walsh series with infinite Fourier series,
4. infinite Walsh series with finite Fourier series.

The last category is of particular interest. It is shown below that if a band-limited signal with a highest normalized frequency component (harmonic) F is applied to a Walsh analyzer whose highest normalized frequency component readout is S , then all F Fourier harmonics of the signal can be determined without error, provided that $S \geq F$. Thus, instruments that yield a finite number of Walsh coefficients can be used for the precise evaluation of the Fourier coefficients of band-limited signals. Furthermore, a substantial easing of hardware requirements in a special-purpose Walsh to Fourier series converter (or of software requirements in a general-purpose computer conversion) is achieved if one puts $S = 2^{M-1}$, where M is an integer related to the number of binary bits in S .

5.1 Series Conversion

Let a function $f(\theta)$ be represented by a sequency-ordered Walsh series;

$$f(\theta) = A_0 + \sum_{s=1}^{\infty} [A_s \text{ cal}(s, \theta) + B_s \text{ sal}(s, \theta)] \quad (5-1)$$

The coefficients A_s and B_s of the even and odd Walsh components, respectively, are defined by Eq. (3-5). $f(\theta)$ has the corresponding Fourier series

$$f(\theta) = \frac{a_0}{2} + \sum_{f=1}^{\infty} [a_f \cos 2\pi f\theta + b_f \sin 2\pi f\theta] \quad (5-2)$$

It is desired to use the Walsh coefficients A_s and B_s in order to derive the Fourier coefficients a_f and b_f . We first consider signals in category 1; i.e., that have both infinite Walsh spectra and infinite Fourier spectra.

The coefficients a_f of the even terms of the Fourier series of a signal are functions only of the coefficients A_s of the corresponding even terms of the Walsh series. Similarly, b_f terms depend only on the B_s terms. Primarily, the coefficients of the odd terms are considered below.

The Walsh to Fourier series conversion relation is derived by equating the terms of each series

$$\sum_{f=1}^{\infty} b_f \sin 2\pi f\theta = \sum_{s=1}^{\infty} B_s \text{ sal}(s, \theta) \quad (5-3)$$

Using superposition, the sal functions are expanded into sets of equivalent Fourier series expressions whose terms have coefficients $b_{f,s}$, where

$$b_{f,s} = 2 \int_0^1 \text{sal}(s, \theta) \sin 2\pi f\theta d\theta \quad (5-4)$$

is the f th Fourier coefficient of $\text{sal}(s, \theta)$. A non-recursive equation for the Fourier transform of a Walsh function, from which the coefficients $b_{f,s}$ can be calculated, is derived in a later section of this chapter. The $s \times f$ matrix of the set $\{b_{f,s}\}$ is denoted \underline{F}_b^T . In the expansion on the right-hand side of Eq. (5-4), terms containing $\sin 2\pi f\theta$ are grouped, yielding b_f values given by

$$b_f = \sum_{s=1}^{\infty} b_{f,s} B_s \quad (5-5)$$

Similarly, for the coefficients a_f ,

$$a_f = \sum_{s=0}^{\infty} a_{f,s} A_s \quad (5-6)$$

where $a_{f,s}$ is the f th Fourier coefficient of the series for $\text{cal}(s, \theta)$.

If \underline{b} represents the $f \times 1$ matrix of the set $\{b_f | f=1, 2, \dots, \infty\}$, and \underline{B} represents the $s \times 1$ matrix of the set $\{B_s | s=1, 2, \dots, \infty\}$, then

$$\underline{b} = \underline{F}_b^T \underline{B} \quad (5-7)$$

However, if only a finite number S of the Walsh coefficients are known, then b_f can only be approximated as \hat{b}_f , where

$$\hat{b}_f = \sum_{s=1}^S b_{f,s} B_s \quad (5-8)$$

The coefficients \hat{b}_f can be considered as the Fourier coefficients of a sequency-limited function. The mean-squared error introduced by the truncation of the series in Eq. (5-5) is

$$\|b_f - \hat{b}_f\|^2 = \left\| \sum_{s=S+1}^{\infty} b_{f,s} B_s \right\|^2 \geq 0 \quad (5-9)$$

Since the $b_{f,s}$ factors are constants, approximation errors in the conversion are dependent on the Walsh series coefficients of the signal. As S increases, errors tend to decrease, but not necessarily monotonically.

Since a number of constants $b_{f,s}$ are shown below to be zero, special cases arise for functions with infinite Walsh spectra and infinite Fourier spectra in which there is no error due to truncation of Eq. (5-5), provided that $s \geq f$. One such case is sawtooth wave which is periodic over the interval $[0,1)$; it has Walsh series coefficients that are non-zero only for s an integral power of 2, so the conversion equation for each b_f has only one non-zero term. (The pattern of non-zero terms in the F_b matrix is discussed later.)

5.2 Sequency-Limited Functions

Signals with spectra in categories 2 and 3 are sequency-limited, with Walsh to Fourier series conversion equations of the form of Eq. (5-5). If $B_s = 0$ for $s > S$, the mean-squared conversion error of Eq. (5-9) is zero provided that all S Walsh coefficients are used to evaluate b_f .

5.3 Frequency-Limited Functions

Functions, other than constants, which have finite Fourier spectra, necessarily have infinite Walsh spectra. If a function $f(\theta)$ is band-limited to become $\hat{f}(\theta)$ with a limited number of harmonics F , and if $\hat{f}(\theta)$ is applied to a Walsh Spectral Analyzer (see Fig. 5-1) to yield the first

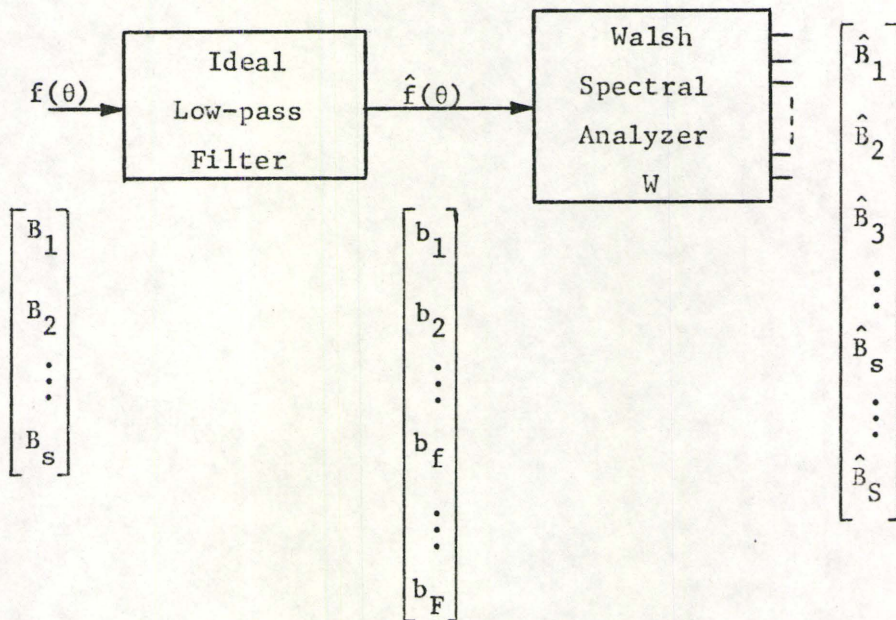


Fig. 5-1 Walsh Spectrum Analysis of a Frequency-limited Function.

S Walsh coefficients, then the F Fourier coefficients of $\hat{f}(\theta)$ can be determined precisely from the S measured Walsh coefficients, provided that $S \geq F$.

Writing

$$\hat{f}(\theta) = \sum_{f=1}^F b_f \sin 2\pi f\theta \quad (5-10)$$

then the Walsh coefficients \hat{B}_s of the band-limited function are

$$\begin{aligned} \hat{B}_s &= \int_0^1 \hat{f}(\theta) \text{sal}(s, \theta) d\theta \\ &= \sum_{f=1}^F \left[\int_0^1 \sin 2\pi f\theta \text{sal}(s, \theta) d\theta \right] b_f \end{aligned} \quad (5-11)$$

or

$$\hat{B}_s = \sum_{f=1}^F B_{s,f} b_f \quad (5-12)$$

where $b_f = 0$ for $f > F$ and where $B_{s,f}$ is the sth Walsh coefficient of $\sin 2\pi f\theta$. In matrix form, Eq. (5-12) can be written

$$\underline{\hat{B}} = \underline{W} \underline{b} \quad (5-13)$$

Since

$$B_{s,f} = \frac{1}{2} \left[2 \int_0^1 \sin 2\pi f\theta \text{sal}(s, \theta) d\theta \right] = \frac{1}{2} b_{f,s} \quad (5-14)$$

$$\underline{W} = \frac{1}{2} \underline{F}^T \underline{b} \quad (5-15)$$

One can solve for \underline{b} in terms of $\underline{\hat{B}}$ as follows:

$$\hat{\underline{B}} = \frac{1}{2} \underline{F}_b^T \underline{b} \quad (5-16)$$

$$\underline{F}_b \hat{\underline{B}} = \frac{1}{2} \underline{F}_b \underline{F}_b^T \underline{b} = \underline{K}_b \underline{b} \quad \text{say,} \quad (5-17)$$

so that

$$\underline{b} = \underline{K}_b^{-1} \underline{F}_b \hat{\underline{B}} \quad (5-18)$$

if \underline{K}_b is non-singular. One can solve for the set $\{b_f\}$ by a system of F linearly independent equations. Thus, S must equal or exceed F . It is shown in a later section that, in particular, for $S = 2^{M-1} \geq F$, \underline{K}_b is indeed non-singular, where M is the number of binary bits in $2S-1$. Thus, the first F Fourier coefficients can be recovered with no truncation error. As $S \rightarrow \infty$, \underline{K}_b becomes the identity matrix and Eq. (5-18) reduces to Eq. (5-7).

5.4 Dual Relationship

A dual relationship permits the determination of Walsh coefficients in terms of Fourier coefficients. Firstly, Eq. (5-16) can be used to find the Walsh coefficients of a band-limited function. There are no errors in conversion if all non-zero Fourier coefficients are used. Secondly, the S Walsh coefficients of a sequency-limited function are derived from the first F Fourier harmonics, provided that $F \geq S$. From Eq. (5-7),

$$\underline{F}_b^T \underline{b} = \underline{F}_b^T \underline{F}_b \underline{B} \quad (5-19)$$

So

$$\underline{B} = [\underline{F}_b^T \underline{F}_b]^{-1} \underline{F}_b^T \underline{b} = \underline{2}^{-1} \underline{K}_b^{-1} \underline{F}_b^T \underline{b} \quad (5-20)$$

if $[\underline{F}_b^T \underline{F}_b]$ is non-singular. For $F = S$; i.e., for a square matrix \underline{F}_b that can be inverted,

$$\underline{B} = \frac{1}{2} \underline{F}_b^T \underline{K}_b^{-1} \underline{b} \quad (5-21)$$

It is seen that the above equation is similar to Eq. (5-16) for the band-limited case. As $F \rightarrow \infty$, \underline{K}_b^{-1} becomes an identity matrix. Conversion equations similar to each of the above apply for the even coefficients a_f and A_s .

5.5 Instrumentation

Digital hardware requirements for a special-purpose Fourier to Walsh or Walsh to Fourier converter (or software requirements for computers to achieve these ends) are eased by using an important property of the matrix \underline{K}_b . It is shown in the following section that if S is an integral power of 2, \underline{K}_b diagonalizes with diagonal elements

$$K_{f,f} = \frac{1}{2} \sum_{s=1}^{2^{M-1}} (b_{f,s})^2 \quad (5-22a)$$

It has also been established that

$$K_{f,f} = \begin{cases} \text{sinc}^2 (f/2^M) , & f < 2^{M-1} \\ 2 \text{sinc}^2 (f/2^M) , & f = 2^{M-1} \end{cases} \quad (5-22b)$$

The diagonalizing property is developed by showing that the rows of \underline{F}_b are mutually orthogonal if S is an integral power of 2 that is equal to or greater than F .

The matrices \underline{F}_b and \underline{K}_b recur in each of the conversion equations (5-7), (5-16), (5-18) and (5-21) for band-limited or sequency-limited functions. By taking advantage of the diagonalizing property of \underline{K}_b , a minimum set of constants can be stored in read-only memories (ROM) of a digital converter if $F = S = 2^{M-1}$. Only the non-zero elements of a $2^{M-1} \times 2^{M-1}$ matrix \underline{F}_b and the 2^{M-1} diagonal elements of \underline{K}_b^{-1} need be stored.

Each element of a matrix \underline{F}_a consisting of the set $\{a_{f,s}\}$ is identical in absolute value with corresponding elements in the matrix \underline{F}_b . However, the signs of the constants may differ. To reduce further the storage requirements of a digital conversion instrument, one read-only memory (ROM) can be used to store the absolute values of the elements in \underline{F}_a or \underline{F}_b , while a smaller ROM stores the corresponding sign bits. Since the elements of the diagonalized \underline{K}_b matrix are squared terms, the same matrix applies to the conversion equations for both a_f and b_f . Consequently, this matrix is henceforth denoted simply \underline{K} . Peripherals about the ROM's in the instrument are used to program each of the conversion equations. Thus, one digital processor can perform the Walsh to Fourier, or the Fourier to Walsh series conversion.

As a general procedure for Walsh series and Fourier series analysis using a Walsh Spectral Analyzer, the following procedure is adopted. If the first F Fourier coefficients of a signal are to be evaluated;

- a) The signal is passed through a low-pass filter to obtain a function with at least F harmonics, i.e., the set \underline{b} .
- b) The function is analyzed using a Walsh spectral analyzer to obtain the first 2^{M-1} Walsh coefficients, i.e., the set $\hat{\underline{B}}$, where 2^{M-1} is

equal to or greater than the number of harmonics contained in the filtered signal.

- c) The set $\hat{\underline{b}}$ is used in a converter that is programmed to solve Eq. (5-18) to evaluate \underline{b} . If only the Walsh coefficients of the original signal are to be measured, the lowpass filter is by-passed.

Similarly, a Fourier spectrum analyzer in conjunction with a series converter can be used for the precise evaluation of Walsh coefficients, provided the signal is sequency filtered before analysis.

5.6 Diagonalization of the \underline{K} Matrix

Calculation procedures for the conversion equations described above are simplified and ROM storage requirements in a digital instrument that affects the conversion processes are minimized if the \underline{K} matrix can be diagonalized. From Eq. (5-17), \underline{K} is defined as

$$\underline{K} = \frac{1}{2} \underline{F}_b \underline{F}_b^T \quad (5-23)$$

It is shown that \underline{K} diagonalizes if the dimensions of \underline{F}_b are $F \times S$ such that S is an integral power of 2 and that $S \geq F$.

Since \underline{K} is a product of \underline{F}_b and its transpose, \underline{K} becomes a diagonal matrix if the rows of \underline{F}_b are mutually orthogonal. That is, if the elements of one row in \underline{F}_b are $b_{f,s}$ and the elements of another row are $b_{R,s}$, then it must be shown that with the aforementioned conditions \underline{K} contains elements $K_{f,R}$ such that

$$K_{f,R} = \frac{1}{2} \sum_{s=1}^S b_{f,s} b_{R,s} = \begin{cases} 0 & , f \neq R \\ K_{f,f} & , f = R \end{cases} \quad (5-24)$$

Multiplication constants do not affect orthogonality and are deleted from each stage of the derivation to follow.

$\text{Sal}(s, \theta)$ can be divided into 2^M uniformly-spaced intervals, where M is the number of bits in the binary representation of $2s-1$, i.e., the order of $\text{wal}(m, \theta)$ corresponding to $\text{sal}(s, \theta)$ [see Eq. (2-6)]. Let the value of the Walsh function in each interval be designated $W_{s,y}$, where $y=0, 1, 2, \dots, 2^M-1$. In each interval, $W_{s,y}$ has a value $+1$ or -1 . Eq. (5-4), which determines $b_{f,s}$, is modified to form a summation of integrals over each section of the sal function;

$$b_{f,s} = 2 \sum_{y=0}^{2^M-1} W_{s,y} \int_{\frac{y}{2^M}}^{\frac{y+1}{2^M}} \sin 2\pi f \theta d\theta \quad (5-25)$$

Let

$$S_{f,y} = \int_{\frac{y}{2^M}}^{\frac{y+1}{2^M}} \sin 2\pi f \theta d\theta \quad (5-26)$$

Then

$$b_{f,s} = 2 \sum_{y=0}^{2^M-1} W_{s,y} S_{f,y} \quad (5-27)$$

Ignoring constants, $b_{f,s}$ is proportional to the summation in Eq. (5-27),

i.e.,

$$b_{f,s} \propto \sum_{y=0}^{2^M-1} W_{s,y} S_{f,y} \quad (5-28)$$

In matrix notation, then,

$$[b_{f,s}] \propto [W_{s,0} \quad W_{s,1} \quad \dots \quad W_{s,y} \quad \dots] \begin{bmatrix} S_{f,0} \\ S_{f,1} \\ \vdots \\ S_{f,y} \\ \vdots \end{bmatrix} \quad (5-29)$$

$$= \underline{W}_s \underline{S}_f$$

The matrix \underline{F}_b which has dimensions $F \times S$ is then expanded as

$$\underline{F}_b \propto \begin{bmatrix} \underline{W}_1 \underline{S}_1 & \underline{W}_2 \underline{S}_1 & \dots & \underline{W}_s \underline{S}_1 & \dots & \underline{W}_S \underline{S}_1 \\ \underline{W}_1 \underline{S}_2 & \underline{W}_2 \underline{S}_2 & & \vdots & & \vdots \\ \vdots & & & \vdots & & \vdots \\ \underline{W}_1 \underline{S}_f & \dots & \dots & \underline{W}_s \underline{S}_f & \dots & \vdots \\ \vdots & & & & & \vdots \\ \underline{W}_1 \underline{S}_F & \dots & \dots & \dots & \dots & \underline{W}_S \underline{S}_F \end{bmatrix} \quad (5-30)$$

The rows of \underline{F}_b are mutually orthogonal if it can be shown that the element by element product of any two rows, say f and R , is zero unless $f = R$. That is,

$$K_{f,R} \propto \underline{W}_1 \underline{S}_f \underline{W}_1 \underline{S}_R + \dots + \underline{W}_s \underline{S}_f \underline{W}_s \underline{S}_R + \dots + \underline{W}_S \underline{S}_f \underline{W}_S \underline{S}_R$$

$$= \begin{cases} 0 & f \neq R \\ \text{constant} & f = R \end{cases} \quad (5-31)$$

Since $\underline{W}_s \underline{S}_f$ represents a scalar quantity [Eq. (5-29)],

$$\underline{W}_s \underline{S}_f = [\underline{W}_s \underline{S}_f]^T = \underline{S}_f^T \underline{W}_s^T \quad (5-32)$$

Therefore, Eq. (5-31) can be factored as

$$K_{f,R} \propto \underline{S}_f^T [\underline{W}_1 \underline{W}_1 + \dots + \underline{W}_s^T \underline{W}_s + \dots + \underline{W}_s^T \underline{W}_s] \underline{S}_R \tag{5-33}$$

Some properties of the matrix form of $\sum_{s=1}^S \underline{W}_s^T \underline{W}_s$ are now investigated. Firstly, $\underline{W}_s^T \underline{W}_s$ is expanded as

$$\underline{W}_s^T \underline{W}_s = \begin{bmatrix} W_{s,0} \\ W_{s,1} \\ \vdots \\ W_{s,y} \\ \vdots \\ W_{s,2^M-1} \end{bmatrix} [W_{s,0} \ W_{s,1} \ \dots \ W_{s,y} \ \dots \ W_{s,2^M-1}] \tag{5-34}$$

A convenient form for representing the expanded product on the right side of Eq. (5-34) is

$$\underline{W}_s^T \underline{W}_s \tag{5-35}$$

$$= \begin{bmatrix} W_{s,0}W_{s,0} & \dots & W_{s,0}W_{s,y-1} & W_{s,0}W_{s,y} & \dots & \dots & W_{s,0}W_{s,2^M-1} \\ \cdot & W_{s,1}W_{s,1} & & & & W_{s,1}W_{s,2^M-2} & \cdot \\ \cdot & \cdot & W_{s,y-1}W_{s,y-1} & W_{s,y-1}W_{s,y} & & & \cdot \\ \cdot & \cdot & \cdot & W_{s,y}W_{s,y} & & & \cdot \\ \cdot & \cdot & \cdot & \cdot & W_{s,y}W_{s,y-1} & & \cdot \\ \cdot & W_{s,2^M-2}W_{s,1} & & & & W_{s,2^M-2}W_{s,2^M-2} & \cdot \\ \cdot & \cdot & \cdot & \cdot & \cdot & \cdot & \cdot \\ W_{s,2^M-1}W_{s,0} & \dots & \dots & \dots & \dots & \dots & W_{s,2^M-1}W_{s,2^M-1} \end{bmatrix}$$

The matrix for $\sum_{s=1}^S \underline{W}_s^T \underline{W}_s$ is identical in form with Eq. (5-35) except that each term involves a summation over s where s has the range 1 to S . The diagonal terms of this matrix are $\sum_{s=0}^S W_{s,y}^2$. Since $W_{s,y}$ can have only the values +1 or -1, $W_{s,y}^2 = 1$ and

$$\sum_{s=1}^S W_{s,y}^2 = S \quad (5-36)$$

The cross-diagonal terms have the form

$$\sum_{s=1}^S W_{s,2^{M-1}-y} W_{s,y}$$

The two components of the product in the above expression represent intervals on the sal function that are on opposite sides of and equidistant from the midpoint of the time-base of the Walsh function (i.e., $\theta=.5$).

Since a sal function is oddly symmetric about $\theta=.5$,

$$W_{s,2^{M-1}-y} = -W_{s,y} \quad (5-37)$$

Hence,

$$\sum_{s=1}^S W_{s,2^{M-1}-y} W_{s,y} = -S \quad (5-38)$$

All other elements of $\sum_{s=1}^S \underline{W}_s^T \underline{W}_s$ can be considered as $\sum_{s=1}^S W_{s,y} W_{s,z}$, where $z \neq y$ and $z \neq 2^{M-1}-y$. It is shown that the minimum value of S for which $\sum_{s=1}^S W_{s,y} W_{s,z} = 0$ is $S = 2^{M-1}$, provided that $y_{\max} = 2^{M-1}$ and the above conditions for z and y are not violated. $W_{s,y}$ can represent both the value of the y th interval of $\text{sal}(s,\theta)$ and the y th sample of discrete $\text{sal}(s,y)$. Hence,

$$\sum_{s=1}^S W_{s,y} W_{s,z} = \sum_{s=1}^S \text{sal}(s,y) \text{sal}(s,z) \quad (5-39)$$

$$= \sum_{s=1}^S \text{wal}(2s-1,y) \text{wal}(2s-1,z)$$

Since y has a limit of 2^{M-1} , the smallest Walsh matrix \underline{W} that can contain all the discrete Walsh functions of Eq. (5-39) is a $2^M \times 2^M$ matrix (see Table 5-1). The sal functions comprise the odd-numbered rows of the matrix. Since the Walsh matrix is its own transpose, the columns also comprise the set of discrete Walsh functions.

Now consider the left half of the Walsh matrix. The elements $W_{m,y}$ of this matrix \underline{W}_α say, where $m = 0, 1, 2, \dots, 2^M - 1$ and $y = 0, 1, 2, \dots, 2^{M-1} - 1$, have the property [1] that for even values of m ,

$$W_{m,y} = W_{m+1,y} \begin{cases} m \text{ even} \\ y = 0, 1, \dots, 2^{M-1} - 1 \end{cases} \quad (5-40)$$

Thus, each pair of rows m and $m+1$ (m even) in \underline{W}_α is identical. Since each column y in \underline{W}_α represents a discrete Walsh function and since the components in the pairs of elements in each column are identical, [Eq. (5-40)], the columns in a matrix comprising only the odd-numbered rows of \underline{W}_α , \underline{W}'_α , say, also form complete discrete Walsh functions. The latter functions are comprised of 2^{M-1} bits, since 2^{M-1} rows were selected. Hence, the minimum value of s that can be used to form complete Walsh functions using odd-numbered bits in each column y for $y = 0, 1, \dots, 2^{M-1} - 1$ is $S = 2^{M-1}$.

s	m	y → 0	1	...	y	...	$2^{M-1}-1$		2^{M-1}	...	2^{M-1-y}	...	2^M-2	2^M-1
↓	↓													
	0	1	1	...	1	...	1		1	...	1	...	1	1
1	1	1	1		1		1		-1		-1		-1	-1
·	⋮	⋮									⋮			
·	y	1	1		1		-1		-1		1		1	1
·	⋮	⋮									⋮			
2^{M-2}	$2^{M-1}-1$	1	1		-1		1		-1		1		-1	-1
·	2^{M-1}	1	-1		-1		-1		-1		-1		-1	1
·	⋮	⋮									⋮			
·	2^{M-1-y}	1	-1		1		1		-1		-1		1	-1
·	⋮	⋮									⋮			
·	2^M-2	1	-1		1		-1		-1		1		-1	1
2^{M-1}	2^M-1	1	-1		1		-1		1		-1		1	-1

Table 5-1 Set of 2^M Discrete Walsh Functions

The matrix \underline{W}_β , say, that forms the right half of \underline{W} contains elements $W_{m,y}$, where $m = 0, 1, 2, \dots, 2^{M-1}$ and $y = 2^{M-1}, 2^{M-1}+1, \dots, 2^M-1$. In this case, the pairs of elements in the columns have the property [1];

$$W_{m,y} = -W_{m+1,y} \begin{cases} m \text{ even} \\ y = 2^{M-1}, 2^{M-1}+1, \dots, 2^M-1 \end{cases} \quad (5-41)$$

By reasoning similar to that for the matrix \underline{W}_α , the matrix comprising the 2^{M-1} odd-numbered rows of \underline{W}_β , $\underline{W}_{\beta'}$, say, has columns which are negative discrete Walsh functions. Again, the minimum value for s is $S = 2^{M-1}$.

Due to odd symmetry of the sal functions, the columns of $\underline{W}_{\beta'}$ are the negatives of the columns of \underline{W}_α , taken in reverse order. That is,

$$\text{sal}(s,y) = -\text{sal}(s, 2^M-1-y) \quad y = 0, 1, \dots, 2^M-1 \quad (5-42)$$

or

$$W_{s,y} = -W_{s, 2^M-1-y} \quad (5-37)$$

Let a new matrix \underline{W}_K be formed by the concatenation of matrices \underline{W}_α , and $\underline{W}_{\beta'}$. The product of any two columns y and z in \underline{W}_K is

$$\sum_{s=1}^{2^{M-1}} W_{s,y} W_{s,z}$$

Since the columns comprise discrete Walsh functions, which form a mutually orthogonal set;

$$\sum_{s=1}^{2^{M-1}} W_{s,y} W_{s,z} = 0 \quad z \neq y, z \neq 2^M-y-1 \quad (5-43)$$

then for each of the 2^M integrals contained in the interval

$$S_{f,y} = -S_{f,2^M-1-y} \quad (y = 0,1,2,\dots,2^M-1) \quad (5-49)$$

Hence, Eq. (5-48) simplifies to

$$K_{f,R} \propto 2 \sum_{y=0}^{2^M-1} S_{R,y} S_{f,y} \quad (5-50)$$

where f and R are equal to or less than the number of Fourier terms F contained in the signal.

It is now shown that the condition $S \geq F$, where $S = 2^{M-1}$, is a sufficient condition to ensure orthogonality of the summation in Eq. (5-50). Thus, the K matrix would become diagonal for the conditions

$$S = 2^{M-1} \geq F \geq f \geq 1 \quad (5-51)$$

By Eq. (5-26),

$$\begin{aligned} \sum_{y=0}^{2^M-1} S_{f,y} S_{R,y} &= \sum_{y=0}^{2^M-1} \int_{\frac{y}{2^M}}^{\frac{y+1}{2^M}} \sin 2\pi f \theta d\theta \int_{\frac{y}{2^M}}^{\frac{y+1}{2^M}} \sin 2\pi R \theta d\theta \quad (5-52) \\ &= \sum_{y=0}^{2^M-1} \left\{ \frac{-1}{2\pi f} \left[\cos 2\pi f \left(\frac{y+1}{2^M} \right) - \cos 2\pi f \left(\frac{y}{2^M} \right) \right] \right. \\ &\quad \left. \cdot \frac{-1}{2\pi R} \left[\cos 2\pi R \left(\frac{y+1}{2^M} \right) - \cos 2\pi R \left(\frac{y}{2^M} \right) \right] \right\} \\ &= \frac{1}{4\pi^2 fR} \sum_{y=0}^{2^M-1} \left\{ \left[-2 \sin \frac{\pi f(2y+1)}{2^M} \sin \frac{\pi f}{2^M} \right] \left[-2 \sin \frac{\pi R(2y+1)}{2^M} \sin \frac{\pi R}{2^M} \right] \right\} \\ &= \left[\frac{1}{\pi^2 fR} \sin \frac{\pi f}{2^M} \sin \frac{\pi R}{2^M} \right] \sum_{y=0}^{2^M-1} \sin \frac{\pi f(2y+1)}{2^M} \sin \frac{\pi R(2y+1)}{2^M} \end{aligned}$$

$$\text{When } f \neq R, \quad \left| \frac{1}{\pi^2 f R} \sin \frac{\pi f}{2^M} \sin \frac{\pi R}{2^M} \right| \geq 0 \quad (5-53)$$

$$\text{When } f = R, \quad \left| \frac{1}{\pi^2 f R} \sin \frac{\pi f}{2^M} \sin \frac{\pi R}{2^M} \right| = \frac{1}{\pi^2 f^2} \left[\sin \frac{\pi f}{2^M} \right]^2 > 0 \quad (5-54)$$

If \underline{K} is to be a non-singular diagonal matrix that can be inverted for use in the conversion equations listed in section 5.5, an element $K_{f,f}$ (i.e., $f = R$) on the diagonal may not have the value zero. With $1 \leq f \leq 2^{M-1}$ according to the conditions specified by Eq. (5-51), the expression in Eq. (5-54) is indeed greater than zero. Hence, $\frac{1}{\pi^2 f R} \sin \frac{\pi f}{2^M} \sin \frac{\pi R}{2^M}$ can be considered as a constant that does not affect the orthogonality of the summation expression in the last line of Eq. (5-52). Thus,

$$K_{f,R} \propto \sum_{y=0}^{2^M-1} \left[\sin \frac{\pi f(2y+1)}{2^M} \sin \frac{\pi R(2y+1)}{2^M} \right] \quad (5-55)$$

If $R = f$, Eq. (5-55) becomes

$$K_{f,f} \propto \sum_{y=0}^{2^M-1} \left[\sin \frac{\pi f(2y+1)}{2^M} \right]^2 \quad (5-56)$$

As previously explained, $K_{f,f}$ may not equal zero. This condition is satisfied if at least one term of the summation in Eq. (5-56) does not equal zero. Since $1 \leq f \leq 2^{M-1}$ [Eq. (5-51)] and $y = 0, 1, 2, \dots, 2^{M-1}-1$, the argument of the sine for at least one term must be $\frac{\pi f}{2^M}$ where

$$\frac{\pi f}{2^M} \leq \frac{\pi f}{2^M} \leq \frac{\pi}{2}$$

and f is an integer. Hence,

$$K_{f,f} \neq 0 \quad [1 \leq f \leq F \leq 2^{M-1} = S] \quad (5-57)$$

If $f \neq R$, it is yet to be shown that the conditions of Eq. (5-51) are sufficient to ensure that $K_{f,R} = 0$. First, let Eq. (5-55) be expanded to

$$K_{f,R} \propto \frac{1}{2} \left\{ \sum_{y=0}^{2^M-1} \cos \frac{2\pi(f-R)(2y+1)}{2^{M+1}} - \sum_{y=0}^{2^M-1} \cos \frac{2\pi(f+R)(2y+1)}{2^{M+1}} \right\} \quad (5-58)$$

From the above,

$$\begin{aligned} \sum_{y=0}^{2^M-1} \cos \frac{2\pi(f-R)(2y+1)}{2^{M+1}} &= \operatorname{Re} \left\{ \frac{1}{2} \sum_{y=0}^{2^M-1} \left[\exp\left(\frac{2j\pi[f-R][2y+1]}{2^{M+1}}\right) \right. \right. \\ &\quad \left. \left. + \exp\left(\frac{2j\pi[R-f][2y+1]}{2^{M+1}}\right) \right] \right\} \\ &= \operatorname{Re} \left\{ \left[\frac{1}{2} \exp\left(\frac{j\pi[f-R]}{2^M}\right) \right] \sum_{y=0}^{2^M-1} \exp\left(\frac{j\pi[f-R]2y}{2^M}\right) \right. \\ &\quad \left. + \left[\frac{1}{2} \exp\left(\frac{j\pi[R-f]}{2^M}\right) \right] \sum_{y=0}^{2^M-1} \exp\left(\frac{j\pi[R-f]2y}{2^M}\right) \right\} \end{aligned} \quad (5-59)$$

where $j = \sqrt{-1}$. Each of the summations in the latter portion of Eq. (5-59) can be represented as a geometric series if the summation is modified to become

$$\sum_{y=0}^{2^M-1} \exp\left(\frac{j\pi[f-R]2y}{2^M}\right) = \sum_{y=0}^{2^M-1} \left(\left[\exp\left(\frac{j\pi}{2^M}\right) \right]^{2[f-R]} \right)^y \quad (5-60)$$

The right side of Eq. (5-60) is a geometric series whose form and sum are

$$\sum_{y=0}^{2^M-1} (q)^y = \left(\frac{q^{2^M} - 1}{q - 1} \right) \quad \text{where } q \neq 1 \quad (5-61)$$

Consequently,

$$\sum_{y=0}^{2^M-1} \left(\exp\left(\frac{j\pi}{2^M}\right) \right)^{2[f-R]y} = \frac{\exp[j2\pi(f-R)]-1}{\exp\left[2\left(\frac{j\pi}{2^M}\right)(f-R)\right]-1} \quad (5-62)$$

Since f and R are integers,

$$\exp[j2\pi(f-R)] = (-1)^{2(f-R)} = 1 \quad (5-63)$$

Hence,

$$\sum_{y=0}^{2^M-1} \exp\left(\frac{j\pi[f-R]2y}{2^M}\right) = 0 \quad \text{if } \exp\left[2(f-R)\left(\frac{j\pi}{2^M}\right)\right] \neq 1 \quad (5-64)$$

Similar expansions of each summation in Eq. (5-58) lead to the following result;

$$K_{f,R} = 0 \quad \text{if } f \neq R \quad (5-65)$$

$$\text{and } \exp\left[\pm(f-R)\left(\frac{j2\pi}{2^M}\right)\right] \neq 1$$

$$\text{and } \exp\left[\pm(f+R)\left(\frac{j2\pi}{2^M}\right)\right] \neq 1 .$$

Since $\exp(j\pi i) = 1$ if i is an integer, the following conditions are required to ensure that the exponential functions in the requirements to satisfy Eq. (5-65) do not equal unity;

$$|\pm(f-R)| \neq 2^M \quad (5-66)$$

$$|\pm(f+R)| \neq 2^M, \quad f \neq R$$

From Eq. (5-51), if $S \geq F$ and $S = 2^{M-1}$,

$$2^{M-1} \geq F \quad (5-67)$$

$$2^M \geq 2F > 2F-1 \quad (5-68)$$

Since $f \neq R$ and both f and R are equal to or less than F , the largest value of $f+R$ is $2F-1$. Hence,

$$2^M > f+R = |\pm(f+R)| \quad (5-69)$$

for the conditions in Eq. (5-51). Similarly, the largest value of $|\pm(f-R)|$ is $F-1$, so that

$$2^M \geq 2F > F-1 \geq |\pm(f-R)| \quad (5-70)$$

Thus, Eq. (5-66) is verified. Consequently, it has been shown that the \underline{K} matrix diagonalizes when the dimensions of the \underline{F}_b matrix are $F \times S$ where $S = 2^{M-1} \geq F$ and M is the number of bits in the binary representation of $2S-1$.

A similar derivation demonstrates the diagonalization of the \underline{K} matrix for use in conversion equations for the coefficients a_f and A_s of the even terms in the Fourier and Walsh series, respectively. However, some small changes in the derivation are required. In order for the matrix involving a summation of terms $\underline{W}_s^T \underline{W}_s$ [comparable to Eq. (5-35)] to have a form similar to Eq. (5-46), s must be in the range $s = 0, 1, \dots, 2^{M-1}-1$. This is easily seen by following a derivation similar to that using the matrices \underline{W}_α , \underline{W}_β , and \underline{W}_K for the b_f and B_s coefficients but using the even-numbered rows of the set of discrete Walsh functions in Table 5-1. 2^{M-1} rows of this matrix, beginning with row 0, must be used to obtain a

matrix for $\sum_{s=0}^{2^{M-1}-1} \underline{W}_s^T \underline{W}_s$ comparable to Eq. (5-46). However, this new matrix

has cross-diagonal elements which are each $+2^{M+i-1}$ rather than -2^{M+i-1} . Consequently, this portion of the derivation indicates that the \underline{F}_a matrix used in the definition of \underline{K} , i.e., $\underline{K} = \frac{1}{2} \underline{F}_a \underline{F}_a^T$ should have the form [cf. Eq. (5-30)];

$$\underline{F}_a \propto \begin{bmatrix} \underline{W}_0 \underline{C}_0 & \underline{W}_1 \underline{C}_0 & \dots & \underline{W}_s \underline{C}_0 & \dots & \underline{W}_{2^M-1} \underline{C}_0 \\ \underline{W}_0 \underline{C}_1 & \underline{W}_1 \underline{C}_1 & & \cdot & & \cdot \\ \vdots & \vdots & & \cdot & & \cdot \\ \underline{W}_0 \underline{C}_f & \cdot & \cdot & \underline{W}_s \underline{C}_f & \cdot & \cdot \\ \vdots & \vdots & & \vdots & & \vdots \\ \underline{W}_0 \underline{C}_{2^M-1} & \cdot & \cdot & \cdot & \cdot & \underline{W}_{2^M-1} \underline{C}_{2^M-1} \end{bmatrix} \quad (5-71)$$

where \underline{C}_f is a matrix whose elements $C_{f,y}$ are

$$C_{f,y} = \int_{\frac{y}{2^M}}^{\frac{y+1}{2^M}} \cos 2\pi f \theta d\theta \quad (y = 0, 1, 2, \dots, 2^M-1) \quad (5-72)$$

As indicated previously, the Fourier coefficients of the Walsh functions, $b_{f,s}$ and $a_{f,s}$, which are proportional to $\underline{W}_s \underline{S}_f$ and $\underline{W}_s \underline{C}_f$, respectively, have the same magnitude, with the possibility of a difference in sign. For the instrument described in section 5.5 it is desirable to store a single matrix \underline{F} which contains only the magnitudes of $b_{f,s}$ or $a_{f,s}$ and which could be used in the conversion of coefficients A_s and B_s to a_f and b_f , respectively. Accordingly, one ROM containing the diagonal elements of \underline{K} would suffice for both conversions.

If the first row and column of \underline{F}_a in Eq. (5-71) could be deleted and if a new row and column containing elements $\underline{W}_1 \underline{C}_{2M-1}$ to $\underline{W}_{2M-1} \underline{C}_{2M-1}$ and $\underline{W}_{2M-1} \underline{C}_1$ to $\underline{W}_{2M-1} \underline{C}_{2M-1}$, respectively, could be concatenated with \underline{F}_a without changing the mutual orthogonality of the rows, then the \underline{F}_a and \underline{F}_b would be identical in form (only the signs of the elements would differ). The pattern of non-zero elements of the Fourier coefficients of Walsh functions (see section 5.9) is such that $\underline{W}_0 \underline{C}_0$ is the only element in both the first row and first column of the matrix in Eq. (5-71) which is non-zero. Thus, deletion of the row and column does not affect the mutual orthogonality of the remaining rows. Similarly, $\underline{W}_{2M-1} \underline{C}_{2M-1}$ is the only non-zero element in the row and column to be concatenated with \underline{F}_a . Again, there is no change in the mutual orthogonality of the rows.

Deletion of the first row and column of \underline{F}_a affects the conversion only of a_0 and A_0 , that is, the average value of each series. Although the average value of the Fourier series was defined as $a_0/2$, this is only for convenience in obtaining a consistent definition for a_f . The average value component of a Walsh series equals the average value component in a Fourier series of the same signal. Thus, no conversion process is required if the average value component in either series is known. In addition, this component does not affect the conversion of any other coefficients, so again it may be ignored in any conversion procedures.

Numerical values of the elements $a_{f,s}$ or $b_{f,s}$ in the \underline{F}_a or \underline{F}_b matrices, respectively, can be evaluated from equations for the Fourier transforms of the corresponding Walsh functions. In the following section, a non-recursive equation that is used to obtain the Fourier transform of any Walsh function is derived.

5.7 A Non-recursive Equation for the Fourier Transform of a Walsh Function

The Fourier transforms of Walsh functions are needed to evaluate the constants in the equations used to convert the Walsh series of a signal to a Fourier series representation. Partial listings of the transforms are available [1,4]. Beyond this range, unlisted transforms may be obtained using a recursive equation [4], which can be tedious, or by using an expression due to Blachman [5] for the Walsh transform of sinusoids, which can be modified to yield the Fourier transform of a Walsh function. In the latter process, sine or cosine terms in the transform are selected accordingly as the sum of adjacent bits in the binary representation of the order is odd or even. An alternative expression for the Fourier transform of a Walsh function is developed below, which differs from previous expressions in that it incorporates the Gray code representation of the order of the function. The expression is non-recursive and it is also unified in the sense that no sine or cosine factor selection process is involved in conjunction with it. This expression leads to an algorithm whereby the transform may be obtained simply from inspection of the bits in the Gray code representation.

Let the two-sided Fourier transform of a Walsh function, $wal(m, \theta)$ be defined by

$$F[wal(m, \theta)] = \int_{-\frac{1}{2}}^{\frac{1}{2}} wal(m, \theta) e^{j2\pi f \theta} d\theta \quad (5-73)$$

where m is the order of the function and θ is the normalized time.

$\text{Cal}(s, \theta)$ and $\text{sal}(s, \theta)$, respectively, have the Fourier transforms

$$F[\text{cal}(s, \theta)] = a(f, s) = \int_{-\frac{1}{2}}^{\frac{1}{2}} \text{cal}(s, \theta) \cos 2\pi f \theta d\theta \quad (5-74)$$

$$F[\text{sal}(s, \theta)] = jb(f, s) = j \int_{-\frac{1}{2}}^{\frac{1}{2}} \text{sal}(s, \theta) \sin 2\pi f \theta d\theta \quad (5-75)$$

Since the Walsh functions are discontinuous, evaluation of Eqs. (5-73) to (5-75) would normally involve a summation of integrals.

It is convenient to view a continuous Walsh function as a convolution of the sequence of unit impulses at points corresponding to samples in a discrete Walsh function over the interval $-\frac{1}{2} \leq \theta < \frac{1}{2}$ with a rectangular pulse of unit magnitude and of width $1/2^M$ equal to the spacing of the unit impulses. The Fourier transform of the continuous Walsh function is then the product of the transforms of the discrete Walsh function and the rectangular pulse. This is shown to be

$$F[\text{wal}(m, \theta)] = (-1)^{g_0} (-j)^\alpha \left[\prod_{k=0}^{M-1} \cos\left(\frac{\pi f}{2^{k+1}} - g_k \frac{\pi}{2}\right) \right] \text{sinc}(f/2^M) \quad (5-76)$$

where $j = \sqrt{-1}$.

g_k is a bit in the Gray code representation of m , as in Eq. (2-17), α is the number of Gray code bits of value ONE, and

$$\text{sinc}(f/2^M) = \frac{\sin(\pi f/2^M)}{\pi f/2^M} \quad (5-77)$$

To derive Eq. (5-76), we begin by defining the discrete Walsh function unit pulse sequence over one period. Referring to the example in Fig. 5-2(a), a discrete $wal(m, \theta)$ in the range $0 \leq \theta < 1$ consists of a sequence of 2^M positive and negative unit impulses, where $\delta(\theta - \theta_y)$ denotes an impulse at $\theta_y = y/2^M$, $y = 0, 1, 2, \dots, 2^M - 1$. Each impulse can also be described in terms of an operator d^y , where

$$d^y \delta(\theta) = \delta(\theta - \theta_y) \quad (5-78)$$

The delay operator has the property

$$d^y d^z = d^{y+z} \quad (5-79)$$

The sign of an impulse at $\theta_y = y/2^M$ can be obtained from a parity check for an even number of ONE's in the Gray code for m that are enabled by the bits y_{M-1-k} of binary y . That is

$$wal(m, \theta_y) = \prod_{k=0}^{M-1} (-1)^{g_k y_{M-1-k}} \quad (2-21)$$

where g_k are the bits of the Gray code [Eq. (2-17)].

In Eq. (2-21) it suffices to consider only those terms for which $y_{M-1-k} = 1$. For example, if $\theta_y = 6/8$, $y = 6 = 110_2$, $M = 3$ and

$$(-1)^{g_0 y_2} (-1)^{g_1 y_1} (-1)^{g_2 y_0} = (-1)^{g_0} (-1)^{g_1} \quad (5-80)$$

The value of the discrete Walsh function at $\theta_y = 6/8$ can then be written

$$wal(m, \theta_6) = (-1)^{g_0} (-1)^{g_1} d^6 \delta(\theta) \quad (5-81)$$

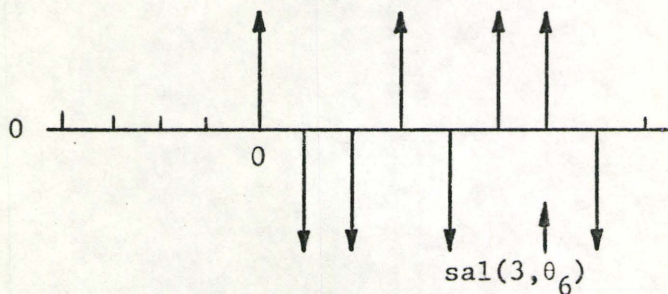
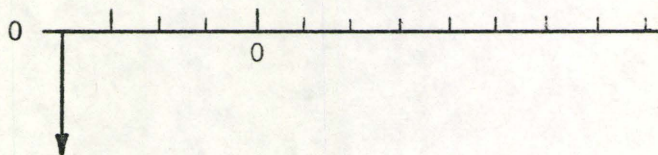
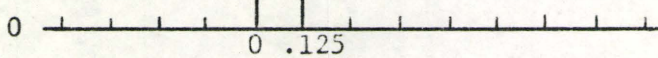
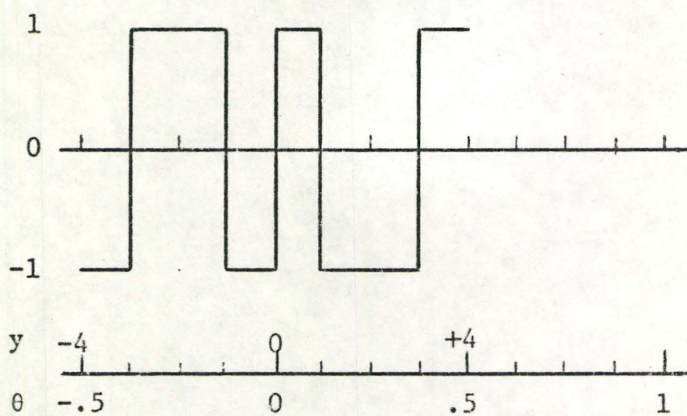
(a) discrete $\text{sal}(3, \theta)$ (b) $\text{sal}(3, -\frac{1}{2})$ (c) $u(\theta) - u(\theta - \frac{1}{8})$ (d) $\text{sal}(3, \theta)$ 

Fig. 5-2 Convolution Quantities to Form $\text{sal}(3, \theta)$
over the Range $-\frac{1}{2} \leq \theta < \frac{1}{2}$.

If now $m = 5$, $wal(5, \theta_6) = sal(3, \theta_6)$; then $m = 101_2 = 111$ Gray. So $g_0 = g_1 = 1$ and $sal(3, \theta_6) = +1 d^6 \delta(\theta)$ [see Fig. 5-2(a)]. Similarly,

$$wal(m, \theta_0) = d^0 \delta(\theta) \quad (5-82)$$

The summation of unit impulses, each of the form of Eq. (5-81), that define a discrete Walsh function over the interval $0 \leq \theta < 1$ may be factored to yield

$$\text{discrete } wal(m, \theta) = \prod_{k=0}^{M-1} [d^0 + (-1)^{g_k} d^{2^{M-1-k}}] \delta(\theta) \quad (5-83)$$

Convolution of a delta function having the same sign as the corresponding continuous Walsh function at $\theta = -\frac{1}{2}$ with Eq. (5-83) achieves a shift in the range of the discrete Walsh function from $0 \leq \theta < 1$ to $-\frac{1}{2} \leq \theta < \frac{1}{2}$. The sign of this δ -function is negative for functions of odd sequency and positive for functions of even sequency. Since the Gray code bit $g_0 = 1$ iff the sequency is odd, the required δ -function at $\theta = -\frac{1}{2}$ can be represented as

$$\text{discrete } wal(\theta, -\frac{1}{2}) = (-1)^{g_0} d^{-2^{M-1}} \delta(\theta) \quad (5-84)$$

The same representation is achieved if the 2's-complement representation for negative values of y are used in Eq. (2-21) (as explained in chapter 2) and then the form of Eq. (5-81) is applied.

The final convolving quantity is a unit amplitude pulse of width $1/2^M$. If $u(\theta - \theta_y)$ defines a unit step at $\theta_y = y/2^M$, then the required pulse is

$$P(\theta_1) = u(\theta) - u(\theta - \theta_1) \quad (5-85)$$

Hence,

$$\text{wal}(m, \theta) = \prod_{k=0}^{M-1} [d^0 + (-1)^{g_k} d^{2^{M-1-k}}] \delta(\theta) \quad (5-86)$$

$$* (-1)^{g_0} d^{-2^{M-1}} \delta(\theta)$$

$$* [u(\theta) - u(\theta - \theta_1)]$$

where $-\frac{1}{2} \leq \theta < \frac{1}{2}$. Examples of the three convolving quantities are shown in Figs. 5-2(a) to 5-2(c), resulting in the continuous Walsh function $\text{sal}(3, \theta)$ shown in Fig. 5-2(d).

The Fourier transform of $\text{wal}(m, \theta)$ is the product of the transforms of Eqs. (5-83) to (5-85). Each unit impulse that comprises the discrete Walsh function has the Fourier transform

$$\begin{aligned} F\left[\prod_{k=0}^{M-1} (-1)^{g_k} d^{y_{M-1-k}} \delta(\theta)\right] &= \left[\prod_{k=0}^{M-1} (-1)^{g_k} d^{y_{M-1-k}}\right] \int_0^1 \delta(\theta - \theta_y) \exp(j2\pi f\theta) d\theta \\ &= \left[\prod_{k=0}^{M-1} (-1)^{g_k} d^{y_{M-1-k}}\right] \exp(j\pi f y / 2^{M-1}) \end{aligned} \quad (5-87)$$

The only change, then, in the summation of impulses that form discrete $\text{wal}(m, \theta)$ and in its transform is that $\exp(j\pi f y / 2^{M-1})$ replaces $d^y \delta(\theta)$. Hence, the sum of the Fourier transforms of the unit impulses of discrete $\text{wal}(m, \theta)$ can be factored in a manner similar to Eq. (5-83). Replacing $d^0 \delta(\theta)$ and $d^{2^{M-1-k}} \delta(\theta)$ by their Fourier transforms, 1 and $\exp(j\pi f / 2^k)$, respectively,

$$F[\text{discrete wal}(m, \theta)] = \prod_{k=0}^{M-1} [1 + (-1)^{g_k} \exp(j\pi f / 2^k)] \quad (5-88)$$

Each factor in Eq. (5-88) can be rewritten as a sine or cosine, depending on the value of the Gray code bit. If $g_k = 1$,

$$[1 - \exp(j\pi f/2^k)] = 2j\exp(j\pi f/2^{k+1})\sin(\pi f/2^{k+1}) \quad (5-89)$$

If $g_k = 0$,

$$[1 + \exp(j\pi f/2^k)] = 2\exp(j\pi f/2^{k+1})\cos(\pi f/2^{k+1}) \quad (5-90)$$

The ONE bits in the Gray code number $G = g_0g_1g_2\dots g_k\dots$ for the order m correspond to the sine factors of the transform [Eq. (5-89)]. If there are α ONE's in G , then the sinusoidal form of Eq. (5-88) is

$$F[\text{discrete wal}(m, \theta)] \quad (5-91)$$

$$= 2^M (-j)^\alpha \exp j\pi f \left(\frac{1}{2} + \frac{1}{4} + \dots + \frac{1}{2^M} \right) \prod_{k=0}^{M-1} \cos \left(\frac{\pi f}{2^{k+1}} - g_k \frac{\pi}{2} \right)$$

$$= 2^M (-j)^\alpha \exp j\pi f \left(1 - \frac{1}{2^M} \right) \prod_{k=0}^{M-1} \cos \left(\frac{\pi f}{2^{k+1}} - g_k \frac{\pi}{2} \right)$$

where

$$\cos \left(\frac{\pi f}{2^{k+1}} - g_k \frac{\pi}{2} \right) = \sin \frac{\pi f}{2^{k+1}} \quad \text{if } g_k = 1.$$

The Fourier transforms of Eqs. (5-84) and (5-85), respectively, are

$$F[(-1)^{g_0} d^{-2^{M-1}} \delta(\theta)] = (-1)^{g_0} \exp(-j\pi f) \quad (5-92)$$

$$F[U(\theta) - U(\theta - \theta_1)] = \frac{1}{2^M} \exp(j\pi f/2^M) \text{sinc}(f/2^M) \quad (5-93)$$

The product of Eqs. (5-91), (5-92) and (5-93) is the non-recursive Fourier transform equation (5-76).

5.8 Algorithm to Determine Fourier Transform of Wal(m,θ)

Using Eq. (5-76), a simple algorithm is now developed for the Fourier transform of a Walsh function. It uses only the bits in the Gray code number G that represents the order m . In Eq. (5-76) it is seen that each factor depends on G ; thus g_0 and g_k are bits in G , α is the number of bits that equal ONE, and M is the number of bits in G .

The first step of the algorithm is to write G as $g_0g_1g_2\cdots g_k\cdots g_{M-1}$. Whenever $g_k = 0$, substitute $\cos(\pi f/2^{k+1})$ and where $g_k = 1$, substitute $\sin(\pi f/2^{k+1})$ to yield an expression in the form of a product of cosine and sine terms. There are as many terms (i.e., M) in the product expression as there are bits in G . The next step is to multiply the expression obtained thus far by $\text{sinc}(f/2^M) = [\sin(\pi f/2^M)]/(\pi f/2^M)$.

The sign of the transform is given by $(-1)^{g_0}(-j)^\alpha$. A simple counting procedure is convenient. Form

$$\beta = \alpha + \langle \alpha/2 \rangle + g_0 \quad (5-94)$$

where $\langle \alpha/2 \rangle$ denotes the integer part of $\alpha/2$. If β is odd, the sign of the transform is negative. If $\alpha/2$ is not an integer, multiply the transform by $j = \sqrt{-1}$. An example to illustrate the algorithm follows.

Let us find, say, the Fourier transform of $\text{sal}(5, \theta)$. $\text{Sal}(5, \theta) = \text{wal}(9, \theta)$, so the order $m = 9 = 1001_2$. The corresponding Gray code number is $G = 1101 = g_3g_2g_1g_0$. Substituting sines and cosines for $g_0 \rightarrow g_3$ yields

$$\sin \frac{\pi f}{2} \cos \frac{\pi f}{4} \sin \frac{\pi f}{8} \sin \frac{\pi f}{16}$$

The above expression is multiplied by $[\sin(\pi f/16)]/(\pi f/16)$.

To obtain the sign, there are three ONE's in G so $\alpha = 3$. Also, $g_0 = 1$. Hence,

$$\beta = 3 + \langle 3/2 \rangle + 1 = 5 \quad (5-95)$$

which is odd, so the sign is negative. Since α is odd, multiply by j . Consequently, the Fourier transform of $wal(9, \theta)$ is

$$jb(f, 5) = -j \sin \frac{\pi f}{2} \cos \frac{\pi f}{4} \sin \frac{\pi f}{8} \frac{\sin^2(\pi f/16)}{\pi f/16} \quad (5-96)$$

To obtain the Fourier series coefficients of a periodic Walsh function, the transform expression is evaluated for integral values of the normalized frequency f . Since the equation (5-76) applies to the two-sided transform, the coefficients obtained using values of $f = 1, 2, \dots$ are doubled to obtain the coefficients of the one-sided series, that is, the coefficients $a_{f,s}$ and $b_{f,s}$. The magnitudes of the coefficients $a_{f,s}$ and $b_{f,s}$ form the \underline{F} matrix, the elements of which are to be stored in a ROM in a digital instrument that performs the Walsh series to Fourier series conversion. To minimize the number of stored constants, it is required to use only the non-zero components. A discussion of the pattern of non-zero elements, i.e., the coefficients $|a_{f,s}|$ or $|b_{f,s}|$, in the \underline{F} matrix, is given in the following section.

5.9 Pattern of Non-zero Elements in the \underline{F} Matrix

The elements $|b_{f,s}|$ of the \underline{F} matrix are derived from

$$b_{f,s} = 2 \int_0^1 \text{sal}(s, \theta) \sin 2\pi f \theta d\theta \quad (5-4)$$

where $f = 1, 2, 3, \dots$. If s is odd, the sal function is oddly symmetric about the centre of its fundamental period $0 \leq \theta < 1$. Thus, these functions have non-zero Fourier coefficients only for the odd-numbered harmonics; that is, $b_{1,s}, b_{3,s}, b_{5,s}, \dots, b_{2Q-1,s}, \dots$ are non-zero ($Q = 1, 2, 3, \dots$). If s is doubled, $\text{sal}(2s, \theta)$ can be considered as a wave $\text{sal}(s, \theta)$ with a time-base that has been halved. Consequently, $\text{sal}(2s, \theta)$ has non-zero coefficients whose harmonic numbers are double those of $\text{sal}(s, \theta)$; that is, $b_{2,2s}, b_{6,2s}, b_{10,2s}, \dots, b_{2(2Q-1),2s}, \dots$ are non-zero. By induction, $\text{sal}(2^x s, \theta)$ has the non-zero coefficients $b_{2^x, 2^x s}, b_{2^x(3), 2^x s}, b_{2^x(5), 2^x s}, \dots, b_{2^x(2Q-1), 2^x s}, \dots$. However, s in each of these cases is an odd number, say, $2X-1$, where $X = 1, 2, 3, \dots$. Hence, all coefficients and only those coefficients of the form

$$b_{f,s} = b_{2^x(2Q-1), 2^x(2X-1)} \quad (5-97)$$

are non-zero. In a row f in \underline{F} , the column numbers containing non-zero elements are $2^x(2X-1)$, where $X = 1, 2, 3, \dots$, and x is determined by f . Any integer f can be represented by $2^x(2Q-1)$ where the binary representation of f is a binary number $2Q-1$ followed by x ZEROS. Say, for example, one wishes to determine the Fourier coefficient b_6 using only the non-zero terms of Eq. (5-8). The coefficient number 6 can be represented as $(2^1)(3)$ or 110_2 . One zero follows binary 3 or 11_2 . Thus, $x = 1$. Consequently, from Eqs. (5-8) and (5-97);

$$b_6 = b_{6,2} B_2 + b_{6,6} B_6 + b_{6,10} B_{10} + \dots + b_{6,2^x(2X-1)} B_{2^x(2X-1)} + \dots \quad (5-98)$$

where $x = 1$ and $X = 1, 2, 3, \dots$. Similarly, if x is determined for any given

Fourier coefficient number, this information can be used to select coefficients from a ROM in a digital Walsh to Fourier series converter, and match the coefficients with the appropriate Walsh coefficients to evaluate b_f . In this manner, only the terms $|b_{f,s}|$ or $|a_{f,s}|$ which are non-zero need be stored in the ROM.

For the F_a matrix [see Eq. (5-71)], it has been indicated that the row $f = 2^{M-1}$ and column $s = 2^{M-1}$ could be concatenated with F_a without affecting the mutual orthogonality of the rows in the matrix. This property holds true only if the coefficient $a_{2^{M-1}, 2^{M-1}}$ is the only non-zero element in either the concatenated row or column. For $f = 2^{M-1} = 2^x(2^0-1)$, $x = M-1$. The first non-zero element in row 2^{M-1} is then $2^x(2^x-1) = 2^{M-1}$, where $x = 1$. Similarly, the first non-zero element in column $s = 2^{M-1}$ is $a_{2^{M-1}, 2^{M-1}}$. Thus, mutual orthogonality of the rows in F_a is preserved despite concatenation of the new row and column.

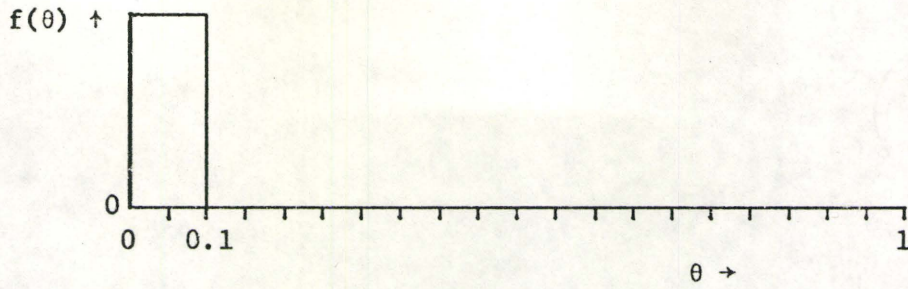
5.10 Comparison of Walsh and Fourier Series Analysis and Synthesis

A number of studies have been made of the usefulness of the Walsh and related spectra in comparison with the more commonly used Fourier spectrum [5-8]. The Walsh spectrum appears to be better suited for analyzing discontinuous functions than is the Fourier spectrum. For example, a square wave has but one Walsh component whereas the Fourier spectrum of the same function is infinite. Conversely, however, the Fourier spectrum displays an obvious advantage in analyzing a sinusoidal wave. This section of the thesis gives only a few graphic examples of waveforms with their corresponding Fourier and Walsh line spectra. The

waveforms are then synthesized in both the Fourier and Walsh sense, using an increasing number of spectral components for each representation. The figures are intended to provide only a feel of waveform synthesis in each domain. A brief, subjective analysis is given for each example.

Fig. 5-3(a) shows one cycle of a rectangular pulse wave with duty cycle of 0.1. All waveforms in the following examples have normalized fundamental periods T over the range $[0,1)$. The first 64 even and odd components of the Fourier spectrum of the pulse wave are shown as line spectra in Figs. 5-3(b) and 5-3(c), respectively. If the waves have a normalized period of T seconds, the spectral lines have a spacing of $1/T$. The corresponding Walsh line spectra are given in Figs. 5-3(d) and 5-3(e). An arbitrary amplitude scale is used for all illustrations, each of which is plotted by computer. It is readily seen in Fig. 5-3 that both Fourier and Walsh spectra oscillate, although the Walsh components appear to diminish in amplitude more rapidly. This effect is displayed to a certain extent in the Fourier series and Walsh series synthesis of the rectangular wave shown in Fig. 5-4. Since each series tends to converge in the least squares sense, the series which diminishes in spectral content more rapidly tends to converge more rapidly when the waveform is synthesized.

Figs. 5-4(a) to 5-4(f) show the synthesis of the Fourier series of the rectangular pulse using 2, 4, 8, 16, 32 and 64 components, respectively. Figs. 5-4(g) to 5-4(l) illustrate the build-up of the corresponding Walsh series, again with double the number of components in each succeeding figure. In this case, Walsh synthesis, which generates a step-function as opposed to a continuous function for Fourier series



(a) Rectangular Pulse

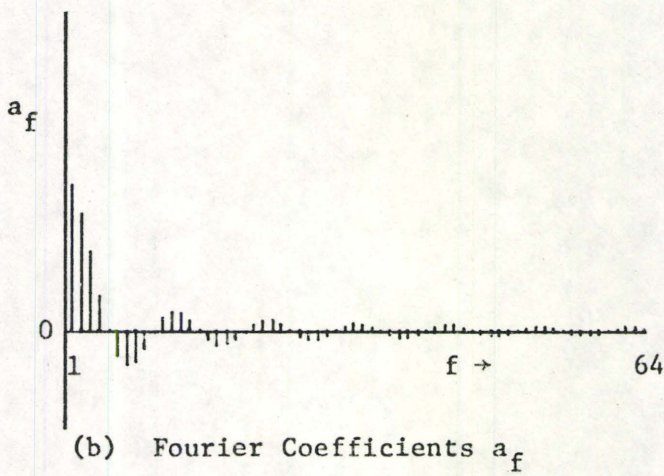
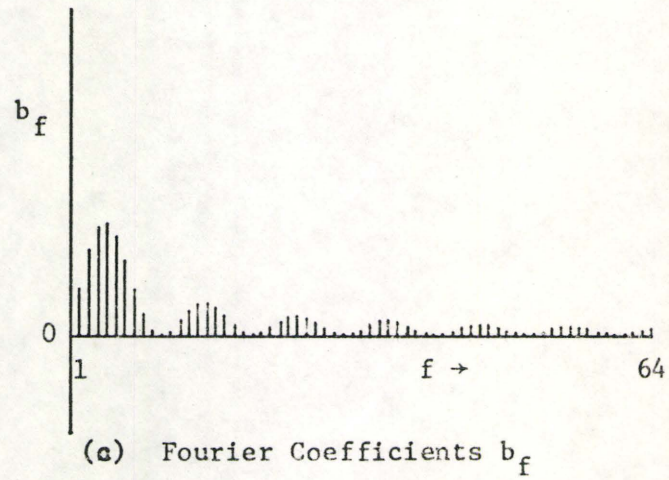
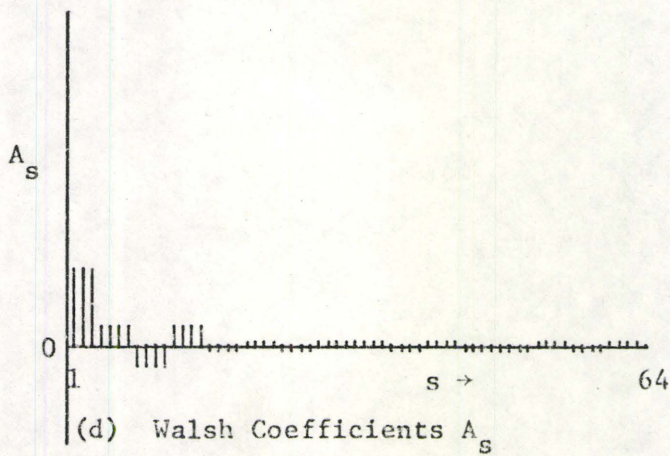
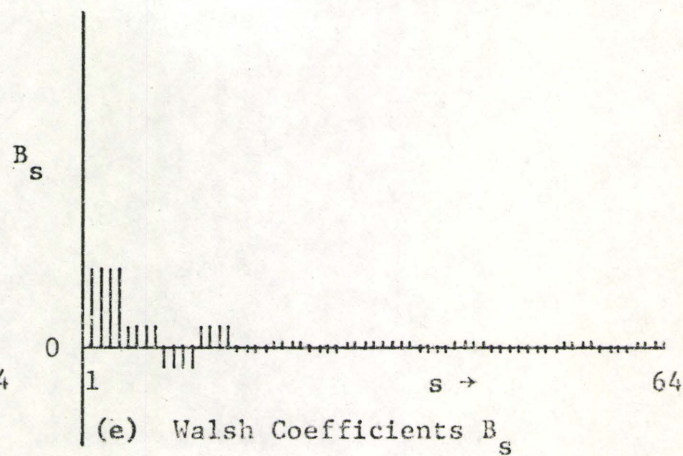
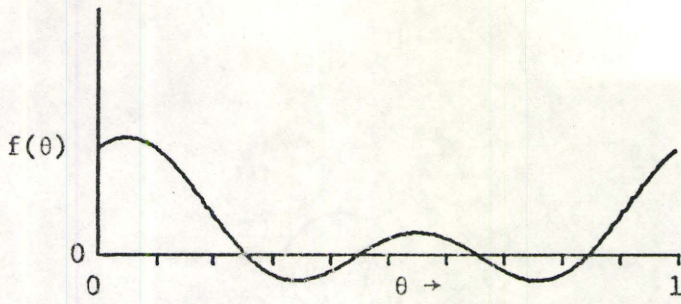
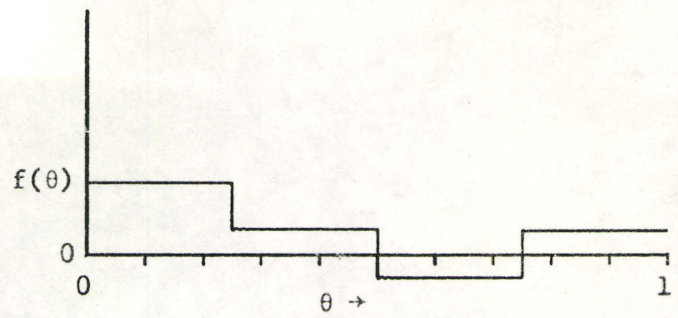
(b) Fourier Coefficients a_f (c) Fourier Coefficients b_f (d) Walsh Coefficients A_s (e) Walsh Coefficients B_s

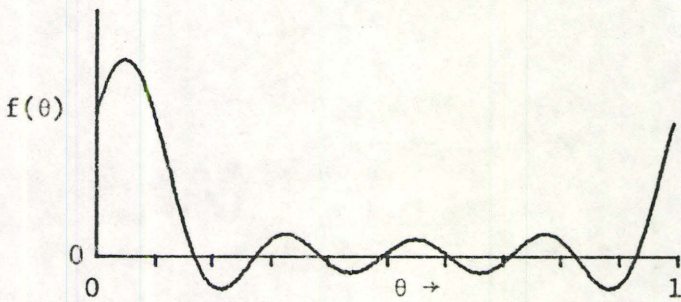
Fig. 5-3 Spectra of Rectangular Pulse (Duty Cycle = 0.1)



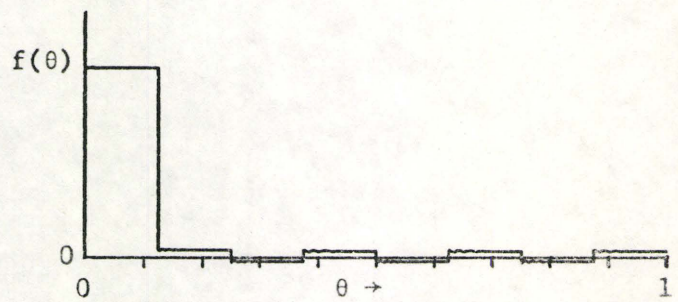
(a) 2 Fourier components



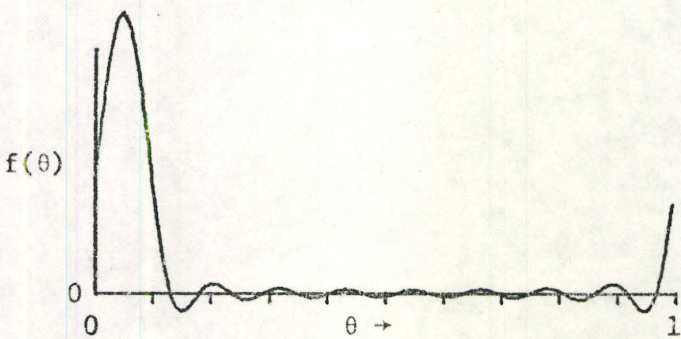
(g) 2 Walsh components



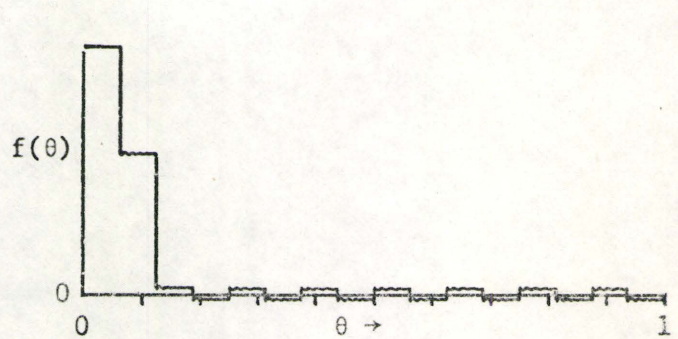
(b) 4 Fourier components



(h) 4 Walsh components

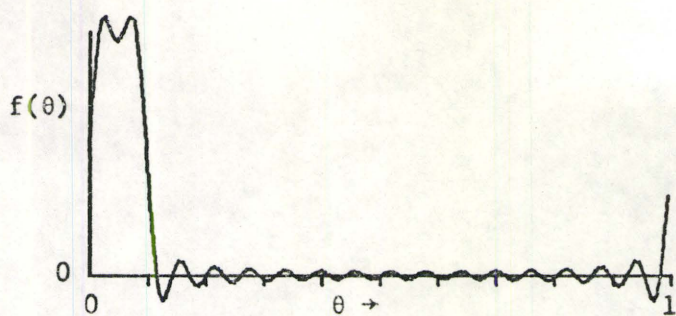


(c) 8 Fourier components

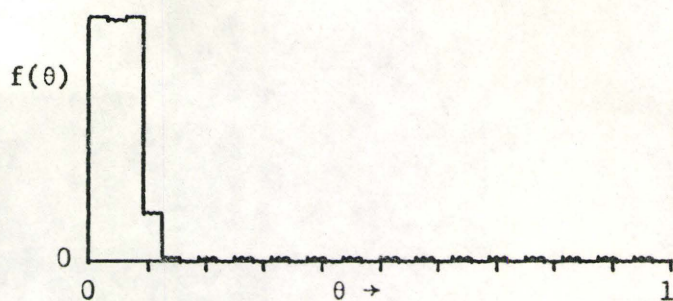


(i) 8 Walsh components

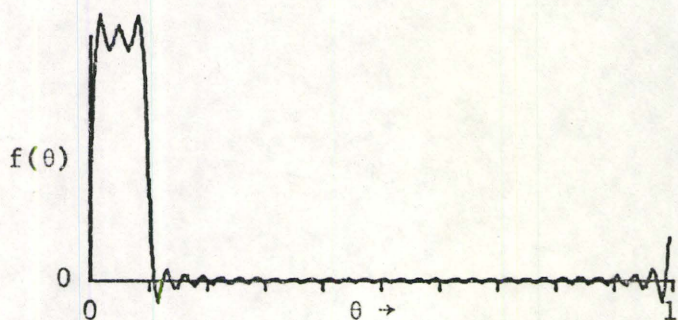
Fig. 5-4 Fourier Series and Walsh Series Synthesis of a Rectangular Pulse (Duty Cycle = 0.1)



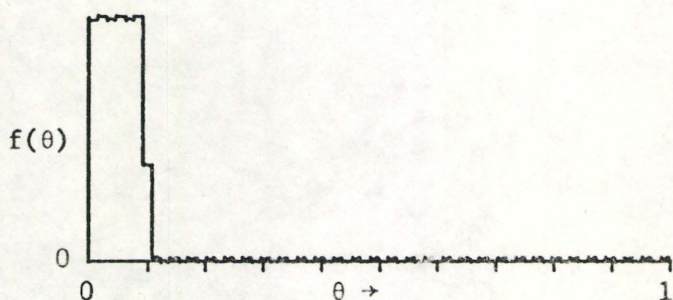
(d) 16 Fourier components



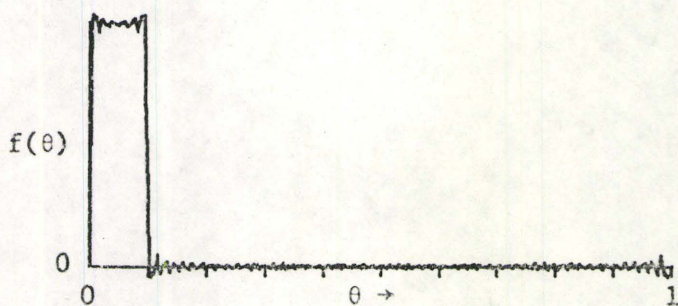
(j) 16 Walsh components



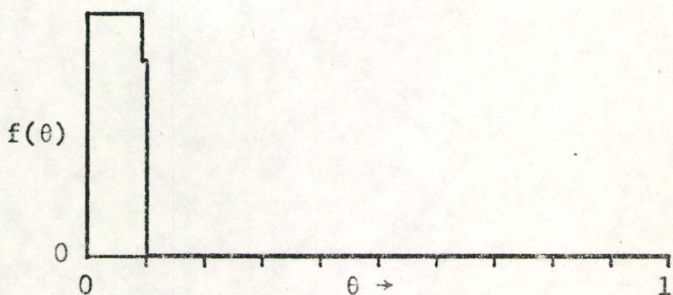
(e) 32 Fourier components



(k) 32 Walsh components



(f) 64 Fourier components



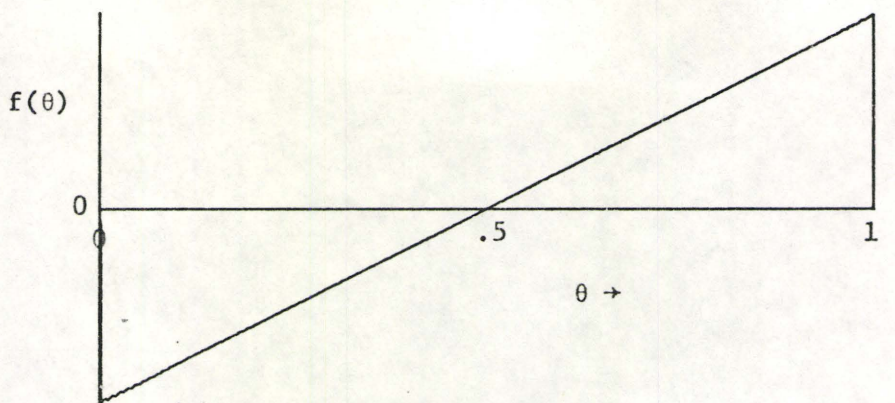
(l) 64 Walsh components

synthesis, appears to yield a function which more closely approximates the original function than does the Fourier synthesis, if the same number of components are used.

Fig. 5-5(a) illustrates a ramp function with its corresponding Fourier and Walsh line spectra in Figs. 5-5(b) and 5-5(c), respectively. Each series contains only odd terms. Although components in each series tend to diminish in amplitude at a similar rate, the Walsh spectrum has many zero-valued components whereas there are none in the Fourier spectrum. Consequently, a greater percentage of the power is concentrated in the first few non-zero Walsh components than in the Fourier domain. Thus, the synthesis of each series using an increasing number of components as shown in Fig. 5-6 again tends to display more rapid convergence to the waveform using the Walsh synthesis.

The third example of Fig. 5-7 shows a triangular waveform in which the Walsh components are more widely distributed than is the Fourier spectrum. The more rapid convergence of the Fourier series synthesis in this case is readily apparent in Fig. 5-8.

A final example illustrates synthesis of a waveform using experimental data taken from the Walsh spectrum instrument described in Chapter 4. The signal input was a slightly skewed sinusoidal wave which had a negative zero-crossing at $\theta \approx .52$. Table 5-2 lists the value of the Walsh coefficients provided by the digital analyzer. The table also lists the Fourier coefficients that were derived from the Walsh coefficients according to Eqs. (5-5) and (5-6). The last column on Table 5-2 is the total harmonic value c_f of the wave, where



(a) Ramp Function

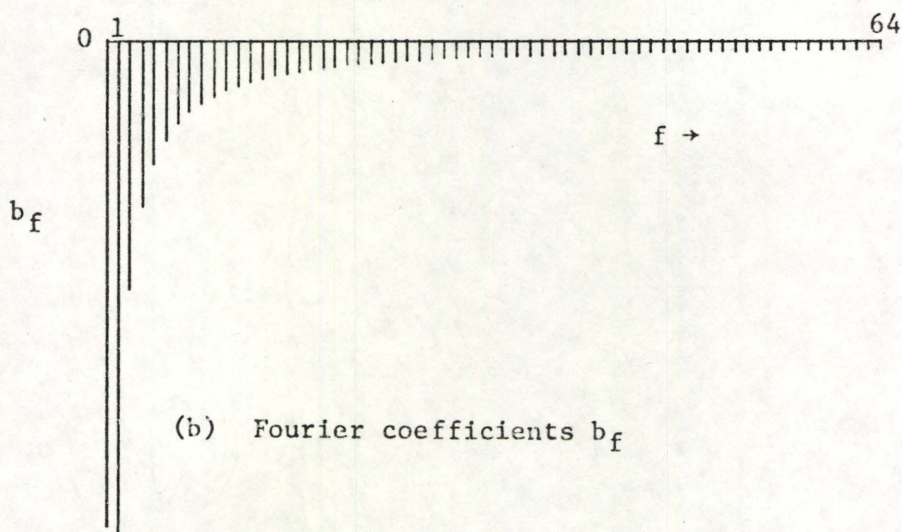
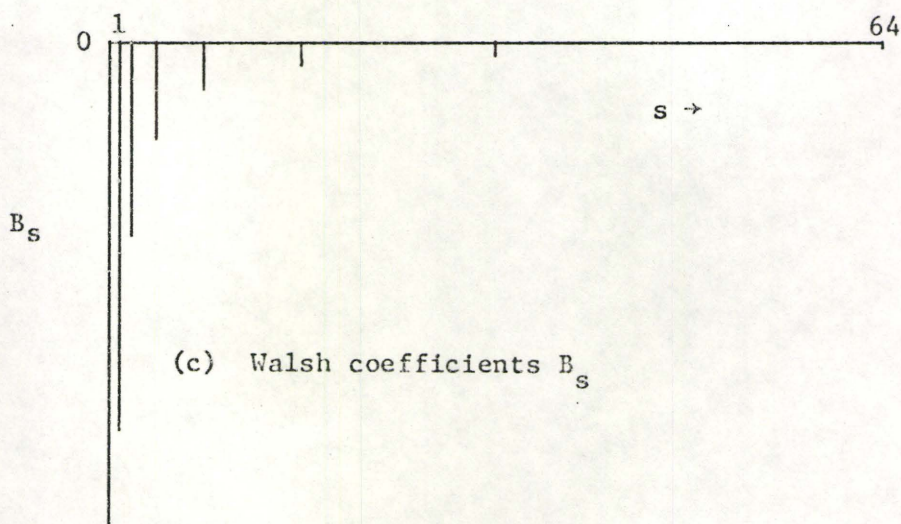
(b) Fourier coefficients b_f (c) Walsh coefficients B_s

Fig. 5-5 Spectra of a Ramp Function

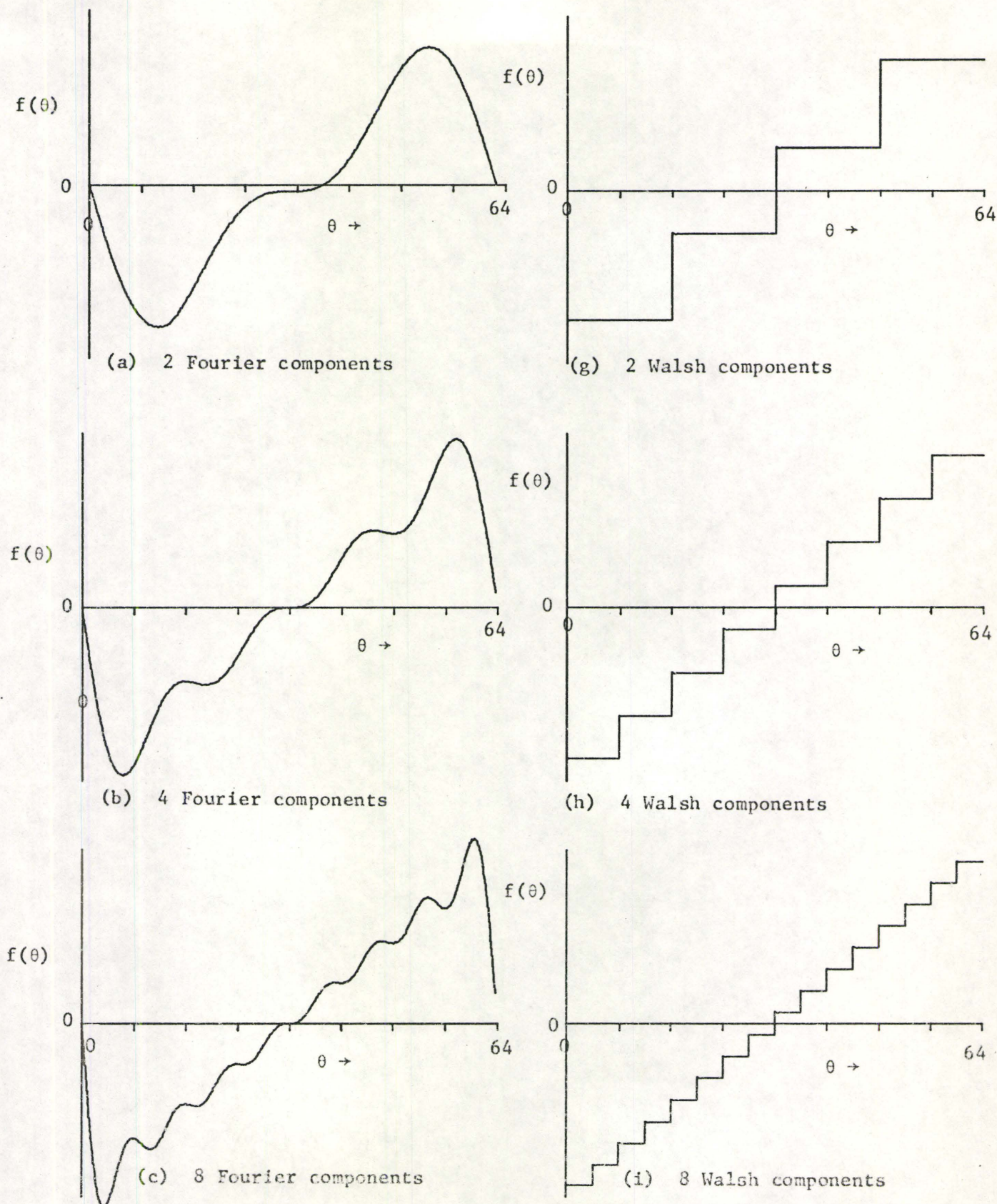


Fig. 5-6 Fourier Series and Walsh Series Synthesis
of a Ramp Function

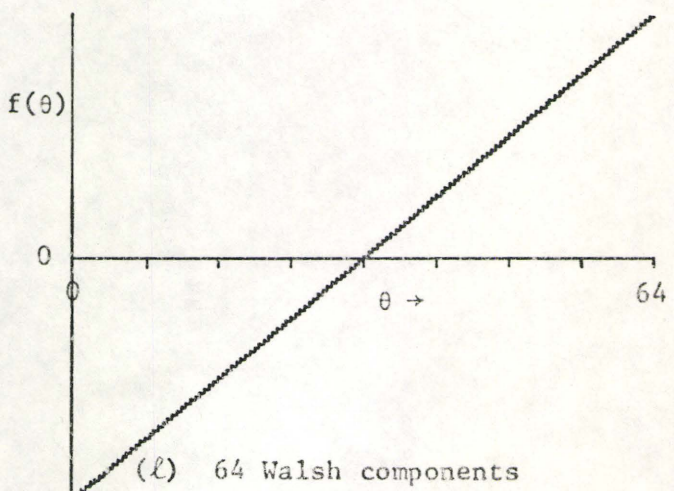
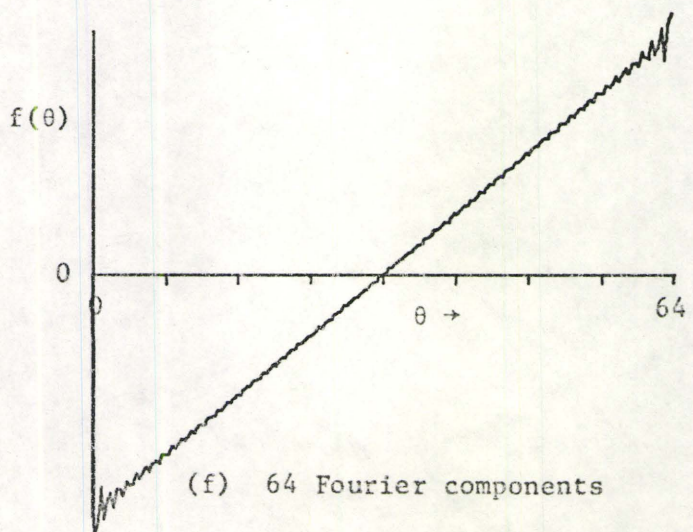
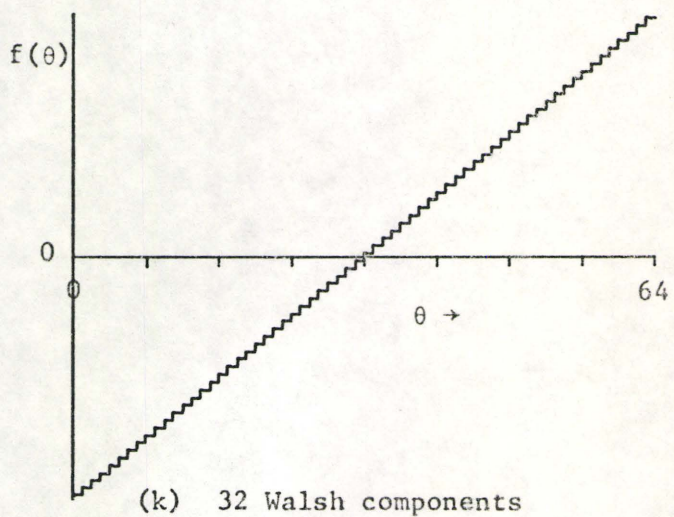
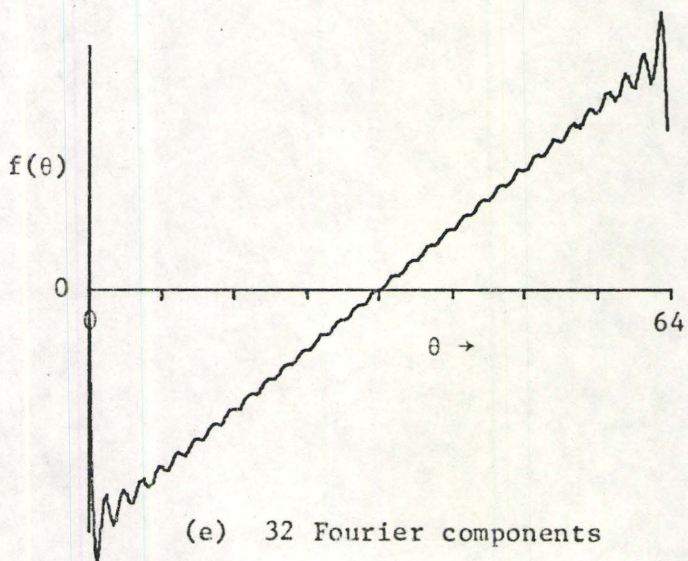
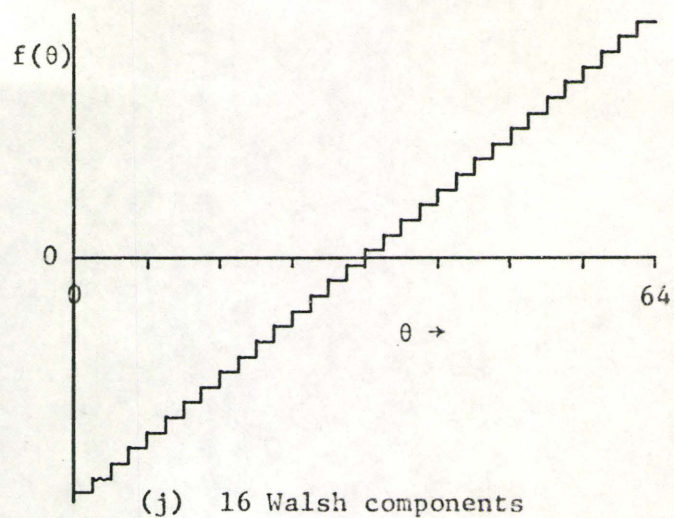
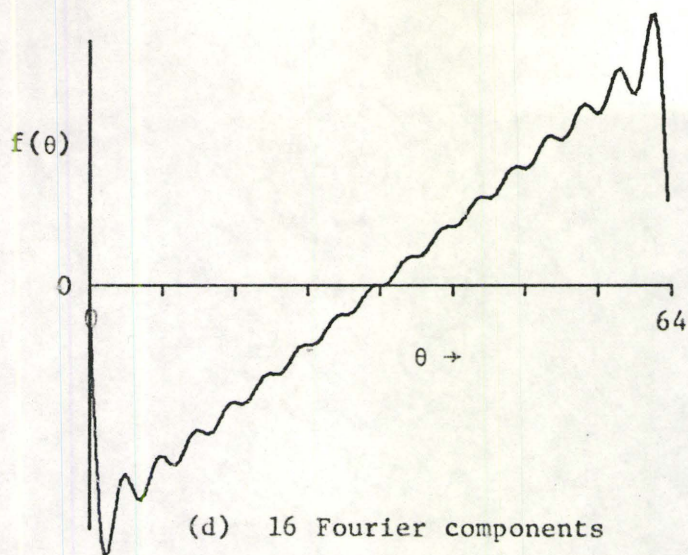
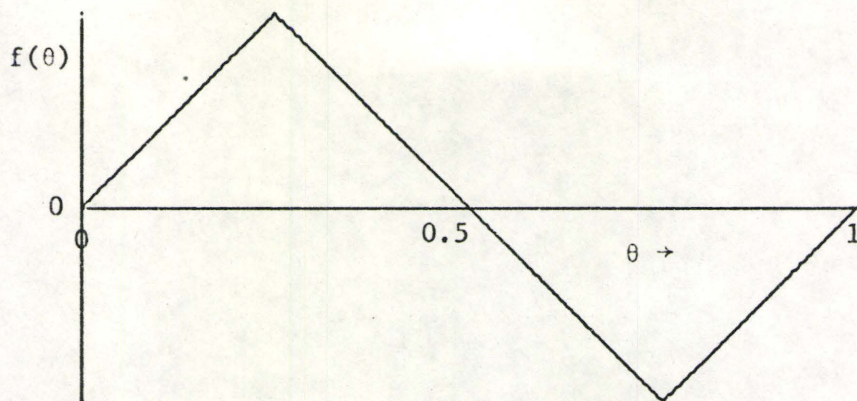


Fig. 5-6 Continued



(a) Triangular Wave

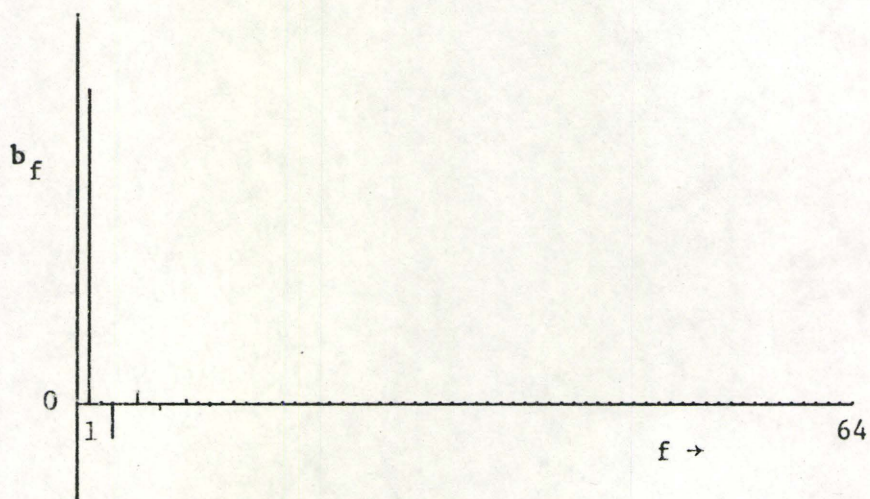
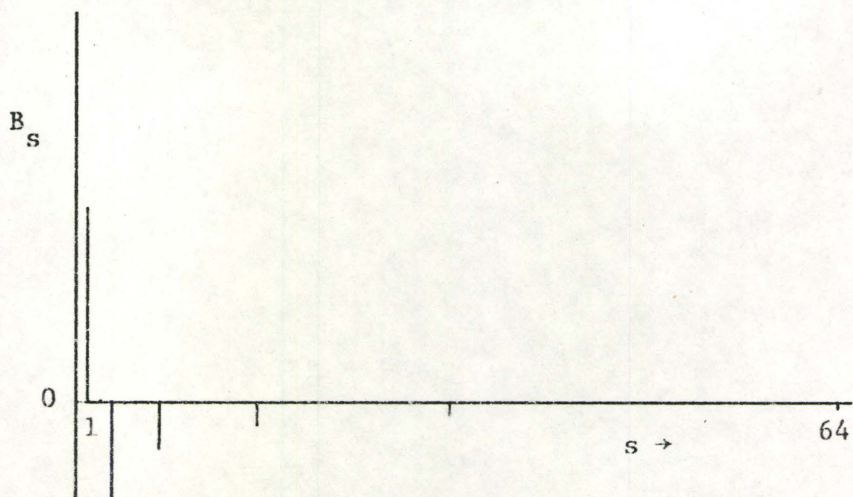
(b) Fourier coefficients b_f (c) Walsh coefficients B_s

Fig. 5-7 Spectra of a Triangular Wave

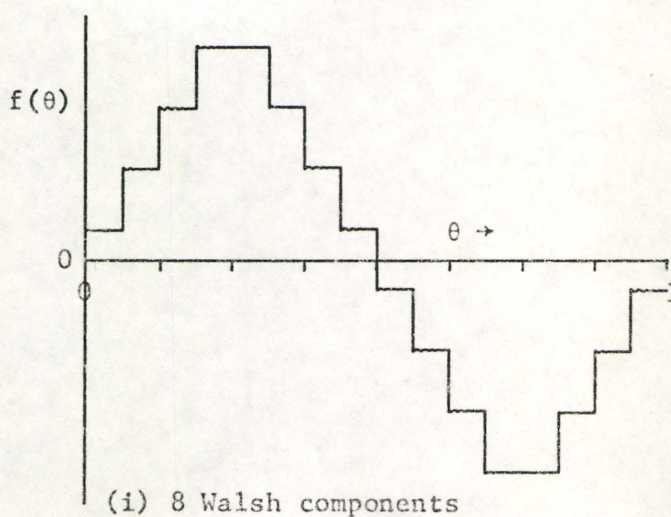
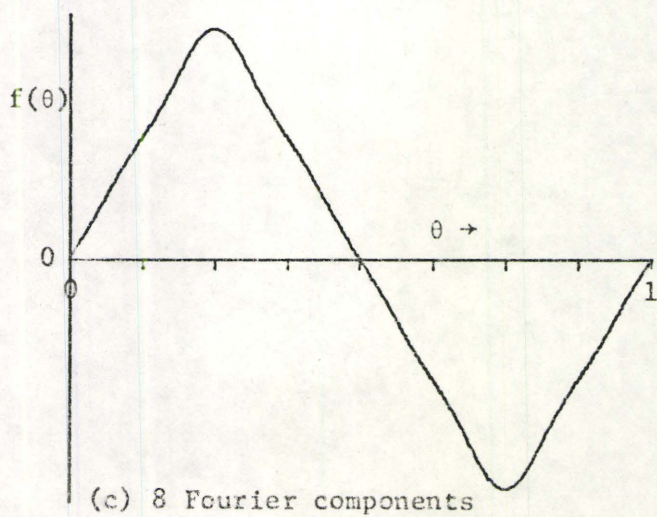
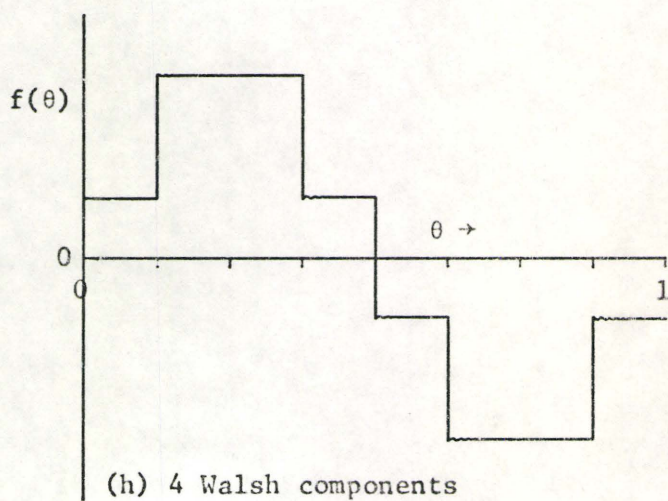
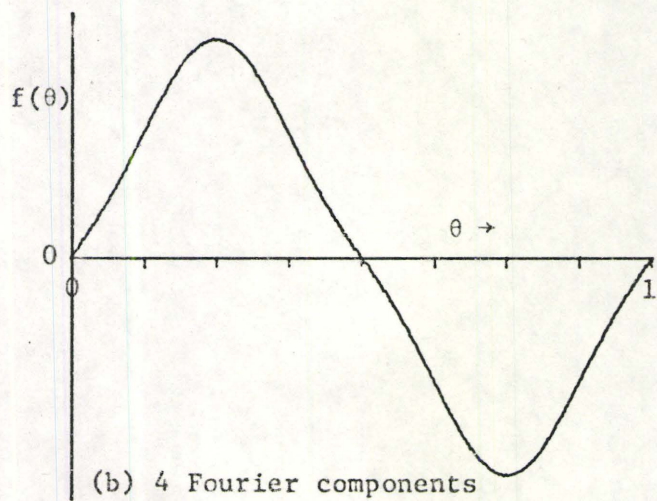
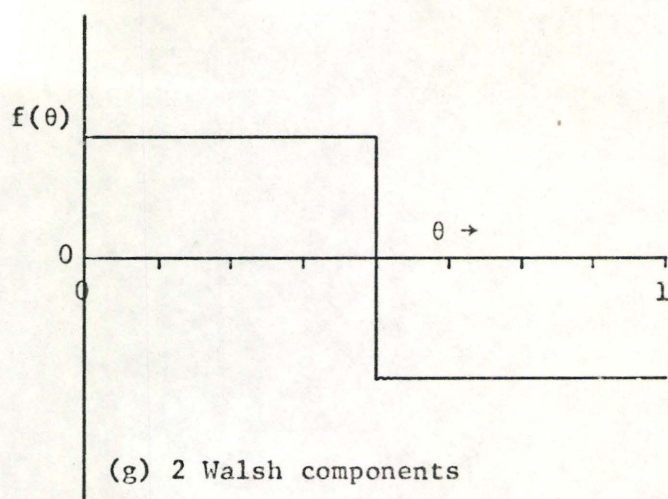
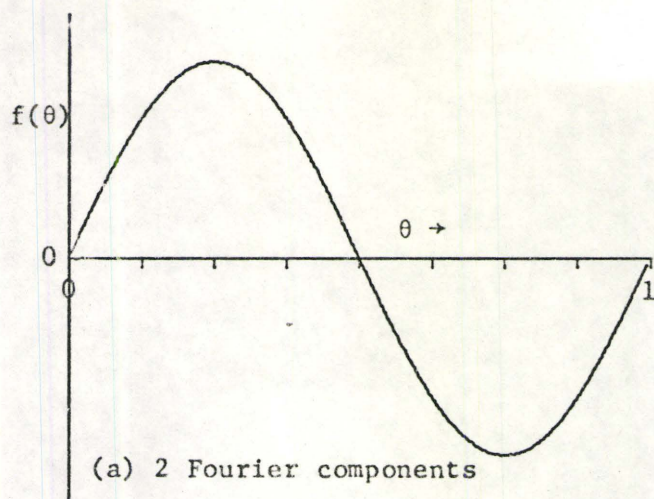


Fig. 5-8 Fourier Series and Walsh Series Synthesis of a Triangular Wave

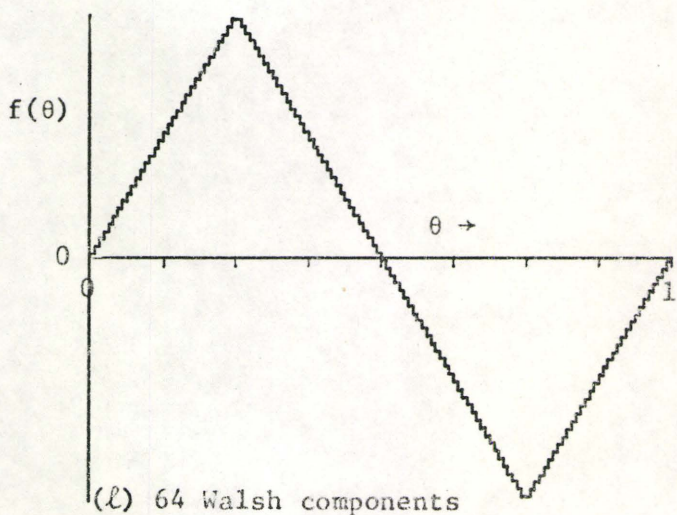
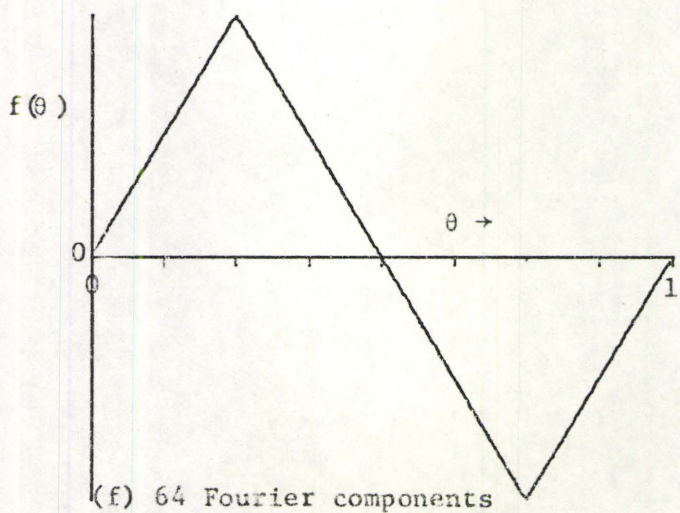
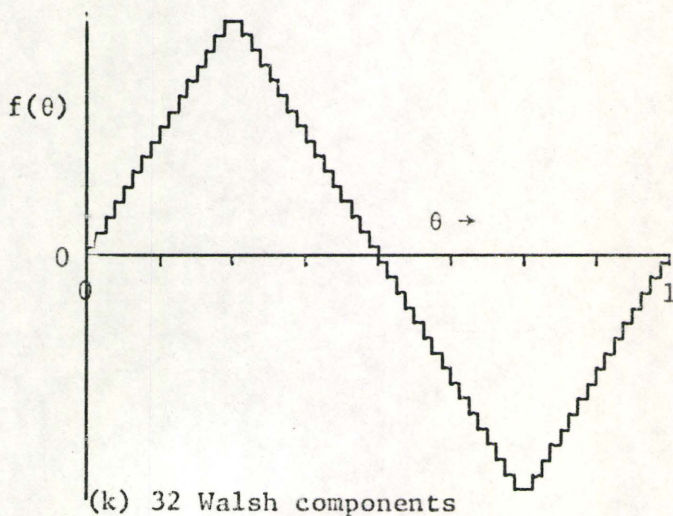
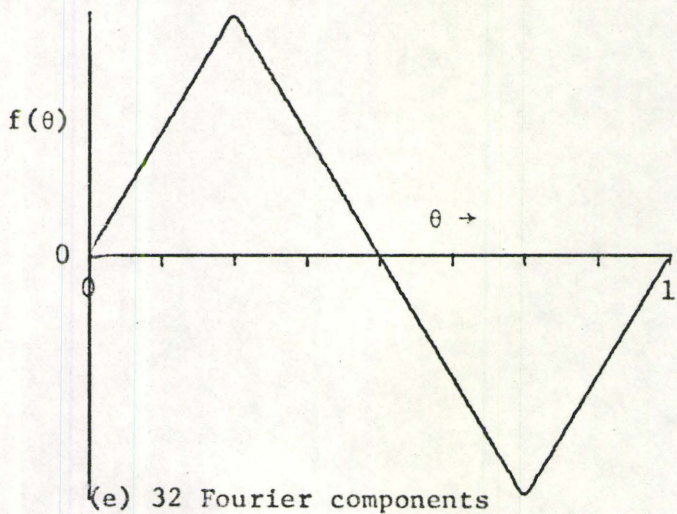
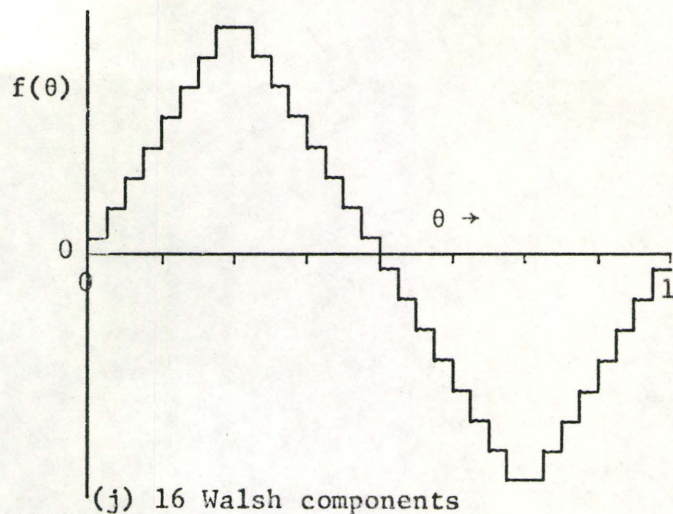
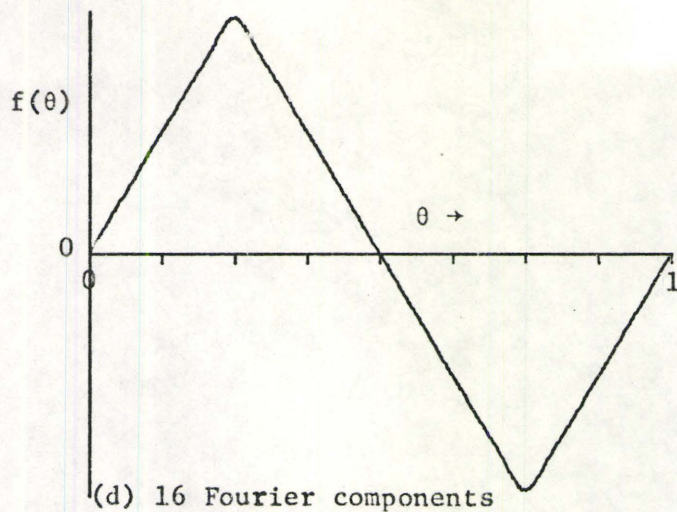


Fig. 5-8 Continued

<u>s or f</u>	Walsh Coefficients		Fourier Coefficients (obtained by conversion)		Harmonic Value
	<u>A</u> _s	<u>B</u> _s	<u>a</u> _f	<u>b</u> _f	<u>c</u> _f
1	-.188152	5.048696	-.291918	7.907939	7.913325
2	.026087	.314130	.041386	.490065	.491810
3	-.073043	-2.061196	.005742	.059299	.059576
4	-.004891	-.019565	-.008284	-.031360	.032436
5	.013804	-.442826	-.004245	-.016169	.016717
6	.011848	-.125978	.000916	.007224	.007282
7	-.034783	-.992065	.004280	.002181	.004804
8	.000435	-.001196	.000267	-.002325	.002340
9	.005435	-.102826	-.001620	-.005503	.005736
10	-.001848	-.029239	.000386	-.000953	.001028
11	-.000109	.039891	.001149	.001131	.001613
12	-.003478	.009565	-.001301	.003069	.003333
13	.010435	-.218587	.002070	-.003756	.004289
14	.004891	-.062174	-.000054	-.001861	.001861
15	-.018696	-.490652	-.001666	-.000151	.001672
16	.001522	-.001630	.001938	-.002076	.002840
17	.000978	-.023913	.001232	-.000792	.001464
18	-.000761	-.005870	.000837	-.000364	.000912
19	.000109	.012174	-.001794	.002284	.002904
20	.000543	0.000000	.001144	-.001215	.001669
21	.000978	.003261	-.000662	.000268	.000714
22	.001304	.001957	.001588	.000164	.001597
23	-.001196	.005217	.000057	-.001036	.001038
24	-.000543	.001522	-.000741	.001052	.001287
25	.002826	-.051848	.001219	-.001044	.001605
26	-.001196	-.014565	-.000962	.000036	.000963
27	.000761	.020978	-.000486	.002017	.002074
28	-.000652	.005543	.000350	.000790	.000864
29	.001630	-.110435	-.001556	.002912	.003301
30	.003370	-.031304	.000799	-.000871	.001182
31	-.007500	-.244891	.001983	-.001080	.002258
32	0.000000	0.000000	0.000000	0.000000	0.000000

MEAN VALUE= .250870

Table 5-2 Walsh Series Coefficients of Experimental Waveform and Fourier Series Coefficients Obtained by Walsh to Fourier Series Conversion

$$c_f = \sqrt{a_f^2 + b_f^2} \quad (5-99)$$

The waveform that was synthesized using the Walsh series coefficients given in Table 5-2 is shown in Fig. 5-9. The corresponding waveform synthesized using the Fourier coefficients is given in Fig. 5-10.

5.11 Conclusion

The feasibility of using Walsh series coefficients to derive the Fourier series of the same function has been demonstrated. Since an ideal low-pass filter [see Fig. 5-1] is required for precise evaluation of coefficients for frequency-limited functions, further studies should be made to investigate the effects of using practical low-pass filters.

The algorithm to determine the Fourier transform of a Walsh function should find application in computer evaluation of either the Fourier transform or the Fourier series coefficients of a Walsh function. Similarly, information regarding the pattern of non-zero elements in the Walsh to Fourier series conversion matrices aids in reducing computation time of the conversion processes.

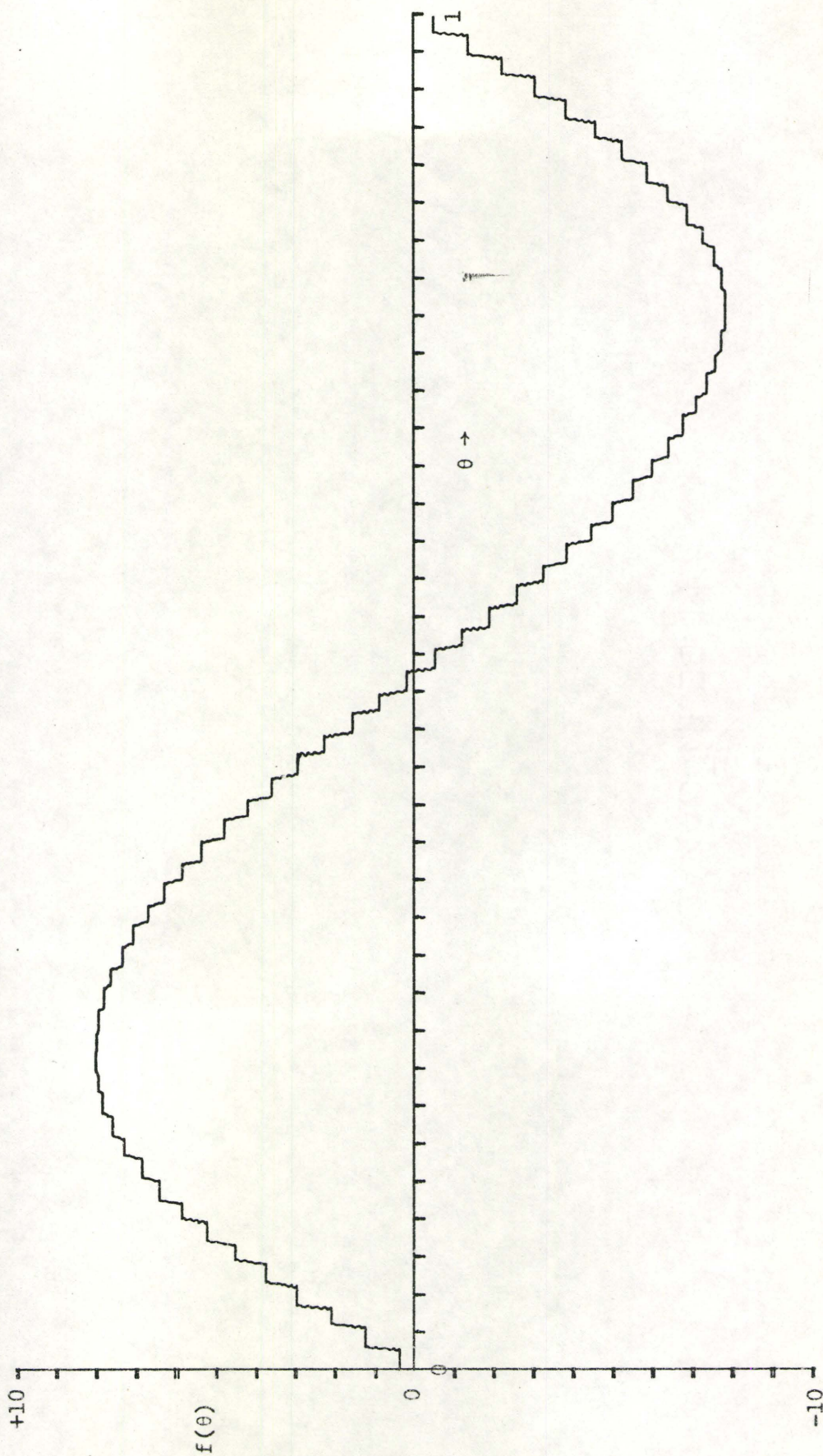


Fig. 5-9 Walsh Series Synthesis of Experimental Waveform

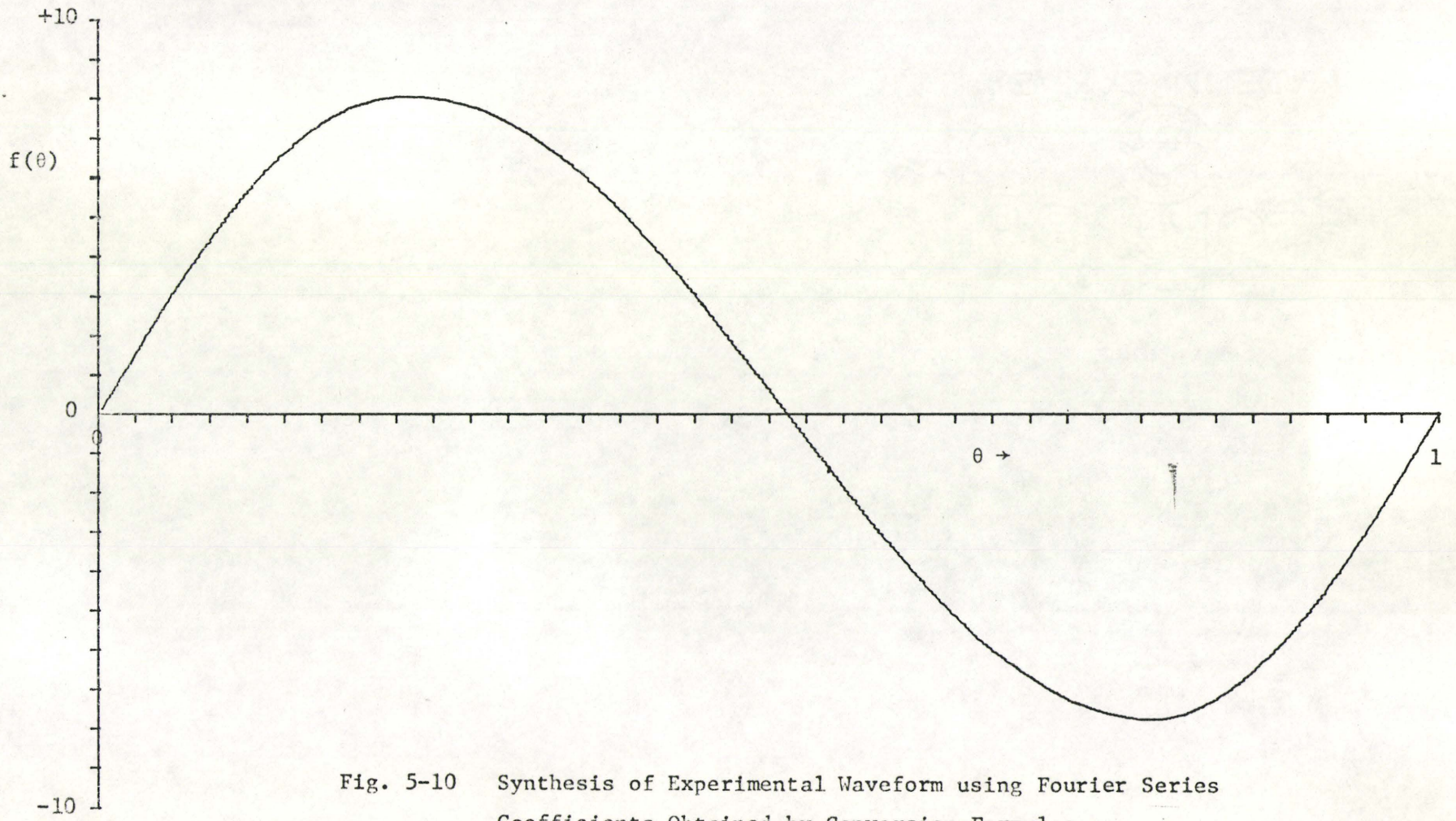


Fig. 5-10 Synthesis of Experimental Waveform using Fourier Series
Coefficients Obtained by Conversion Formulae

CHAPTER 6

CONCLUSIONS

The use of non-recursive definitions of Walsh functions results in simple coding algorithms for evaluating an arbitrary point on a Walsh function. The algorithms have been used to design and construct compact digital Walsh function generators whose outputs are free of hazards. Tests conducted on the generators show that they operate satisfactorily at input clock rates of over 10 MHz.

A generator that produces 64 Walsh functions simultaneously on parallel output lines has been incorporated into the design of a digital Walsh spectral analyzer. For periodic signals, the analyzer obtains a measure of the fundamental period of the signal to be analyzed and yields the first 64 coefficients of the sequency-ordered Walsh series at the end of the second complete cycle of the input waveform. Since coefficient values are available at that time, the analyzer can be considered as a real-time instrument. A sample is processed completely before the next input sample is taken so that fast processing is enabled without storage of the samples.

Further development of the spectral analyzer should entail a more flexible design of the controls that would enable the instrument to operate in any of the 6 modes of operation outlined in Chapter 3. The instrument would then become more versatile: Both periodic and non-periodic waveforms could be analyzed. The time-base of measurement may be time-locked to the fundamental period of a periodic wave, or it

may be preset arbitrarily. The sample size may be left indefinite or it may be preselected. Both analog signals and ready-quantized data may be analyzed. With appropriately high master-clock rate and a sufficiently fast A/D converter, the Walsh Spectral Analyzer can be extended easily to analyze signals in the entire audio range. There is no lower frequency limit. However, a complete error analysis of the instrument is yet required to establish more precise error characteristics.

The complexity of the instrument increases approximately in a linear manner for an increasing number of Walsh series coefficients. Since a sample accumulator and readout counter are required for each coefficient that is to be determined, these portions represent the bulk of the instrument. If a commercial Walsh Spectral Analyzer were developed, it would be advisable to manufacture LSI (large scale integration) circuits for each accumulator and counter. Several other sections of the analyzer could also be produced in LSI form, e.g., the Walsh function generator or the generator that produces pulses to clock the W.F.G. A 16-pin IC package could be used to contain a programmable W.F.G. that can generate 1024 Walsh functions.

Another project that is being undertaken is the development of a special-purpose instrument that will perform the Walsh series to Fourier series conversion and vice versa. A minimum number of constants are stored in the ROM of the conversion instrument if the number of coefficients to be used in the conversion is an integral power of two. A particularly useful study following the design of such an instrument would be an extensive study of the cost and versatility of a Fourier processor (possibly an FFT system) in comparison with the analyzer

described in this thesis in conjunction with a Walsh to Fourier series converter. Since sample storage and multiplication circuits are not required in the Walsh series analyzer, it is felt that this process leads to faster and less-expensive instrumentation than a Fourier series analyzer. The WSA not only yields the Walsh series coefficients, but in conjunction with the conversion instrument, may provide a less costly method obtaining the Fourier series coefficients. However, complexity of instrumentation for increasing numbers of coefficients to be determined may not increase at the same rate for the Walsh analysis with the conversion process as it does for the Fourier process. In light of this, further studies are required to reveal whether or not there is a range of operation for which instrumentation for one process is advantageous over the other.

APPENDIX

APPENDIX A

Summary of Walsh Function Definitions Derived in Chapter 2

(a) $wal(0, \theta) = 1$ (2-16)

$$wal(m, \theta) = \prod_{k=0}^{M-1} m_k \{R_k(\theta)\}$$

where m_k is a binary presence operator (see P. 15),
 m_k are bits in the binary representation of m ,
 M is the number of binary bits in m ,
 $R_k(\theta)$ are Rademacher functions of order k .

(b) $wal(m, \theta) = \prod_{k=0}^{M-1} g_k \{R_k(\theta)\}$ (2-18)

where g_k is a Gray code presence operator (see P. 15).
 g_k are bits in the Gray code for m .

(c) $wal(m, \theta_y) = \prod_{k=0}^{M-1} (-1)^{y_k g_{M-1-k}}$ (2-21)

$$= \prod_{k=0}^{M-1} (-1)^{g_k y_{M-1-k}}$$

where y_k are bits in the binary representation of $y = 2^M \theta_y$.

(d) $wal(m, \theta_y) = (-1)^{\sum_{k=0}^{M-1} y_k g_{M-1-k}}$ (2-22)

$$(e) \quad \text{wal}(m, \theta) = \prod_{k=0}^{M-1} m_k \{ \text{wal}(2^k, \theta) \} \quad (2-26)$$

$$= \prod_{k=0}^{M-1} \text{wal}(m_k 2^k, \theta)$$

$$= \text{wal} \left(\sum_{k=0}^{M-1} m_k 2^k, \theta \right)$$

$$(f) \quad \text{wal}(m, \theta) = \exp j\pi \left[\sum_{k=0}^{M-1} \langle m_k 2^k \theta \rangle \right] \quad (2-31)$$

where $\langle x \rangle$ denotes nearest integer to x .

$$(g) \quad \text{wal}(m, \theta) = \exp j\pi \left[\sum_{k=0}^{M-1} m_k (\theta_{k-1} + \theta_k) \right] \quad (2-33)$$

$$(h) \quad \text{wal}(m, \theta) = \exp j\pi \left[\sum_{k=0}^{M-1} m_k (\theta_{k-1} \oplus \theta_k) \right] \quad (2-34)$$

$$(i) \quad \text{wal}(m, \theta) = (-1)^{\sum_{k=0}^{M-1} m_k \gamma_k} \quad (2-36)$$

$$= \prod_{k=0}^{M-1} (-1)^{m_k \gamma_k}$$

where γ_k are bits in the Gray code representation of θ .

BIBLIOGRAPHY

Chapter 1

- [1] H.F. Harmuth, Transmission of Information by Orthogonal Functions, Springer-Verlag, New York, 1969.
- [2] F.F. Fowle, "The Transposition of Conductors", Trans. AIEE, vol. 23 (1905), pp. 659-687.
- [3] J.L. Walsh, "A Closed Set of Normal Orthogonal Functions", Amer. J. Math., vol. 45, 1923, pp. 5-24.
- [4] H.A. Rademacher, "Einige Saetze ueber Reihen von allgemeinen Orthogonalfunktionen", Math. Ann., vol. 87, 1922, pp. 112-138.
- [5] S. Kaczmarz, "Ueber ein Orthogonalsystem", Comptes Rendus du Premier Congres des Mathematiciens Pays Slaves, Warsaw, 1929, pp. 189-192.
- [6] R.E.A.C. Paley, "A Remarkable Series of Orthogonal Functions", Proc. London Math. Soc., vol. 34, 1932, pp. 241-279.
- [7] N.J. Fine, "On the Walsh Functions", Trans. Amer. Math. Soc., vol. 65, May 1949, pp. 372-414.
- [8] N.J. Fine, "The Generalized Walsh Functions", Trans. Amer. Math. Soc., vol. 69, July 1950, pp. 66-77.
- [9] N.J. Fine, "Cesaro Summability of Walsh-Fourier Series", Proc. Nat. Acad. Sci. USA, vol. 45, 1955, pp. 588-591.
- [10] H.F. Harmuth, "A Generalized Concept of Frequency and Some Applications", IEEE Trans. on Information Theory, vol. 14, May 1968, pp. 375-382.
- [11] H.F. Harmuth, "Applications of Walsh Functions in Communications", IEEE Spectrum, November 1969, pp. 82-91.
- [12] H.F. Harmuth, "Survey of Analog Sequency Filters Based on Walsh Functions", Proc. Symp. Appl. of Walsh Functions, Washington, 1970, pp. 208-219.
- [13] H.F. Harmuth, "Electromagnetic Walsh Waves in Communications", Proc. Symp. Appl. of Walsh Functions, Washington, 1970, pp. 248-259.

- [14] C.A. Bass (Editor), Proc. 1970 Symposium and Workshop on Applications of Walsh Functions, Washington, April 1970.
- [15] R.W. Zeek and A.E. Showalter (Editors), Proc. 1971 Symposium on Applications of Walsh Functions, Special Issue, IEEE Trans. Electromagnetic Compatibility, vol. EMC-13, Aug. 1971.

Chapter 2

- [1] J.L. Walsh, "A Closed Set of Normal Orthogonal Functions", Amer. J. Math., vol. 45, 1923, pp. 5-24.
- [2] F. Pichler, "Das System der sal-und cal-Funktionen als Erweiterung des Systems der Walsh-Funktionen und die Theorie der sal-und cal-Fourier Transformation", Doctoral Thesis, University of Innsbruck, 1967.
- [3] H.F. Harmuth, "A Generalized Concept of Frequency and Some Applications", IEEE Trans. on Information Theory, vol. 14, May 1968, pp. 375-382.
- [4] H.F. Harmuth, Transmission of Information by Orthogonal Functions, Springer-Verlag, New York, 1969.
- [5] K.W. Henderson, "Some Notes on the Walsh Functions", IEEE Trans. Computers, vol. EC-13, Feb. 1964, pp. 50-52.
- [6] N.J. Fine, "On the Walsh Functions", Trans. Amer. Math. Soc., vol. 65, May 1949, pp. 372-414.
- [7] C.K. Yuen, "Comments on 'Application of Walsh Transform to Statistical Analysis'", IEEE Trans. Systems, Man, and Cybernetics, vol. SMC-2, Apr. 1972, pp. 294.
- [8] R.B. Lackey and D. Meltzer, "A Simplified Definition of Walsh Functions", IEEE Trans. on Computers, vol. C-20, Feb. 1971, pp. 211-213.
- [9] R. Kitai and K.H. Siemens, "Comment on a Simplified Definition of Walsh Functions", IEEE Trans. on Computers, vol. C-21, May 1972, p. 512.
- [10] T.S. Durrani and J.M. Nightingale, "Sequential Generation of Binary Orthogonal Functions", Electronics Letters, vol. 7, July 1971, pp. 377-380.
- [11] A.C. Davies, "On the Definition and Generation of Walsh Functions", IEEE Trans. Computers, vol. C-21, Feb. 1972, pp. 187-189.

- [12] D.D. Givone, Introduction to Switching Circuit Theory, New York: McGraw-Hill, 1970, pp. 442-462.
- [13] R. Kitai and K.H. Siemens, "A Hazard-free Walsh-Function Generator", IEEE Trans. Instrumentation and Measurement, vol. IM-21, Feb. 1972, pp. 80-83.
- [14] I.A. Davidson, "The Use of Walsh Functions for Multiplexing Signals", Proc. Symp. Appl. of Walsh Functions, Washington, 1970, pp. 23-25.
- [15] F. Bagdasarjanz and R. Loretan, "Theoretical and Experimental Studies of a Sequency Multiplex System", Proc. Symp. Appl. of Walsh Functions, Washington, 1970, pp. 36-40.
- [16] F.J. Lebert, "Walsh Function Generator for a Million Different Functions", Proc. Symp. Appl. of Walsh Functions, Washington, 1970, pp. 52-54.
- [17] K.H. Siemens and R. Kitai, "Digital Walsh-Fourier Analysis of Periodic Waveforms", IEEE Trans. on Instrumentation and Measurement, vol. IM-18, Dec. 1969, pp. 316-321.
- [18] J.C. Majithia, "Simple Design for Up/Down Gray-Code Counters", Elect. Lett., Nov. 1971, vol. 7, pp. 658-659.
- [19] K.H. Siemens, "Digital Walsh-Fourier Analyzer for Periodic Waveforms", M.Eng. Thesis, McMaster University, Hamilton, Ontario, Canada, 1969.

Chapter 3

- [1] J.L. Walsh, "A Closed Set of Normal Orthogonal Functions", Amer. J. Math., vol. 45, 1923, pp. 5-24.
- [2] G.W. Morgenthaler, "On Walsh-Fourier Series", Trans. Am. Math. Soc., vol. 84, March 1957, pp. 472-507.
- [3] N.J. Fine, "On the Walsh Functions", Trans. Amer. Math. Soc., vol. 65, May 1949, pp. 372-414.
- [4] N.J. Fine, "The Generalized Walsh Functions", Trans. Amer. Math. Soc., vol. 69, July 1950, pp. 66-77.
- [5] N.J. Fine, "Cesaro Summability of Walsh-Fourier Series", Proc. Nat. Acad. Sci. USA, vol. 45, 1955, pp. 588-591.

- [6] H.F. Harmuth, Transmission of Information by Orthogonal Functions, Springer-Verlag, New York, 1969.
- [7] C. Watari, "Best Approximation by Walsh Polynomials", Tohoku Math. J., Series 2, vol. 15, Mar. 1963, pp. 1-5.
- [8] C. Watari, "A Note on Saturation and Best Approximation", Tohoku Math. J., Series 2, vol. 15, Sept. 1963, pp. 273-276.
- [9] C. Watari, "Contraction of Walsh-Fourier Series", Proc. Amer. Math. Soc., vol. 15, April 1964, pp. 189-192.
- [10] C. Watari, "Mean Convergence of Walsh-Fourier Series", Tohoku Math. J., Series 2, vol. 16, June 1964, pp. 183-188.
- [11] C. Watari, "Multipliers for Walsh-Fourier Series", Tohoku Math. J., Series 2, vol. 16, Sept. 1964, pp. 239-251.
- [12] C. Watari, "On Decomposition of Walsh-Fourier Series", Tohoku Math. J., Series 2, vol. 17, March 1965, pp. 76-86.
- [13] C. Watari, "Approximation of Functions by a Walsh-Fourier Series", Proc. Symp. Appl. of Walsh Functions, Washington, 1970, pp. 166-169.
- [14] W.S. Burdick, Radar Signal Analysis, Englewood Cliffs, N.Y.: Prentice-Hall, Inc., 1968.
- [15] H.F. Harmuth, "A Generalized Concept of Frequency and Some Applications", IEEE Trans. on Information Theory, vol. 14, May 1968, pp. 375-382.
- [16] H.C. Andrews and K.L. Caspari, "A Generalized Technique for Spectral Analysis", IEEE Trans. on Computers, vol. C-19, Jan. 1970, pp. 16-25.
- [17] J.L. Shanks, "Computation of the Fast Walsh-Fourier Series", IEEE Trans. on Computers, vol. C-18, May 1969, pp. 457-459.

Chapter 4

- [1] J.L. Shanks, "Computation of the Fast Walsh-Fourier Series", IEEE Trans. on Computers, vol. C-18, May 1969, pp. 457-459.
- [2] Burr-Brown Research Corp.: "Handbook of Operational Amplifier Applications", 1963.
- [3] Digital Equipment Corp.: "Digital Logic Handbook", 1969, pp. 218-249.
- [4] Les Brock, "Designing with MSI, Vol. 1", Signetics, 1970, pp. (3-1)-(3-8).

Chapter 5

- [1] K.H. Siemens, "Digital Walsh-Fourier Analyzer for Periodic Waveforms", M.Eng. Thesis, McMaster University, Hamilton, Ontario, Canada, 1969.
- [2] K.H. Siemens and R. Kitai, "Digital Walsh-Fourier Analysis of Periodic Waveforms", IEEE Trans. on Instrumentation and Measurement, vol. IM-18, Dec. 1969, pp. 316-321.
- [3] C. Boesswetter, "Analog Sequency Analysis and Synthesis of Voice Signals", Proc. Symp. Appl. of Walsh Functions, Washington, 1970, pp. 220-229.
- [4] H.H. Schreiber, "Bandwidth Requirements for Walsh Functions", Proc. Symp. Appl. of Walsh Functions, Washington, 1970, pp. 46-51.
- [5] N.M. Blachman, "Spectral Analysis with Sinusoids and Walsh Functions", IEEE Trans. Aerospace and Electronic Systems, vol. AES-7, Sept. 1971, pp. 900-905.
- [6] J.E. Gibbs, "Sine Waves and Walsh Waves in Physics", Proc. Symp. Appl. of Walsh Functions, Washington, 1970, pp. 260-274.
- [7] H.F. Harmuth, Transmission of Information by Orthogonal Functions, Springer-Verlag, New York, 1969.
- [8] S.J. Campanella and G.S. Robinson, "A Comparison of Orthogonal Transformations for Digital Speech Processing", IEEE Trans. on Commun. Tech., vol. COM-19, Dec. 1971, pp. 1045-1050.